Dynamic Modeling of Environmental Systems

Book · January 2000

DOI: 10.1007/978-1-4612-1300-0 · Source: RePEc

2 authors:

Michael L. Deaton
James Madison University
53 PUBLICATIONS **1,318** CITATIONS
SEE PROFILE

James J. Winebrake
University of North Carolina Wilmington
157 PUBLICATIONS **7,137** CITATIONS
SEE PROFILE

"DYNAMIC FUGACITY MODELING IN ENVIRONMENTAL SYSTEMS"

A Dissertation
Presented to
The Academic Faculty

By

Sinem Gokgoz Kilic

In Partial Fulfillment
of The Requirements for the Degree
Doctor of Philosophy in the
School of Civil and Environmental Engineering

Georgia Institute of Technology

April 2008

DYNAMIC FUGACITY MODELING
IN ENVIRONMENTAL SYSTEMS

Approved by:

Dr. Mustafa Aral (Advisor)
School of Civil and Environmental Engineering
Georgia Institute of Technology

Dr. Jiabao Guan
School of Civil and Environmental Engineering
Georgia Institute of Technology

Dr. Spyros Pavlostathis
School of Civil and Environmental Engineering
Georgia Institute of Technology

Dr. Sotira Yiacoumi
School of Civil and Environmental Engineering
Georgia Institute of Technology

Dr. Turgay Uzer
School of Physics
Georgia Institute of Technology

Date Approved: 24 March 2008

Aileme

ACKNOWLEDGEMENTS

This PhD has been a long and adventurous journey with many ups and downs. I was able to complete this endeavor because I was lucky to be surrounded with many wonderful people. I must first express my gratitude towards my advisor Dr. Mustafa M. Aral. He was not only an advisor during my PhD, but also a mentor. His professionalism, his hard work, and work ethics set an example I would like to match someday. I consider myself fortunate to have the opportunity to work with him.

I would like to also thank my committee members Dr. Sotira Yiacoumi, Dr. Spiros Pavlosthatis, Dr. Jiabou Guan, and Dr. Turgay Uzer for their time, effort and enlightening suggestions towards improvement of the quality of this thesis. I am very grateful for their input.

I would like to thank my previous and current lab mates as well. MESL, our lab, has always been a friendly and comforting environment for me. I feel very fortunate to have met all of my friends and colleagues, whom I have shared an office with. Thank you very much Dr. Orhan Gunduz, Dr. Chen He Park, Dr. Wonyong Jang, Dr. Elcin Kentel, Kijin Nam, Scott Rogers, Jinjun Wang, Recep Kaya Goktas, Ilker Telci, and Radhika Dhingra. I also would like to thank my good friends at the department of Civil and Environmental Engineering, Evren, Ulas, Burcak, and many more that would be very hard to list here.

I would like to thank my good friends, Nazmiye Acikgoz, Melda Ormeci, and Atay Kizilaslan for all the coffee breaks we have shared and the joyful conversations to go with the coffee. Without those coffee breaks, this thesis would never have finished. During the length of my PhD at Georgia Tech, many good friends helped me through bad times and give me courage to continue on this path. I cannot express my gratitude for you Meltem Alemdar, Funda Golcuklu and Nevbahar Ertas. You were always there when I needed help through bad times, offered me a shoulder to cry on, helped keep my sanity, and made me a better person. It is not possible to list everyone who helped me through this journey, but I thank you all very much.

I am very grateful for my parents Semra and Sevki Gokgoz, and my sister, Ozlem Gokgoz Aksoy, for their unconditional love and support. Without your belief in me, I could never have come so far. Someone told me once that only those who have enough support to fall back on can go further in life. If I have come this far, it is because I knew that my family would always be there to pick me up and help me go on.

I do not even know the words to thank my beloved husband, Hakan. Hakan: you have held my hands through hard times, you have kept me going when I wanted to give up, and you have given me hope when I thought I lost it all. I do not believe I would have been able to finish this thesis had it not been for you. I cannot express how much it means to have you and your love in my life.

TABLE OF CONTENTS

LIST OF TABLES

LIST OF FIGURES

SUMMARY

Fully-dynamic, continuous fugacity-based fate and transport models have been developed to examine all natural processes and interactions in the aquatic water systems. Within a body of surface water such as a lake or a river, a dynamic interaction among different media takes place. Chemical compounds are continuously dissolving, adsorbing into solid particles, attaching to suspended particles, resuspending, reacting, diffusing, and advecting. As the inclusion of all these interactions into a model is complex, the use of fugacity concept instead of concentration, renders the modeling task relatively easy. Fugacity, which is described as the escaping tendency of a chemical from a medium, is continuous among different phases, thus easier to follow the movement of the chemical.

The first model has been developed to be used as an emergency response model by decision makers. It models the fate and transport of any contaminant in a shallow water environment with three compartments; air, water, and sediments. Due to uncertainties involved in the examination of long term response of a water system to any contaminant in a short amount of time, Monte Carlo simulations have been performed. The fate of three representative contaminants, polychlorinated biphenyls (PCBs), atrazine, and benzene and the concentration profiles of each contaminant in all compartments are examined with this model.

The second model developed in this thesis, is a continuous, dynamic river fugacity-based water quality model. In order to develop a continuous model, the velocity and the depth values along the river need to be established. This is done through the solution of river hydrodynamics, namely Saint-Venant equations. Water depth and velocity at each point along the river are used in the advection-dispersion equation to determine the fate and transport of a contaminant. Interactions between different phases are also incorporated into the advection-dispersion equation which is solved numerically and coupled with a mass balance equation derived for the same contaminant in the sediments.

The third model is a multispecies contaminant fate and transport model which can be used for the fate of a single contaminant and its daughter products. Trichloroethylene (TCE) and its daughter products, dichloroethylene (DCE) and vinyl chloride (VC), are used as representative of multispecies contaminants. The fate and transport of TCE and its daughter products has been analyzed first in a lake environment, and then in a river environment. For the lake application, a model that has four compartments; water, air, sediment, and biofilm compartments have been developed. For the river application, hydrodynamics of the river is solved first and then advection dispersion equation is developed for three compounds in the water column. Mass balance equations for the three compounds in biofilm and sediment compartments are also solved simultaneously along with the advection dispersion equation derived for the water column.

CHAPTER 1

INTRODUCTION

Surface waters are an important component of the natural environment. As human survival depends on fresh water sources, lakes, rivers, and streams need to be protected from pollution. However, they are under constant threat from contaminants, including both conventional and hazardous substances (Chuco 2004).

Among all the sources of fresh water, the most susceptible to contamination is the surface water since it interacts with the atmosphere, groundwater, soil and open water bodies such as seas and oceans through estuaries. Furthermore, since rivers and lakes are habitats for many aquatic species, they are also susceptible to the same contamination. Therefore, the fate and transport of contaminants in surface waters have long been the focus of research in which environmental scientists and engineers have applied various approaches to water quality modeling. This study focuses on contaminants that are difficult to follow in the environment as they partition between different phases that exists in the water column. As these contaminants partition, they may follow various pathways, and pose myriad of risks. As an example, they may end up in the food chain and eventually pose health risk to humans. To examine the behavior of these

contaminants, models that deal with the aqueous phase alone may not be suitable and more effective tools are necessary.

As the contaminants are distributed among all the possible media in the vicinity of a water column, such as suspended particles, fish, aerosols, sediments, and air, an environmental model that examines only aqueous phase transport cannot accurately predict the fate and transport of these contaminants. The interactions between all the possible phases in the surface water column can be analyzed with the fugacity approach, as used in this study.

Within a body of surface water such as a lake or a river, a dynamic interaction among different media takes place. Chemical compounds are continuously dissolving, adsorbing into solid particles, attaching to suspended particles, resuspending due to diagenesis (bioturbation on the active surface of sediments) or shear force of the flowing water on top of the sediments, and reacting, diffusing, and advecting with bulk water movement. As the inclusion of all these interactions into a model is complex, the use of fugacity concept instead of concentration, renders the modeling task relatively easy. Fugacity, which is the pressure or chemical potential a compound exerts wherever it exists, can also be described as the escaping tendency of a chemical from a medium. The fugacity values of a chemical in water, sediments, and air tell us the direction of the movement a chemical will make between phases. Using the fugacity concept to track the fate and transport of contaminants in rivers and lakes, this study aims to incorporate thermodynamic knowledge into the contaminant transport model in surface waters.

The study is organized into three main parts in ascending complexity. The first presents a probabilistic approach to evaluate the extent of pollution in a lake environment after a natural disaster or accidental deliberate contamination event. In this approach, the hydrodynamic analysis remains simple with the use of a well-mixed reactor assumption. The lake environment is defined as a collection of three compartments: air, a water column, and a sediment compartment. Each compartment, in turn, is a collection of solid, liquid, and gas phases. The first compartment, air, contains aerosols (i.e., particulate matter in air) and an air gas phase. The second, a water column, is composed of water and suspended particles. The last, a sediment compartment, consists of a soil matrix under saturated conditions. The compartments are continuously interacting, and such interactions are reflected in the mass balance equations written for each compartment. The air compartment acts as a sink, as wind-induced air flow removes chemicals volatilized into the air from the system. Sometimes, the volatilized chemicals return to the water column through wet and dry deposition and rain. Sediments may become secondary sources of pollution as they slowly release chemicals that are adsorbed into the solid phase in the water column and settle on the bottom. The water column allows chemicals to exit via tributaries and to interact with the adjacent air and sediment compartments. In this first stage, contaminants are considered non-reactive and only decay on their own in each compartment according to their half-lives in that particular environment.

In this study, the fate of three representative contaminants, polychlorinated biphenyls (PCBs), atrazine, and benzene, are modeled using the fugacity approach, and the concentration profile of each contaminant in all compartments is examined. To resolve the uncertainty involved in the model parameters, Monte Carlo analysis is used. The resulting model is a simple, general, and effective tool that can be used as an emergency response model by decision makers.

In the second part of this study, the water quality in rivers is examined. In the past, the fugacity concept has been applied to river water quality modeling with a simple approach in which many completely stirred tank reactors (CSTR) are connected in series and discrete analysis is performed. However, in this part of this thesis, a fully dynamic and continuous contaminant fate and transport model for rivers is developed and solved. First, the velocity and the depth distribution in a river are established through the solution of river hydrodynamics. Saint-Venant Equations are derived and solved for a natural river so that the hydrodynamics can be analyzed. As a result, the water depth and velocity at each node in the model is obtained. This information is then used for the fate and transport of a contaminant by application of advection-dispersion equation written in fugacity form.

In addition, three compartments are used with the interactions between them, as in the lake case discussed. However, instead of including the solution of air dynamics, this study assumes the air compartment is semi-infinite. Thus, the air compartment acts as a sink. All the interactions between the air and water columns are used, but they would

never be sufficient to change the air concentration in the long run, so this concentration is kept constant throughout the analysis. While the water column flows with the velocities calculated in the hydrodynamic solution, the sediment compartment is immobile yet interacts with the water column above. The chemicals are still non-reactive. This dynamic and continuous water quality analysis of a river system has never been attempted with the fugacity approach before. As mentioned earlier, when fugacity is used, modeling is much easier regarding the flux of a chemical from one compartment to another and this advantage is also made use of in this study.

Thus far, only abiotic reactions such as hydrolysis, photosynthesis, and decay have been considered. Nevertheless, in nature, particularly in rivers, many microorganisms live and interact with chemical compounds. In the third part of this thesis, the fate and transport of a multi-species compound, namely trichloroethylene (TCE), is examined. TCE may undergo both aerobic and anaerobic transformation in the presence of a microbial population. As anaerobic bacteria use TCE as an energy source, a chlorine atom is removed from the chemical, and through anaerobic biotransformation, TCE may produce daughter products. The first is dichloroethylene (DCE) and then with further removal of another chlorine atom, vinyl chloride (VC), which has only one chorine atom left, may be produced. When that final chlorine atom is removed by the activities of anaerobic microbes, the harmless ethane is produced. All daughter products are substances considered harmful to human health. Hence, the disappearance of TCE from an aquatic system, which results in the production of other toxic chemicals, is not necessarily positive. Thus, the by-products, or daughter products, need to be considered when TCE

is being modeled. When TCE or any of its daughter products go through aerobic transformation, they can completely be mineralized, that is, they turn into water and carbon dioxide.

The microbial population in aquatic environments is generally concentrated on the sediment-water interface, and they form a biofilm. Depending on the oxygen penetration depth of this biofilm, both aerobic and anaerobic transformations may occur here. In this final part of the thesis, these biotrasformations are added to the already developed dynamic fugacity-based river water quality model. Using this approach, the fate of DCE and VC is also followed in addition to that of TCE. To perform this analysis, a biofilm, the upper layer on top of sediments, is introduced into the model as an additional compartment in which all the biological transformations occur.

The result of this research is the development of a fully dynamic fugacity-based model with a sophisticated representation of all the natural processes that may take place in a river or lake environment.

Scope of the Study

This study is organized in six main chapters. In Chapter 2, background literature is given about the river hydrodynamics, river water quality models, application of fugacity, the contaminant transport, and biofilm applications. In Chapter 3 the application of the fugacity concept in water quality modeling is given through development of a simple, yet

effective emergency response model. The model developed is used to examine the effects of short term measures taken in Lake Pontchartrain after Hurricane Katrina. This application does not involve water hydrodynamics. In Chapter 4 the hydrodynamics of water flow in natural rivers is discussed. In this chapter, the set of coupled, non-linear, unsteady equations describing the conservation of mass and conservation of momentum in rivers, which are known as Saint Venant equations are derived. In Chapter 5, a contaminant fate and transport model with a fugacity approach is derived for a river system. Then the model is applied to Altamaha River System using the results of the hydrodynamics solution as well. Chapter 6 introduces multispecies fate and transport using a fugacity approach. In this chapter, TCE and its two daughter products are modeled first in Lake Pontchartrain, and then in the Altamaha River System. The biotransformation reactions take place on top of sediments where microorganisms are concentrated forming biofilms. Biofilm is added as another compartment to the model developed to account for multispecies fate and transport. In Chapter 7 the summary and conclusions of all these studies are provided.

CHAPTER 2

BACKGROUND AND LITERATURE REVIEW

An integral part of the natural environment, rivers supply fresh water for domestic and industrial uses, convey wastewater discharges (treated and untreated), and supply economic value through electric generation, fishing, transportation, and irrigation. Therefore, for the sake of both ecological and human welfare, the maintenance of rivers is crucial if they are to remain clean, sustainable, and protected from sources of contamination. However, such maintenance requires the enforcement of environmental regulations. Compliance of these regulations can be assessed and assured with the use of river water quality models.

River water quality models are based on the conservation of mass principle, i.e., within a finite section of a river, mass is neither created nor destroyed and thus has to be conserved. To account for all transfers of matter across the system's boundaries and all transformations occurring within the system quantitatively, mass balance equations needs to be developed. Further, a comprehensive river water quality model should incorporate temporal as well as spatial variability. To develop a completely dynamic river water quality model, this research will first address the complex hydrodynamic routing

component and then discuss the complex pollutant fate and transport routing component. The advection-dispersion equation is used for the transport of a contaminant through the river system while conserving its mass.

The term “advection” refers to the movement of bulk water that contains all the dissolved substances and particulate matter. The calculation of advection requires the velocity of a river along its path, and in almost all cases, the velocity can be calculated independently of the water-quality model. A wide variety of models that calculate the flow in a river system have been developed. They are based on full or simplified forms of the Saint Venant equations, which represent the conservation of mass and momentum in a one-dimensional domain consistent with the typical geometry of rivers. Two- and three-dimensional representations are also available, but they require considerable computational complexity and rely on significant number of parameters which may be difficult to characterize. A comprehensive review of these models is provided by (Bedford et al. 1988). Many water quality models favor the use of simple measures of stream velocity such as time-of-travel studies rather than complex hydrodynamic calculations (Kilpatrick and Wilson 1989). This study uses the full form of the Saint Venant equations.

2.1. The Saint-Venant Equations

Rivers and streams, natural, open channels with a free surface, can be characterized as a streamline along which the pressure is constant and equal to the atmospheric pressure

(Sturm 2001). Due to the existence of the free surface, flow boundaries are no longer fixed by channel geometry but change to accommodate given flow conditions. Another aspect of open channel flow in rivers is the wide variability of the cross-sectional shape and roughness of a channel. Because of the free surface, gravity is the driving force instead of pressure, as is the case in closed conduits (Sturm 2001).

Because water flow in natural channels is almost always unsteady (Mahmood and Yevjevich 1975), this aspect of open channel flow requires a complex solution. The procedure to predict the temporal and spatial variations of a flood wave as it traverses a river reach or reservoir is known as flood routing (Baltas 1988).

Saint-Venant equations form the basis of the general mathematical model of unsteady, non-uniform flow in channels. The set of full, not-simplified forms of the Saint-Venant equations is referred to as the dynamic wave model. These equations can be simplified if some terms yielding a number of approximate distributed flow models are neglected. The full dynamic wave model is the only one that can accurately simulate backwater effects in a channel. This form of the equation is given below:

$$V\rho\frac{\partial u}{\partial t}+V\rho u\frac{\partial u}{\partial x}=-V\rho g\frac{\partial h}{\partial x}+F_p\ , \tag{2.1}$$

where V is the volume [L^3], ρ [M/L^3] is the density, u [L/T] is the velocity, t [T] is time, g [L/T^2] is the gravitational acceleration, h [L] is the water surface elevation, x [L] is the distance along the river, and F_p [L/T^2] is the frictional resistance.

In Equation (2.1), the first term is the local acceleration, the second term is the convective acceleration, the third term represents the effect of gravity on the water surface slope, and the last term represents the frictional resistance. If the local and convective acceleration terms in the momentum equation are neglected, the remaining portion of the equation is then referred to as the diffusion wave model. This model can be used to simulate flow in a channel when the backwater effects are not significant, and it can be simplified by dropping the pressure force term to obtain the simple kinematic wave model, which is known as the simplest channel flow model. The kinematic wave model assumes that the friction slope is equal to the channel bed slope and that it does not allow the simulation of backwater effects, as a flood wave can travel only downstream (Sturm 2001).

The complete Saint-Venant equations are a set of partial differential equations with two independent $\{x, t\}$ and two dependent variables $\{u, h\}$. The conservation of momentum is given in Equation (2.1), and the other equation, required to solve for the two unknowns, is the conservation of mass for incompressible fluids, referred to as the continuity equation.

$$\frac{\partial A}{\partial t} + \frac{\partial Q}{\partial x} = q_L \ , \tag{2.2}$$

where A [L^2] is the cross-sectional area, Q [L^3/T] is the volumetric flow rate, t [T] is time, x [L] is the distance along the river, and q_L [L^2/T] is the lateral flow entering the reach per length of the reach.

These two equations, also known as the Saint-Venant equations, together form the system of equations representing unsteady flow in channels. They are coupled, nonlinear, first-order partial differential equations of the hyperbolic type whose solutions require one initial and two boundary conditions (Baltas 1988). In addition, they have no analytical solution other than a few special cases (Gunduz 2004; Gunduz and Aral 2004). However, several numerical methods that solve the Saint-Venant equations have been developed. Among these methods, the finite difference method is used in this study.

The finite difference method involves the transformation of governing differential equations into algebraic equations through the approximation of the derivative in terms of difference equations. In an explicit finite difference method, the solution is advanced from point to point along one time line until all the unknown values in that particular time line have been calculated. In the next time step, the same principle is applied. In an implicit finite difference method, the solution from one time line to the next is performed simultaneously for all the discretization points of the idealization. While solutions for explicit methods are straightforward and easily programmed but restricted by conditions for stability, those for implicit methods are more complex and difficult to program but are unconditionally stable for the most part (Fread 1985).

2.2. Contaminant Fate and Transport Models (Water Quality Models)

Contaminant fate and transport in a river are often described by the advection-dispersion (mass-balance) equation, based on the principle of conservation of mass and Fick's laws.

$$\frac{\partial C}{\partial t}+\frac{\partial (Cu)}{\partial x}+\frac{\partial (Cv)}{\partial y}+\frac{\partial (Cw)}{\partial z}-\frac{\partial}{\partial x}\left(D_{Hx}\frac{\partial C}{\partial x}\right)-\frac{\partial}{\partial y}\left(D_{Hy}\frac{\partial C}{\partial y}\right), \\ -\frac{\partial}{\partial z}\left(D_{Hz}\frac{\partial C}{\partial z}\right)=\sum \text{Reaction}+\text{ interactions} \qquad (2.3)$$

where C [M/L^3] is the concentration of the contaminant, t [T] is time, u, v, and w [L/T] are velocities in x, y, and z [L] directions, respectively, and D_{Hx}, D_{Hy}, and D_{Hz} [L^2/T] are dispersion coefficients in x, y, and z directions, respectively. The reaction and interactions term on the right hand side of the equation represents all water column reactions such as decay, hydrolysis, and photolysis as well as the sinks and sources for contaminants that may enter and exit the aqueous phase.

Equation (2.3) above can be simplified into a one-dimensional form because rivers are much longer than they are deep or wide. Generally, river water quality models can be approximated as one-dimensional models. The solution of the one-dimensional advection dispersion equation requires the solution of Saint Venant equations for the velocity distribution in a river. As the solution of the Saint Venant equations is complicated, many modelers search for simplifications in terms of conceptual models.

$$\frac{\partial C}{\partial t}+\frac{\partial (Cu)}{\partial x}-\frac{\partial}{\partial x}\left(D_{Hx}\frac{\partial C}{\partial x}\right)=\sum \text{Reaction + interactions}. \qquad (2.4)$$

Rivers are usually faced with two major water quality issues: eutrophication (algal bloom due to nutrient enrichment) and contamination by hazardous substances. Eutrophication models follow the fate of algae (phytoplankton) and green plants and their effect on the dissolved oxygen and nutrient concentration of a river. The complexity of the model varies tremendously from the simplest Streeter-Phelps Oxygen Sag Curve to extended models such as QUAL1 (Masch and Associates 1970), QUAL2 (WaterResourcesEngineers 1973), QUAL2E (Brown and Barnwell 1987), and QUAL2K (Park and Lee 2002). The latest version of QUAL2E has been adapted in various water quality simulators, including ISIS (WallingfordSoftware 1994), DUFLOW-EUTRO (Alderink et al. 1995) and MIKE11 (DHI 1992). Some other eutrophication models such as WASP5 (Ambrose and Martin 1993) and SWAT (Neitsch et al. 2000) are also based on the principles of QUAL2E. More recently, an International Water Association (Iwasa and Aya) task group has developed a more complex eutrophication model called River Water Quality Model No. 1 (RWQM1) (Reichert et al. 2001).

In this report, the interest is not in the modeling of eutrophication but in the fate and transport of hazardous substances in a river. Contamination by hazardous substances in rivers is usually examined under the heading of contaminant fate models, which describe the fate and transport of contaminants in the environment. These models can be categorized as local-scale, regional-scale and continental-scale models. Local-scale models such as GREAT-ER (Schowanek et al. 2001) describe the fate of contaminants in

river water, and they may also include soil models such as SoilFug (DiGuardo et al. 1994) or wastewater treatment plant models such as WW-TREAT (Cowan et al. 1993). A regional-scale model that describes the fate of contaminants in user-defined regions is ChemCAN (Mackay et al. 1996a).

Although many types of contaminant fate models are available in literature, they fall into two distinctive types: those that follow a multimedia fugacity approach and those that follow a concentration based analysis. Models that follow the fugacity approach use fugacity instead of the conventional concentration for the quantification of all contaminants of concern in the system. The use of such an approach simplifies the modeler's understanding of the path of contaminant fluxes from one phase to the next (e.g., sediment to water, water to air, and so forth) and reduces the number of constants used in the model. More detailed information on fugacity and its application is provided in the next section.

Multimedia fugacity models can be categorized into four levels in the literature: Levels I, II, III, and IV (Mackay 2001). In Level I fugacity models, steady-state and equilibrium conditions are assumed between environmental compartments (air, water, soil, sediment, and biota). In Level II fugacity models, chemical transformations and advection are considered with the assumption of steady-state and equilibrium conditions. Level III models assume steady-state, but non-equilibrium conditions between environmental compartments. Level IV models consider non-equilibrium conditions between environmental compartments under unsteady-state conditions. Level IV approaches are

the most realistic. However, these models are seldom applied due to their complexity and data requirements. Thus, Level III models are the most widely used. Contaminant fate and transport models based on Level III fugacity models include the EQC model (Mackay et al. 1996a), ChemCAN ((Mackay et al. 1996b), CalTOX (McKone 1993), Fug3ONT (Maddalena et al. 1995), EUSES, and SimpleBOX. The EUSES and SimpleBOX models are used by the European Union to describe the fate of new or existing chemicals in the environment (Chuco 2004). Level III models are also widely used in the screening phase of exposure assessments (Chuco 2004).

Hazardous contaminants cause toxicity, which depends on the duration and frequency of exposure, so a dynamic model in the receiving waters of the hazardous substance is of great importance. The exposure assessment models derived in the framework of Level III models do not address the temporal and spatial variability of the contaminant.

Although Level IV models introduce the temporal variability of a contaminant's fate and transport in the environment, these models treat the environment as a single well-mixed box. The well-mixed box approach can rarely be applied to a river, as the contaminant concentration varies spatially. To account for spatial variability, Mackay and Diamond (1989) proposed another modeling approach and developed a model called the Quantitative Water Air Sediment Interaction (QWASI) model. In the QWASI model, the river is treated as a series of connected lakes or reaches, each of which is assumed to be well-mixed. The larger the number of reaches, the more accurately river behavior is simulated. In fact, this is not a new approach. The series of connected, well-mixed

sections has been applied as a simplification for the advection-dispersion model. CSTRs (Completely Stirred Tank Reactors) are the simplest systems that can be used to model a natural water body (Chapra 1997). This simple conceptual approach, also known as the moving segment model, or the cells-in-a-series model, has been successfully applied to river water quality modeling (Beck and Reda 1994; Lewis et al. 1997; Park and Lee 1996; Park and Lee 2002; Sincock and Lees 2002).

However, the practical difficulty in the application of this approach is that changes in flow volume and velocity cannot be easily included. Furthermore, although everything in nature is continuous, this approach produces a discrete model. Hence, this report propose the development of a totally dynamic continuous fate and transport model that integrates the solution of the Saint Venant equations with the solution of the advection-dispersion transport equation along with a fugacity approach.

The transport and transformation processes taking place in rivers include interactions with phases in the vicinity of the water column, i.e., sediments and air. When modeling the fate and transport of contaminants, these compartments must be incorporated into the model because most of the toxic substances adsorb onto suspended particles and sediments. In addition, atmospheric input or output can affect the mass balance of contaminants. In shallow rivers in particular, benthic activity contributes significantly to the conversion processes (Shanahan et al. 2001b). The use of fugacity in our model simplifies the modeling of different compartments in the river system.

The following paragraphs briefly present background information on the processes that determine the fate of hazardous substances in streams and rivers as well as on the mathematical equations representing these processes. These processes make up the reaction term in the advection dispersion equation. All these transport and transformation processes are presented in the schematic diagram in Figure 2.1.

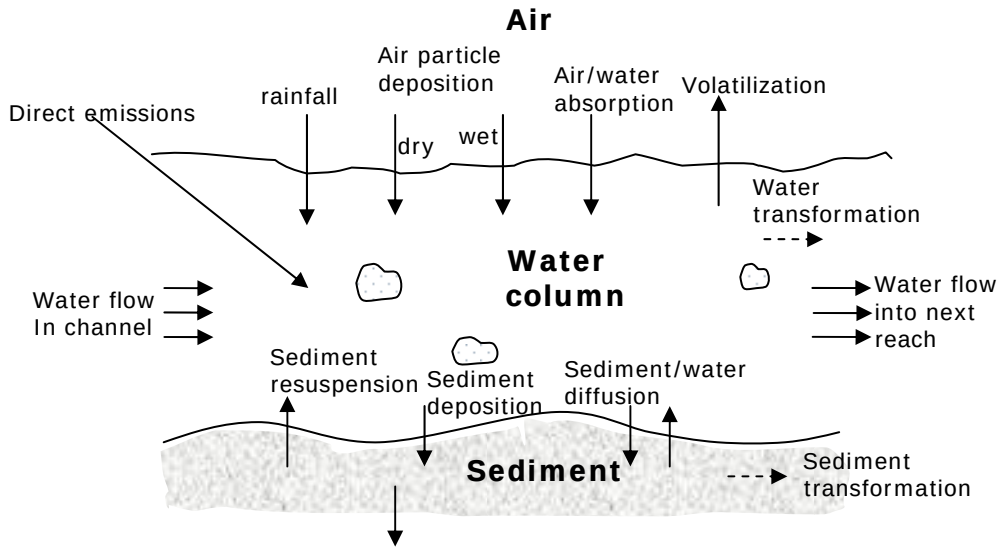

Figure 2.1. Processes in a river reach

The major processes/reactions include dry and wet particle deposition from the air, sediment deposition and resuspension, sediment burial, diffusive flux between air and water and between sediment and water, and transformations occurring in each compartment. These transformations include chemical hydrolysis, oxidation/reduction, decay, photodegradation, and sorption onto particles. Abiotic transformations (photolysis, hydrolysis, oxidation, and reduction) can be lumped together and denoted with a first-order reaction rate constant derived from the contaminant's half-life. If biotic

transformations are considered, they should be included into the model following Michealis-Menten kinetics for the growth of microorganisms and transformation of the substrate (i.e., the contaminant).

Diffusive air-water and water-sediment fluxes are represented by Whitman's two-film theory and the deposition of the particles by Stoke's formulation for the settling velocity of particles. Resuspension is denoted using shear velocity at the bottom. These interactions are further examined in the sections below.

2.2.1. Interactions between Compartments

Air and water, air and soil, water and soil and water and sediment all interact. However, sediments and soil or air and sediments do not directly interact. In this section, these interactions are explained and representations of their well-known mathematical forms are presented.

Air to water interaction involves diffusion, rain dissolution, or dry and wet deposition. Water to air interaction involves only volatilization. From air to soil, the same list of diffusion, rain dissolution, and wet and dry deposition applies. From soil to air, the only means of mass transfer occurs via diffusion. Between soil and water, diffusion and deposition from water to soil and soil runoff and water runoff from soil to water occur. Water to sediment interaction can be listed as diffusion and deposition and sediment to water interaction can be listed as diffusion and resuspension.

All of these interactions can be classified into diffusive flux processes, material transport processes, and reactive processes. Diffusive flux processes involve the transport of a chemical between two phases due to a concentration gradient and may occur in both directions while material transport involves the transport of a bulk amount of a chemical from one phase to another in strictly one direction.

2.2.2. Diffusive Flux Processes

The process in which a chemical spreads is called "diffusion." The fundamental mechanism of diffusion is the random action of molecules on a very small scale, primarily by Brownian motion (Chin 2000). The diffusion between water and a gas phase has been the most frequently investigated process, but the same principles apply to diffusion from sediment to water, soil to air or water, and even biota to water (Mackay 2001). Traditionally, mass transfer between two phases has been explained by the Whitman Two-Resistance mass transfer coefficient approach, simply known as the two-film theory. In this approach, two films of very small thickness lie on each side of the interface separating two phases forming boundary layers in each phase. The flux through each film must be equal and the concentrations at the interface in equilibrium.

$$N = \frac{(F_w - F_a)}{\frac{H}{K_w A_{water}} + \frac{RT}{K_a A_{water}}} = A_{water} \frac{(F_w - F_a)}{\frac{H}{K_w} + \frac{RT}{K_a}} = T_{D_{w,a}} (F_w - F_a), \qquad (2.5)$$

in which, K_w [L/T] is the water mass transfer coefficient, K_a [L/T] is the air mass transfer coefficient, H is Henry's law constant, R [J/mol.K] is the universal gas constant, T [K] is the temperature, and A_{water} [L^2] is the water surface area. F_w [Pa] is the fugacity in water and F_a [Pa] is the fugacity in air. All the constant terms are collected in the diffusive flux transport term, T_D.

Diffusion between the water column and sediment and that between air and water can be similarly expressed. While the mass transfer coefficients differ, the approach is the same. The resulting equation is as follows:

$$N = \frac{(F_w - F_{sed})}{\frac{H}{K_w A_{sed}} + \frac{H}{K_{sed} K_p \rho_{sed} A_{sed}}} = A_{sed} \frac{(F_w - F_{sed})}{\frac{H}{K_w} + \frac{H}{K_{sed} K_p \rho_{sed}}} = T_{D_{w,sed}} (F_w - F_{sed}), \qquad (2.6)$$

where K_{Sed} [L/t] is the mass transfer coefficient for sediments, K_p [L^3/M] is the partition coefficient between sediments and water columns, and A_{Sed} [L^2] is the area of sediments, H is Henry's law constant, F_w [Pa] is the fugacity in water and F_s [Pa] is the fugacity in sediments, and ρ_{sed} [M/L^3] is the density of the sediment particles.

The air and water side mass transfer coefficients have been measured in wind-wave tanks and in lakes as a function of wind speed. Schwarzenbach et al. (1993) have reviewed the correlation between wind speed and air and water side mass transfer coefficients. Some estimates can be calculated using the following equations:

$$K_a = 10^{-3} + 0.0462U^*(Sc_a)^{-0.67} \quad (2.7)$$

$$K_w = 10^{-6} + 0.0034U^*(Sc_w)^{-0.5} \quad (2.8)$$

$$U^* = 0.01(6.1 + 0.63U_{10})^{0.5}U_{10} \ , \quad (2.9)$$

where U^* [m/s] is the friction velocity that characterizes the drag of wind on water surface, U_{10} [m/s] is the wind velocity at a height 10 m above the ground, $Sc_{w,}$ the Schmidt number in water, is usually about 1000, and Sc_a, the Schmidt number in air, generally ranges between 0.6 and 2.5 (Mackay 2001).

2.2.3. Material Flux Processes

Material transport involves the transport of a chemical in bulk form from one phase to another phase. Deposition of particles to the bottom of a lake or river and the resuspension of particles from sediment into water column are two examples. The atmospheric depositions onto water or soil can also be listed among the material transport processes.

These processes are dependent on a velocity of the flow rate. With this information, a certain amount of a chemical is carried into another face. In the mass balance equation,

this can be shown using the product of the flow rate and the fugacity of the medium from which the chemical is carried out and the fugacity capacity of the chemical in that medium. In this section, flow rate calculations explain all the material transport processes.

Atmospheric deposition consists of wet and dry deposition from the air. Wet deposition of a compound from the atmosphere occurs when that compound is scavenged from the atmosphere by rain, snow, or fog. The efficiency of wet deposition of a compound is directly related to its water solubility and vapor pressure. For wet deposition to occur, the compound should dissolve in rain water or snow and scavenged.

Rain dissolution can be calculated by simply multiplying the rain rate (given as $m^3 \text{rain} / m^2 \text{area}.h$) with the volume fraction of aerosols (very small particles in the air that hold the contaminant) with the area of air in contact with the compartment into which rain dissolution will occur as follows:

$$\text{Rain dissolution} = A_w U_R v_Q \ , \tag{2.10}$$

where A_w [L^2] is the surface area of water (in the case of the air-water interaction), U_R [L/T] is the rain rate, and v_Q [L^3/L^3] is the volume fraction of aerosols.

Wet deposition incorporates the scavenging of the contaminant into the medium by rain or snow. The same simple approach used in rain dissolution can be used with the

incorporation of a scavenging ratio. In the case of the air-water interaction, the equation would be

$$\text{Wet Deposition} = A_w U_R Q v_Q \ , \tag{2.11}$$

where A_w [L^2] is the surface area of water, U_R [L/T] is the rain rate, Q is the scavenging ratio, and v_Q [L^3/L^3] is the volume fraction of aerosols.

Dry particle deposition of particle-bound chemicals in a water body depends on the deposition layer, particle size, and macro and micrometeorology. In the simplest case, dry depositional flux can be described by the area of the compartment into which the deposition would occur, the dry deposition rate, and the volume fraction of a contaminant in the aerosol phase:

$$\text{Dry Deposition} = A_w U_Q v_Q \ , \tag{2.12}$$

where A_w [L^2] is the surface area of water, U_D [L/T] is the dry deposition rate, and v_Q [L^3/L^3] is the volume fraction of aerosols. For the case of air-soil interactions, the same equations hold with the substitution of a soil surface area for a water surface area. Soil runoff describes the amount of contaminant transfer from soil to water via solid particles running off into the water from the soil. Average annual runoff rate of solids multiplied by the area of soil can be used for this transport mechanism. The use of $2.3x10^{-8}\ m^3/m^2h$ $(0.0002\ m/year)$ has been suggested by Mackay (2001) for the average runoff rate of solids from soil to water. The estimate is

$$\text{soil runoff} = A_s U_{\text{solids runoff}} \ , \tag{2.13}$$

where A_s [L^2] is the soil surface area, $U_{solids\ runoff}$ [L/T] is the solids runoff rate. Similar to soil runoff, water runoff, the contaminant transfer during the runoff of water from soil to water, can be estimated in a similar fashion using the average runoff rate. Mackay (2001) also suggests an average value for runoff rate of water from soil, which is $3.9x10^{-5}\ m/h$ ($0.34\ m/year$). The formula is

$$\text{water runoff} = A_s U_{\text{water runoff}} \ , \tag{2.14}$$

where A_s [L^2] is the soil surface area, $U_{solids\ runoff}$ [L/T] is the solids runoff rate.

Sediment deposition can be explained in terms of the fall velocity of particles onto which contaminant is sorbed. The velocity of a settling particle is given by the well-known equation of the fall velocity (Kiely, 1997):

$$V_{fall} = \sqrt{\frac{4(\rho_s - \rho)gd}{3\rho C_D}} \ , \tag{2.15}$$

where g [L/T^2] is the gravitational acceleration, d [L] is the effective particle diameter, and C_D is the drag coefficient.

For laminar flow, the drag coefficient is equal to 24/Re, and Re is the Reynold's number. Thus, the equation for the fall velocity becomes Stoke's Law for the velocity of a settling particle.

$$V_{fall} = \frac{gd^2}{18}\left(\frac{\rho_s - \rho}{\mu}\right), \tag{2.16}$$

where μ [L^2/T] is the kinematic viscosity of the water. Although the particle diameter is a variable, the average particle diameter can be used as the effective diameter of the particles. Hence, a constant average settling velocity can be described for the flow domain. When possible, sediment traps can be used to check the reliability of this equation.

The deposition onto the sediments is the result of the multiplication of this settling velocity and the area onto which the particles will fall.

$$\text{Deposition} = V_{fall}.A_{sed} = A_{sed}\,\frac{gd^2}{18}\left(\frac{\rho_s - \rho}{\mu}\right). \tag{2.17}$$

When the shear stress on the bottom of the water column exceeds a critical value, the resuspension of settled sediments occurs. The resuspension rate is directly proportional to excess shear stress on the surface of the sediments. Several different expressions, all complicated, have been used to describe the resuspension process. Thus, for the purpose of simplification, an average resuspension rate for the whole water body can be used to estimate the resuspension process. Mackay (2001) suggests an average value for the

resuspension of contaminants from a small lake as $1.1x10^{-8}\, m^3/m^2h$ $(0.0001\, m/year)$. Resuspension occurs over the entire area of the sediments, so the resuspension flux is estimated by multiplying the resuspension rate by the area from which the resuspension occurs:

$$\text{Resuspension} = U_{resuspension} . A_{sed} \ . \tag{2.18}$$

All the values calculated in this section can be multiplied with appropriate fugacity capacities and converted to transportation constants for each medium for a specific chemical. We can combine all of the above information and form a static steady state fugacity model and use the resulting single concentration value for each medium as the average concentration for an exposure assessment study. This model assumes that each compartment is well mixed and attains one single value for concentration and that all the parameters are defined in the model.

2.2.4. Reactive Processes

Reaction of a chemical, which can occur in any medium (i.e., water, soil, sediments, or air) usually involves the degradation of the chemical into other forms, or a decay process based on the half-life of a contaminant. For simplification, first-order decay is assumed for the non-reactive contaminants in this thesis. If we substitute the concentration with fugacity, we have the following equation to represent reaction terms in our equations:

$$Reaction = kC = kZF \tag{2.19}$$

Where k [1/T] is the first order reaction rate, Z [mol/L^3.Pa] is the fugacity capacity, and F [Pa] is the fugacity. The first-order reaction rate constant is calculated half-life of a chemical in a certain medium.

2.3. Fugacity Concept

The tendency of a chemical to escape from a medium is referred to as "fugacity." Derived from the Latin root *fugere,* meaning "to flee" or "escape," fugacity is the pressure that the chemical exerts on a medium and the chemical potential of a substance in that medium (Gobas and MacLean 2003). The chemical potential of a system is the change in the energy of the system when an additional chemical is introduced into the system while the entropy and the volume of the system remain constant. Although the chemical potential is related to the concentration through a logarithmic relationship, fugacity is linearly related to the concentration (C) of a chemical through a proportionality constant, known as the fugacity capacity. The fugacity capacity (Z) is a function of the natural chemical properties of the medium and the temperature. The Z value of a chemical is deduced using a dimensionless partition coefficient (K_{12}) between phases 1 and 2. The definition of Z starts in the air phase and then progresses to other media (Mackay and Hickie 2000b).

The relationship between concentration and fugacity at low concentrations can be represented mathematically with the proportionality constant, or the fugacity capacity, as in Equation (2.20):

$$C = ZF \,, \tag{2.20}$$

where C [M/L^3] is the concentration, F [Pa] is the fugacity, and Z [M/L^{3}Pa] is the fugacity capacity.

Fugacity, the chemical equilibrium criterion between the phases, can be used as a tool to predict the partitioning of a chemical from the aqueous phase to other phases available in the environment. Given enough time, equilibrium is reached between all phases available in the water column. The concentration in each phase can be calculated in terms of the compound's aqueous concentration using the fugacity capacity of the contaminant in that phase.

Fugacity simplifies our understanding of the equilibrium between two different phases because they reach a common fugacity while attaining different concentrations. For example, oxygen in equilibrium between air and water has a concentration of about 0.3 mol/m^3 (10 mg/L) in water and 8.0 mol/ m^3 in air (Mackay, 1979).

To understand the concept of fugacity, one can examine the analogy of heat transfer between two phases with different temperatures. Heat flows from one phase to another

until the temperature in all the phases becomes equal. The heat transfer is directly proportional to the heat capacity of a chemical. The heat capacity describes the capacity of a phase to absorb enough heat to raise the temperature of that phase 1°C. For example, an increase in the temperature of 1 g of water by 1°C requires 4.2 J of heat energy. A similar increase in the temperature of 1 g of copper requires 0.38 J of heat, and that of hydrogen 14.3 J. Fugacity capacity is based on a similar concept. A phase with a high-fugacity capacity would absorb greater amounts of a chemical but will retain lower fugacity. In contrast, phases with low fugacity capacities would absorb smaller amounts of a chemical but will retain higher fugacity. In conclusion, chemicals tend to partition into phases with higher fugacity capacities and build up large concentrations with low fugacity capacities. As an example, ***d****ichloro-****d****iphenyl-****t****richloroethane* (DDT) has a very high fugacity capacity in fish and a low fugacity capacity in water. Hence, at equilibrium conditions, DDT will reach much higher concentrations in fish although the fugacity in fish and water will be the same, as fish have a greater capacity to store DDT at low-fugacity values.

When equilibrium is not reached among the different phases, the fugacity gradient becomes the driving force for a chemical to move from one phase into another because chemicals seek equal fugacity among different phases.

In summary, fugacity is a thermodynamic quantity used as an equilibrium criterion with units of pressure. Thus, it represents the partial pressure for ideal gases. Fugacity is linearly related to concentration through a proportionality constant, or fugacity capacity.

2.3.1. Calculation of fugacity capacities

Fugacity in a gaseous phase, given as in Equation (2.21), is defined in thermodynamic textbooks (Stumm and Morgan 1996).

$$F = y\phi P_T\,, \tag{2.21}$$

where y is the mole fraction of a chemical in a gaseous phase, ϕ is the fugacity coefficient, and P_T [Pa] is the total (atmospheric) pressure. The multiplication of total pressure by the mole fraction produces the partial pressure of a chemical in the atmosphere:

$$P = yP_T\,. \tag{2.22}$$

Assuming that the ideal gas law is applicable:

$$P_T V = nRT \qquad \Rightarrow \qquad PV = ynRT\,, \tag{2.23}$$

where P [Pa] is the partial pressure, y is the mole fraction, n [moles] is the number of moles, V [L^3] is the volume, R [J/M.K] is the universal gas constant, and T [K] is the absolute temperature in Kelvin.

If both sides of Equation (2.23) are divided by the volume, the *n/V* term becomes the molar concentration (mol/m^3), and by definition, concentration is linearly related to fugacity:

$$C = \frac{n}{V} = \frac{Py}{RT} = Z_a F \,. \tag{2.24}$$

If Equation (2.21) is substituted for *F* in Equation (2.24), then the fugacity capacity for the chemicals in the gas phase becomes:

$$Z_a = \frac{1}{\phi RT}. \tag{2.25}$$

Under certain environmental conditions, the fugacity coefficient, ϕ, is usually unity, so it can be dropped from Equation (2.25). In this way, the fugacity capacity of all non-interacting chemicals in the gaseous phase becomes:

$$Z_a = \frac{1}{RT}, \tag{2.26}$$

and the fugacity of all the chemicals in the gaseous phase becomes the partial pressure of the chemical. Exceptions may occur at low temperature or high pressure, or when molecules interact in the gas phase.

In the liquid phase, fugacity can be calculated using mole fractions, activity coefficients, and a reference fugacity value based on Raoult's Law. This relation is given in Equation (2.27):

$$F_i = x_i \gamma_i F_R , \tag{2.27}$$

where F_i [Pa] is the fugacity of chemical i in the liquid phase, x_i is the mole fraction, γ_i is the activity coefficient, and F_R [Pa] is the reference fugacity.

The molar concentration of the chemical in water can be given as the moles of the chemical in the water divided by the total volume of the chemical and water. Furthermore, the volume of water is much higher than the volume of the chemical, so the relationship can be given as

$$C_i = \frac{n_i}{V_i + V_w} \simeq \frac{n_i}{V_w} , \tag{2.28}$$

in which C_i is the concentration of contaminant, n_i is the number of moles of the contaminant, V_i is the volume of the contaminant, and V_w is the volume of water.

The mole fraction is by definition the ratio of the moles of the chemical to the moles of the water plus the chemical. By similar deduction, the moles of the chemical are much lower than the moles of the water:

$$n_i = \frac{n_i}{n_i + n_w} \simeq \frac{n_i}{n_w}, \tag{2.29}$$

where n_i is the number of moles of the contaminant and n_w the number of moles of the water.

The volume of the water can be written as the molar volume by the moles of water:

$$V_w = n_w v_w, \tag{2.30}$$

where n_w is the moles of water, and v_w [L^3/mol] is the molar volume of water. Therefore, the concentration of the chemical in water becomes

$$C_i = \frac{x_i}{v_w}, \tag{2.31}$$

if Equation (2.31) is substituted for the molar fraction in Equation (8), and fugacity is equated with concentration times fugacity capacity:

$$F_i = C_i v_w \gamma_i F_R = (F_i Z_w) v_w \gamma_i F. \tag{2.32}$$

Then the fugacity capacity of a chemical in water becomes

$$Z_w = \frac{1}{v_w \gamma_i F_R}. \tag{2.33}$$

Equation (2.33) can also be expressed in terms of aqueous solubility, $C_{s,}$ [M/L^3], and vapor pressure. For liquid chemicals, solubility is given as $1/v_w\gamma_i$ and reference fugacity is the vapor pressure of the chemical. Hence, the fugacity capacity of a chemical in water becomes the ratio of its vapor pressure to aqueous solubility, which is the reciprocal of Henry's Law constant, H [Pa.L^3/M] :

$$Z_w = \frac{C_s}{P^s} = \frac{1}{H}. \tag{2.34}$$

So far, the fugacity capacities in the air and water phases have been derived. The fugacity capacity calculations in the solid phases can be similarly derived. Nevertheless, it is not typical for chemicals to have solubility values in solids, except in some plastics. In this case, instead of solubility, sorption characteristics, which explain the partitioning of a chemical into a solid matrix, are used. The same argument can be used for the intake of chemicals into the structure of living beings (partition into biota). In this case, a sorption or partition coefficient is used together with the water fugacity capacity to calculate the tendency of escaping from a solid phase:

$$Z_{solids} = \frac{K_{sw}\rho_s}{H} = K_{sw}\rho_s(Z_{water}) \tag{2.35}$$

$$Z_{biota} = \frac{K_{bw}\rho_{biota}}{H} = K_{bw}\rho_{biota}(Z_{water}), \tag{2.36}$$

where K_{sw} [L^3/M] is the solids-water partition coefficient, K_{bw} [L^3/M] is biota-water partition coefficient, ρ_s is the solids density, ρ_{biota} is the biota density, and H [Pa.L^3/M] is the Henry's Law constant.

Thus, the fugacity capacity of chemicals can be calculated using the formulae below (Kiely, 1996):

$$\begin{aligned} Z_{air} &= \frac{1}{RT} \\ Z_{water} &= \frac{1}{H} = \frac{C^s}{P_s} \\ Z_{soil} &= \frac{K_{sw}\rho_s}{H} = K_{sw}\rho_s(Z_{water}) \\ Z_{biota} &= \frac{K_{fw}\rho_f}{H} = K_{fw}\rho_f Z_{water} \end{aligned}, \tag{2.37}$$

where R [8.314 Pa.m^3/mol.K] is the universal gas constant, T [K] is temperature, C^s [M/L^3] is aqueous solubility, P_s [Pa] is vapor pressure (Pa), H [Pa.L^3/M] is the Henry's Law constant, K_{sw} [L^3/M]is solid-water partition coefficient, ρ_s [M/L^3] is the density of solids, K_{fw} [L^3/M] is the bioconcentration factor (biota-water partition coefficient), and ρ_f [M/L^3] is the density of biota.

2.4. Persistent Organic Pollutants

Researchers have been concerned about the presence of several persistent and semi-volatile chemicals that tend to bioaccumulate and produce toxic effects at low concentrations. These chemicals have been collectively referred to as "persistent organic pollutants" (POPs) (Wania and Mackay, 1999). Twelve such substances identified as POPs by the Stockholm Convention include the pesticides aldrin, dieldrin, dichloro-diphenyl-trichloroethane (DDT), endrin, chlordane, mirex, and toxaphene; the industrial chemicals hexachlorobenzene and polychlorinated biphenyls (PCBs); and the industrial by-products dioxins and furans (Eckley, 2001).

The issue of POPs in the environment has been the focus of many studies and numerical models. The scale of such models is very broad, ranging from 10^{-6} m for a single cell to a global scale of 10^{7}m. Among the many POPs models, a few examples may shed light on the diversity of existing models. Dulfer et al. (1998) studied the transport of PCBs across a cell membrane. MacLachlan (1994) simulated the transfer of polychlorinated dibenzo-p-dioxins and furans (PCDD/Fs) from grass to cow's milk. Goss (1994) studied the enrichment of organochlorine pesticides in fog droplets. Mackay (1989) quantified the sources and the sinks of PCBs in Lake Ontario, and Thomann et al. (1991) modeled the fate of PCBs in the Hudson River. Wania et al. (2000) developed a mass balance model that could be applied to any persistent organic pollutant in the Baltic Sea Region.

2.4.1. Polychlorinated biphenyls (PCBs)

PCBs are a class of chlorinated, aromatic compounds in which one to ten chlorine atoms are attached to a biphenyl ring at different positions. Possible human carcinogens and toxic to many aquatic biota, PCBs are calcitrant and can be observed almost every medium.

PCBs are a combination of two benzene rings linked at a C-1 carbon, forming a biphenyl ring. The remaining ten carbons in the ring can hold chlorine atoms, and hence the origin of the term polychlorinated. The possible combinations of the various number of chlorine atoms in the ortho, meta, and/or para position lead to 209 compounds referred to as PCB congeners. When PCBs are classified according to the number of chlorine atoms, the term "homologue" is used. PCBs of a given homologue with different chlorine substitutions are called "isomers." Each homologue contains a total of 1 to 10 chlorine atoms and 1-46 isomers (Abramowicz 1990; Wiegel and Wu 2000). Figure 2.2 shows the structure of the biphenyl ring and the possible 10 sites to which the chlorine atoms can attach.

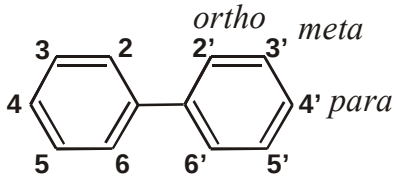

Figure 2.2. Structure of a biphenyl ring. (The numbers indicate the numbering scheme for the possible chlorine positions and nomenclature for the resulting PCB compounds.)

Generally, because PCBs have low vapor pressure and low water solubility, they are hydrophobic. Their chemical properties show stability to oxidation, flame resistance, and relative inertness (Imamoglu 2001). In addition, they are synthetic chemicals, manufactured by the catalytic chlorination of biphenyl as complex mixtures containing specific weight percentages of chlorine (Imamoglu 2001). As a result of their chemical and physical properties such as low vapor pressure, low water solubility, excellent dielectric properties, and stability to oxidation, flame resistance, and relative inertness, PCBs were widely used in industry (Abramowicz 1990; Wiegel and Wu 2000). PCB mixtures were originally used as coolants and dielectric fluids in transformers and capacitors as heat transfer fluids and coatings to reduce the flammability of wood products. Later on, they were incorporated into paints, inks, dust control agents, carbonless copy paper and pesticides (Imamoglu 2001) and extensively used as heat-transfer fluids, hydraulic fluids, solvent extenders, plasticizers, flame retardants, organic diluents, and dielectric fluids (Abramowicz 1990). However, most manufacturers of such products reduced or stopped production in the 1970s.

In 1971, the major manufacturer of PCBs, the American company Monsanto, voluntarily restricted the sales of PCBs to closed electrical systems. In 1976, however, the United States Congress banned the manufacture, processing, distribution, and use of PCBs except in totally enclosed systems such as electrical transformers, capacitors, and electromagnets. Shortly after, in 1977, Monsanto ceased production of all PCBs (Imamoglu 2001). However, between 1929 and 1977, Monsanto manufactured a majority of the approximately 5.7×10^8 kg of commercially-produced PCBs, of which

approximately 2 x 10^8 kg (35%) still remains in environmental reservoirs (Eisenreich 1987). According to (Abramowicz 1990) the approximately 1.4 billion pounds of PCBs were produced within a 50-year period.

The extensive use of PCBs between 1929 and 1978 resulted in extensive contamination of air, water, soil, and sediments (Gevao et al. 1997; Imamoglu and Christensen 2002; Wiegel and Wu 2000). Although the production and use of PCBs was banned in the late 1970s, PCB-contaminated sediments remained a significant source of pollution to water bodies and biota, long after the original source of contamination was removed (Ghosh et al. 2003), as further contamination can occur if PCB-contaminated sludge and sediments are disturbed (Wiegel and Wu 2000).

(Haque et al. 1974) was the first to report the volatilization of PCBs from sands and soils, and then (Beurskens and Stortelder 1995; McFarland and Clarke 1989; Sanders et al. 1992), and (Chiarenzelli et al. 1997) showed that PCBs released from the underlying sediments to the water column above in lakes and rivers volatilize into the atmosphere.

Although all of PCB congeners are not toxic, their toxicity is closely related to the number and configuration of the chlorine atoms. As an example, the closer the congeners approach the molecular configuration of 2,3,7,8-tetrachlorodibenzo-*p*-dioxin, the higher their potential toxicity becomes (Beurskens and Stortelder 1995; McFarland and Clarke 1989).

The discovery of the widespread environmental occurrence of PCBs, followed by increased public concern regarding the toxic and carcinogenic effects of PCBs, prompted the regulation of PCBs by the Toxic Substances Control Act of 1976, and the role of the enforcer of the regulations was the Environmental Protection Agency (EPA) (Imamoglu and Christensen 2002).

2.4.2. Atrazine

Atrazine, which has no known natural source, is the most common broad-leaf herbicide used in agricultural and other weed-control practices. Despite its wide use, atrazine is not available to the general public, as it was classified in 1990 as a "restricted use pesticide" (RUP) (ATSDR 2003). The structure of atrazine can be seen in Figure 2.3:

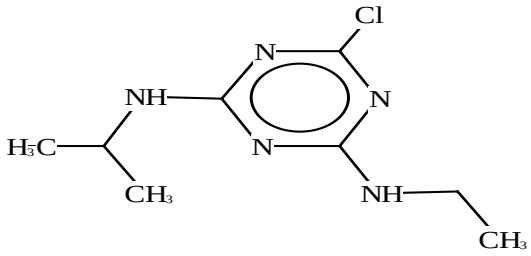

Figure 2.3. The structure of atrazine

Atrazine enters the environment principally through spraying on farm crops. Some loss or transport from the soil into the atmosphere may occur, resulting in the deposit of atrazine into the soil or bodies of water. Volatilization of atrazine has been measured up to 14% of the applied amount (ATSDR 2003). Once in the air, atrazine exists in both the particulate and vapor phases due its high vapor pressure. It may also be transported by

runoff into surface water and percolate into groundwater, where it persists in surface and groundwater while moderately absorbing into sediments. Its persistence in water enables atrazine to enter food chain (ATSDR 2003). Depending on the availability of sunlight, oxygen, and microorganisms, the half-life of atrazine in water is about six months.

2.4.3. Benzene

Benzene, a sweet-smelling organic chemical compound with the formula C_6H_6, is a colorless and highly flammable carcinogenic liquid used abundantly as an industrial solvent. Once an additive in gasoline, it is now restricted and used only as a precursor in the production of drugs, plastics, synthetic rubber, and dyes and as a natural constituent of crude oil. In this study, benzene has been selected as a representative compound of harmful and volatile chemicals.

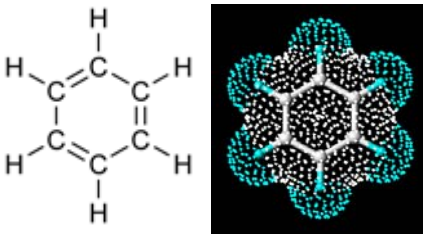

Figure 2.4. The chemical structure of benzene

Since its discovery, benzene has been a difficult compound for scientists to understand. Micheal Faraday (1791-1867), famous for his insights into electricity and magnetism, was the first to identify and determine the composition of benzene. However, he did not

understand how a chemical compound made up of six atoms of carbon and six atoms of hydrogen could remain stable. Based on the ratio of carbon to hydrogen atoms in benzene, it was considered unsaturated. However, unlike most unsaturated compounds, it did not easily react with hydrogen. Further findings led to more unanswered questions concerning the nature of benzene. Many structures were proposed, but none withstood the scrutiny of experimental evidence. It was not until 1865, when a young German by the name of Friedrich August Kekule (1829-1896), that the hexagonal structure which is known as the structure of benzene today was discovered (as shown in Figure 2.4).

After its discovery, benzene was used as an after-shave lotion because of its pleasant smell in the nineteenth and early twentieth centuries, and around the turn of the twentieth century, benzene was being used to decaffeinate coffee. In addition, before the 1920s, benzene was also used as a metal degreasing solvent. However as its toxicity became obvious, such uses were abandoned. Today, benzene is being used as a petrol additive. In the United States, as much as 1% benzene is added to gasoline. Due to its toxicity, however, benzene is used mainly as an intermediate in the manufacture of other chemicals, such as polymers, plastics, resins, and adhesives. Small amounts of benzene can be found in some types of rubbers, lubricants, dyes, detergents, drugs, explosives, napalm, and pesticides. Therefore, as a ubiquitous chemical compound, this study has denoted benzene as a representative of a harmful but widely-used compound.

2.4.4. Trichloroethylene (TCE) and daughter products

Trichloroethylene (TCE), a chlorinated solvent, was widely used for metal degreasing, but it is now a common contaminant at hazard waste sites and many federal facilities. TCE has been identified in at least 1,500 hazardous waste sites regulated under the Superfund or the Resource Conservation and Recovery Act. Besides its use in degreasing, TCE has been used as an extractant and as a chemical intermediate. Most TCE used in the United States is released into the atmosphere from vapor degreasing operations. It can enter surface waters via direct discharges and groundwater through leaching from disposal operations and Superfund sites; the maximum contaminant level for TCE in drinking water is 5 ppb. Furthermore, TCE can be released into indoor air from the use of consumer products that contain it, vapor intrusion through underground walls and floors, and volatilization from the water supply (EPA, 2004).

Under anaerobic conditions, TCE produces daughter products by releasing a chlorine atom at each step. The removal of one chlorine atom from TCE produces the first daughter product, dichloroethylene (DCE). The further removal of another chlorine atom produces vinyl chloride (VC). Then the removal of the single chlorine atom in vinyl chloride, ethane, produces a harmless hydrocarbon. Under aerobic conditions, all of these compounds undergo total mineralization. DCE contains three isomers: 1,1-DCE, cis-1,2-DCE, and trans-1,2-DCE. About 95% of all DCE compounds are cis-1,2-DCE (also referred to as cDCE), and only this isomer is considered in this study. Thus, from

this point on, when DCE is mentioned, it refers to cis-1,2-DCE. Both DCE and VC are more toxic to humans then TCE.

Hence, the selection of TCE as a target contaminant not only gives us an opportunity to examine multi-species fate and transport in aquatic environments but also allows for the modeling of three highly toxic common environmental contaminants.

2.5. Biofilms in Natural Aquatic Environments

Microorganisms are capable of growing on most solid surfaces in aquatic environments. In fact, bacteria in natural aquatic populations have a tendency to adhere to surfaces, eventually forming biofilms. The formation of biofilms on surfaces is a survival strategy for bacteria. Bacterial populations exist in a highly-protected environment within the biofilm matrix, and nutrients are abundant on the water/solid surface interface (Costerton et al. 1987). Clean surfaces that are submerged in natural water soon show evidence of a microbial colony on them. The development of microbial colonies has been observed on glass slides immersed in aquatic systems as well as on sand grains, pebbles, and detritus (Costerton et al. 1987; Marshall 1992).

When nutrients accumulate on a surface, motile microorganisms with chemo tactic responses are attracted to them, and they swim along a concentration gradient of the nutrients toward this surface. Other mechanisms by which microorganisms are attracted to and attach to surfaces in aquatic environments are physicochemical attraction forces.

Reported modes of microbial attachment onto aquatic surfaces are Brownian motion, electrostatic attraction, van der Waals forces, and hydrophobic interactions (Marshall 1992).

Following some form of attraction, microorganisms establish contact with the surface. Most microorganisms adhere to a surface by means of extracellular polymers that anchor the organisms permanently to the surface. Some of these extracellular materials include pili, flagella, acidic polysaccharides, and specific extracellular proteins (Costerton et al. 1987; Marshall 1992).

Experiments show that the initial colonization of surfaces is a selective process. First, small rods (<0.8 μm long) adhere within an hour of immersion of a surface, followed by adhesion of coccoidal, spiral, and larger rod forms within six to eight hours. Stalked or budding microorganisms appear after 24 hours, and diatoms and protozoa appear around the same time. Eventually biofilms, which are the extensive growth of microorganisms on aquatic surfaces exposed to flowing water systems, develop. The nature of the developed mature films differs depending on the conditions in the aquatic ecosystem. As the thickness of the film increases, some of the microorganisms in the film matrix become nonviable as the nutrient diffusion becomes limited (Marshall 1992).

As many different organisms pile up on the aquatic surface, the biofilm becomes a micro-cosmos with a variety of diverse species. An increase in interspecific and intraspecific interactions results in the formation of mixed cultures (Costerton et al. 1987; Marshall

1992; Rauch et al. 1999; Tartakovsky et al. 2005). An illustration of biofilm formation is given in Figure 2.5.1 below. Another illustration shows the steps of biofilm formation in Figure 2.5.2.

Biofilm buildup depends on the nutrient load and biofilm-forming microorganisms. Activity in the biofilm increases as the biofilm thickness increases to a certain level above, the activity of which is not affected by the biofilm thickness. Diffusion of nutrients into the biofilm from the bulk water occurs over the active depth (Khlebnikov et al. 1998). Similarly, oxygen can only penetrate up to a certain depth in the film, and the amount of oxygen diffusion into the inner portions of the biofilms affects the metabolic efficiency of microorganisms in the film (Marshall 1992).

Gerhardt and Schink (2005) state that the variable oxygen profile formed due to the limits of the oxygen penetration depth provide bacteria with new chances and challenges. These challenges help the formation of mixed cultures with aerobic and anaerobic transformations.

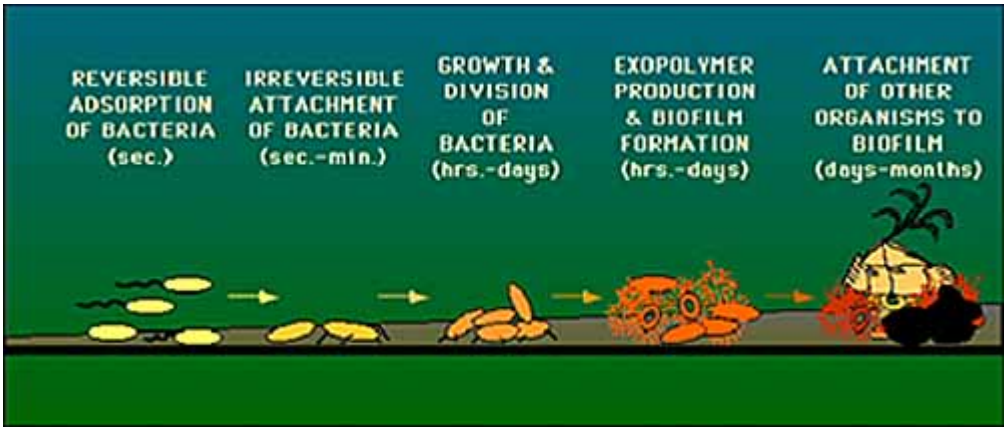

Figure 2.5.1. Biofilm formation (source: http://www.biofilmsonline.com/cgi-bin/biofilmsonline/ed_how_primer.html

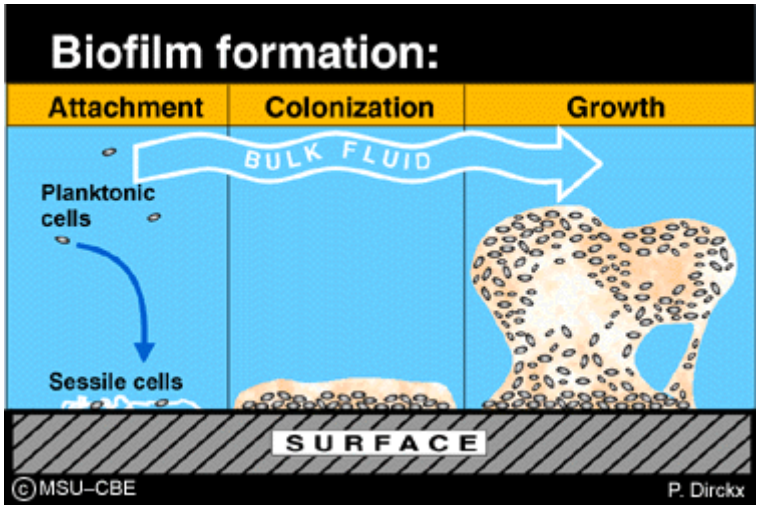

Figure 2.5.2. Steps in biofilm formation (source: http://www.erc.montana.edu/CBEssentials-SW/bf-basics-99/bbasics-01.htm

Oxygen is very rapidly consumed in most natural water systems due to the high rate of mineralization. Thus, the oxygen penetration depth is generally less than 10 mm and results in the formation of anoxic environments in sediments. In aerobic sediments,

heterotrophic bacteria can completely mineralize organic matter into carbon dioxide. In anaerobic sediments, organic matter is decomposed in more complex and less energy efficient pathways that require colonies of physiologically different microorganisms. Each of the microbial groups participates in the decomposition process, forming an end product used by other groups of microbes until decomposition is complete (Holmer and Storkholm 2001; Tank and Dodds 2003).

The aerobic and anaerobic zones occur due to limitations of oxygen penetration into the biofilm, as depicted in Figure 2.5.3 below:

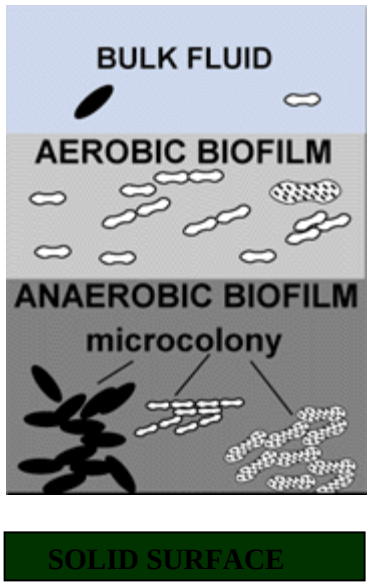

Figure 2.5.3. Portions of aerobic and anaerobic microorganisms in biofilms. (Source: http://www.erc.montana.edu/CBEssentials-SW/bf-basics-99/bbasics-01.htm)

After several experiments, (Hibiya et al. 2004) developed some empirical equations that related oxygen penetration depth with biomass concentration and the effective oxygen diffusion coefficient with oxygen penetration depth as follows:

$$X = 2.5x10^{4} + 1.5x10^{5} \exp\left(-\frac{\delta}{175}\right), \tag{2.38}$$

where X [M/L^3] is the biomass concentration and δ [L] is the biofilm thickness. This empirical equation is used to estimate the effective oxygen diffusion coefficient as

$$D_e = (3.5^{-19} + 1.5^{-21}\delta)^{0.5}, \tag{2.39}$$

where D_e [L^{2}T^{-1}] is the effective oxygen diffusion coefficient.

Higashino and Stefan (2005) developed a model that estimates the diffusion of oxygen from the water column to sediments and "sediment oxygen demand," which is the oxygen in the sediment that the microbial colony requires to continue their activities. Their model is suitable for laminar flow, which causes the formation of a laminar diffusive boundary layer on top of the sediment/water interface. The illustration for their model is given in Figure 2.5.4. below:

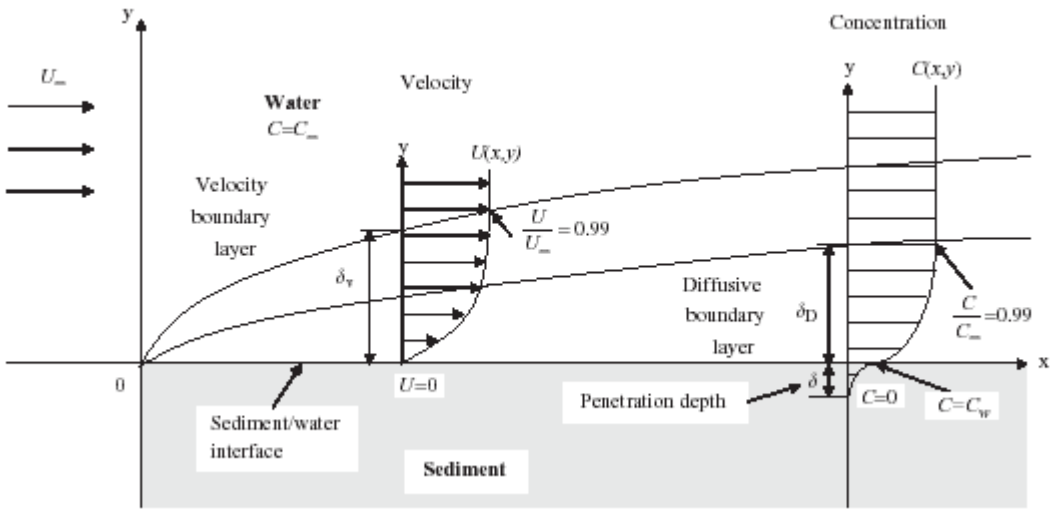

Figure 2.5.4. The velocity and dissolved oxygen profiles for a reactive sediment/water interface (Source: (Higashino and Stefan 2005))

They have concluded that the free-stream velocity has very little effect on the oxygen penetration depth and that the oxygen penetration depth depends very strongly on the maximum biomass concentration. Hence, the oxygen penetration depth can be calculated independent of the stream velocity and can be assumed constant over the entire length of a river, given the biomass concentration is also assumed to be constant.

2.6. Data Requirements

For the developed model to work properly, data used in the simulations is very important. Since the developed model will be dynamic and continuous, and will be based on spatial variability of parameters over the entire river domain, the input data are expected to be compatible and satisfy the needs of each model component. Therefore, the data required

for all processes which are included in the model needs to be available at the earlier stages while the model formulation is done.

The major data requirement in the one-dimensional channel flow model is the characterization of the channel that involves the analysis of channel topographic features (i.e., reach lengths, bottom elevations above a datum and slopes) and channel conveyance characteristics (i.e., tables relating water surface elevation to channel top width and roughness coefficients). Another crucial data requirement for a channel flow model is the time dependent boundary condition data that drives the model. Access to stage and discharge hydrographs or stage-discharge rating curves is extremely important for accurate simulations of channel flow processes. Finally, reasonably accurate initial condition data is also important for successful start up of a model. Without such data, the numerical model could easily create stability problems which would eventually invalidate the simulation.

The major data requirement for the contaminant transport portion of the data includes the phsico-chemical properties of the contaminants. These can be found from reference handbooks. The fugacity capacities are calculated using the guidelines given in the chapter previously. Biofilm data can also be found from reference handbooks and previous studies.

Using the background information given in this chapter, a dynamic and continous fugacity-based contaminant transport model has been developed. The details will be

explained in the coming chapters of this thesis. The proposed model not only suitable for the analysis of single species contaminants, but with the inclusion of a biofilm compartment, the proposed model can also be used in the analysis of multispecies contaminant fate and transport in rivers.

CHAPTER 3

PROBABILISTIC FUGACITY ANALYSIS OF LAKE PONTCHARTRAIN POLLUTION AFTER HURRICANE KATRINA

This chapter is an application of fugacity-based water quality models as assessment tools following a natural disaster and accidental or deliberate contaminant spillage in a surface water body. After Hurricane Katrina hit the Gulf of Mexico in August 2005, the floodwaters covering New Orleans were pumped into Lake Pontchartrain as part of a process to rehabilitate the city. However, this environmentally critical decision will have long-term consequences. In this chapter, we examine how Lake Pontchartrain will respond to the load of contaminants in the flood waters by modeling several hypothetical scenarios. As a preliminary outcome, this study provides a tool that will effectively assess the extent of damage inflicted on the natural water resources of Southern Louisiana and similar environments elsewhere. This study will examine the effects of contaminants on surface water bodies with different physicochemical characteristics using an unsteady state fugacity model. This model yields continuous fugacity values in water, air, and sediment phases that can easily be transformed into concentrations. Due to

a limited amount of available data on the event. In this study we also demonstrate the use and performance of an uncertainty analysis to address the variability issues of the parameters used in the model using a Monte Carlo analysis.

The results of the study indicate that Lake Pontchartrain, which was recovering from earlier assaults on its water quality, will continue on a path to recovery for a long while. This study will analyze three representative contaminants likely to have been found in the waters discharged into Lake Ponchartrain. The recovery time, in which the levels of the three contaminants dropped below maximum contaminant levels (MCL) values, range from approximately a year to sixty-eight years. The model developed in this study can be used to create scenarios of similar emergency situations and predict their environmental consequences, and thus, as a useful decision-making tool, can be used to assist policymakers and city officials.

3.1. Introduction

As a result of Hurricane Katrina, the city of New Orleans was flooded and large sections of the city declared uninhabitable. The first and immediate attempt to make the city habitable again was to drain the flood waters and assess the structural and environmental damage to the city. Even though draining the flood waters into Lake Pontchartrain seemed to be an effective solution at the time, the long-term effects of the resulting pollution were not examined thoroughly, as the water being drained into the lake contained various potentially hazardous contaminants. Since industrial complexes as well

as chemical warehouses were flooded, it is likely that hazardous chemicals escaped into the floodwaters. The news media reported incidents in which fish literally jumped out of water at or nearby discharge points. At the time, it was assumed that dilution and other natural processes in the lake could effectively cleanse the water of these contaminants. However, this was not the case. Thus, in this chapter, the effects of these natural processes on the persistence of hypothetical loads of three potentially harmful constituents in the flood waters are examined. The objective of this chapter is to provide preliminary answers to the long-term effects of environmental decisions made at the time of the crisis.

In the analysis of the response of the lake to a wide range of pollutants, this thesis will discuss three chemicals, each with different physicochemical properties. Since gasoline leakage resulted from the flooding of New Orleans, benzene, as it is a constituent of gasoline and found in abundant quantities in the flood waters, is the first, representing a volatile compound. Since warehouses that stored agricultural products were also inundated by flood waters, atrazine, which is water soluble and the most common agricultural herbicide, is the second. As they are abundant in nature and thus, PCBs represent the third chemical in this study. Although banned in the 1970s, PCBs remain highly toxic and abundant in nature, so this study has selected them to represent the group of hydrophobic contaminants. All three chemicals are potentially harmful to human health and biota in lakes.

All chemicals behave differently in nature; they partition into different pathways when introduced into a surface water system such as a lake. Some of the contaminants volatilize, some of them adsorb into solid materials, and some of them remain in the aqueous phase. In any attempt to determine the fate of these chemicals in surface water environments, the existence of sediments, suspended particles, and an air phase must also be considered. Thus, this thesis considers the existence of different phases in the vicinity of a water column through the application of fugacity analysis. The use of fugacity instead of concentration can provide a clearer understanding of the direction of chemical flow in an aquatic system. Furthermore, a fugacity analysis can establish a chemical equilibrium between phases and predict partitioning among the various compartments. Since fugacity is continuous between phases while concentration is discontinuous, one can more easily follow a chemical as it passes from one phase to another with the fugacity approach (Mackay 2001; Stumm and Morgan 1996).

Site-specific information on pollutant levels in flood waters gathered immediately after Hurricane Katrina is not available. The extensive data collection necessary for the evaluation of the consequences of pumping flood waters into Lake Pontchartrain was not conducted due to the requirements of immediate emergency response decisions at the time. This study provides an alternative approach to conducting such an analysis. Nevertheless, lack of data would introduce significant uncertainties to the outcome. Thus, to evaluate the uncertainty effects, Monte Carlo analysis is applied. Thus, instead of using single deterministic values, probability distributions for mass transfer coefficients, decay rate coefficients, and most importantly, the source rate, are used. Consequently, the

recovery time of the lake becomes a probability density outcome instead of a single value outcome. Hence, a better understanding of the expected pollution levels and recovery time of the lake can be achieved. For the uncertainty analysis, this study has selected a subset of all the uncertain parameters and performed a sensitivity analysis of all the parameters.

3.2. Model Development

A lake system consists of different phases which dynamically interact with each other. These interactions play an important role in the persistence of chemicals in each phase. Air, water, and sediment phases make up the three compartments of a lake system. The water phase, occurring in the middle of the other two phases, is in contact with both the air and sediment compartments. Three unsteady state mass balance equations among these compartments establish the basis of the model.

All three compartments are assumed to be well mixed. The interactions between the air and water compartments involve wet and dry deposition from air to water and diffusive flux at the air and water interface. The interactions between the sediment and water phases may involve diffusive flux at the water-sediment boundary, deposition of water particles onto sediments, and resuspension of particles from sediments. In addition, water outflows from the lake via tributaries and chemicals are removed through wind-induced air flow just above the lake. The sediments are assumed to be immobile.

Moreover, in each phase, chemicals follow first-order decay reactions that cause the system to remove the compound.

Instead of concentration, fugacity is used in the development of mass balance equations, as it provides an easier representation of mass flow among phases (Mackay 2001; Stumm and Morgan 1996). Fugacity, *F*, and concentration, *C*, are linearly related through a proportionality constant, *Z* as

$$C = ZF \tag{3.1}$$

Each phase contains particles. Air consists of gas and aerosols, which are the small particulate matter in the air. Aerosols provide a solid surface that can adsorb a chemical. Likewise, a water column includes suspended particles that form the solid phase available for adsorption. Similarly, only a portion of bottom sediments comprises solid material, as sediments form a porous medium in which pores fill up with water. Thus, each phase has its bulk fugacity capacity representing its physicochemical characteristics. Bulk fugacity capacities can be calculated using volume fractions. The fraction of aerosols in the air is stated in the literature as 30 $\mu g/m^3$, which corresponds to a value of 2×10^{-11} as the volume fraction. The fraction of suspended solids in water is stated in the literature as 5 mg/L, which corresponds to 2.08×10^{-7} as the volume fraction. The literature considers sediments 15% solid materials by volume (Mackay and Diamond 1989). Hence, the bulk fugacities in each phase can be calculated as

$$Z_{bw} = Z_p n_w + Z_w (1 - n_w), \tag{3.2}$$

where Z_{bw} [M/L^3.Pa] is the bulk water fugacity capacity, Z_p [M/L^3.Pa] is the water particle fugacity capacity, and Z_w [mol/m^3.Pa] is the pure water fugacity capacity. n_w is volume fraction of particles in the water.

$$Z_{ba} = Z_{aerosol} n_a + Z_a (1 - n_a), \tag{3.3}$$

where Z_{ba} [M/L^3.Pa] is the bulk air fugacity capacity, $Z_{aerosol}$ [M/L^3.Pa] is the aerosol fugacity capacity, and Z_a [M/L^3.Pa] is the pure air fugacity capacity. n_a is the volume fraction of aerosols in air.

$$Z_{bs} = Z_s n_s + Z_w (1 - n_s) \tag{3.4}$$

where Z_{bs} [M/L^3.Pa] is the bulk sediment fugacity capacity, $Z_{sediment}$ [M/L^3.Pa] is he sediment fugacity capacity, and Z_w [M/L^3.Pa] is the water fugacity capacity. n_s is the volume fraction of solid particles in a sediment.

The fugacity capacity of suspended sediments (water particles) is assumed to be the same as that of sediments because they share similar physical characteristics (i.e., the same density and particle-water partition coefficient).

Given the above information, the time rate of change in the fugacity of each compartment relates to the fugacity in all the compartments. The following set of three equations depicts the mass balance of a lake system in terms of fugacities:

$$V_w Z_{bw} \frac{dF_W}{dt} = S + (K_{aw} A_w Z_w + Q_{dry} Z_{aerosol} + Q_{wet} Z_{aerosol}) F_A + (Q_{res} Z_s + K_{sw} A_s Z_w) F_S - (k_w V_w Z_w + Q_{dep} Z_p + Q_{out} Z_{bw} + K_{aw} A_w Z_w) F_W \quad (3.5)$$

$$V_a Z_{aw} \frac{dF_A}{dt} = (K_{aw} A_w Z_w) F_W - (Q_{dry} Z_{aerosol} + k_a V_a Z_a + Q_{wet} Z_{aerosol} + Q_{air} Z_{ba} + K_{aw} A_w Z_w) F_A \quad (3.6)$$

$$V_s Z_{bs} \frac{dF_S}{dt} = (Q_{dep} Z_p + K_{sw} A_s Z_w) F_W - (k_s V_s Z_s + Q_{res} Z_s + K_{sw} A_s Z_w + Q_{bury} Z_s) F_S \quad (3.7)$$

in which F_W [Pa] is the fugacity of the water compartment, F_A [Pa] is the fugacity of the air compartment, and F_S [Pa] is the fugacity of the sediment compartment. S [M/T] is the source rate of contaminants in the water phase. V_w [L^3], V_a [L^3], and V_s [L^3] represent the volumes of water, air, and sediment compartments, respectively. Similarly, A_w [L^2] and A_s [L^2] represent the surface areas of water and sediment. Q_{dry} [L^3/T] is the dry deposition rate from air, Q_{wet} [L^3/T] is the rate of wet deposition from the air, Q_{res} [L^3/T] is the resuspension rate of sediments, Q_{dep} [L^3/T] is the deposition rate of suspended particles in the water column, Q_{air} [L^3/T] is the wind induced air flow rate on the lake, Q_{out} [L^3/T] is the rate of water flowing out of the lake, and Q_{bury} [L^3/T] is the burial rate of the bottom sediments. The fugacity capacity of water is Z_w [M/L^3.Pa], that of air is Z_a [M/L^3.Pa], that of sediments is Z_s [M/L^3.Pa], that of water particles (suspended solids) is Z_p [M/L^3.Pa], that of aerosols (particulate matter in the air) is $Z_{aerosol}$ [M/L^3.Pa], that of bulk water is Z_{bw} [M/L^3.Pa], that of bulk air is Z_{ba} [M/L^3.Pa], and that of bulk sediment is

Z_{bs} [M/L^3.Pa]. Whereas K_{aw} [L/T] is the mass transfer coefficient between the air and the water compartments, K_{sw} [L/T] is that between the sediment and the water compartments. k_w [1/T], k_a [1/T], and k_s [1/T] are the first-order decay rate constants in the water, the air, and the sediment compartments, respectively. The processes that this thesis considers are depicted in Figure 3.1.

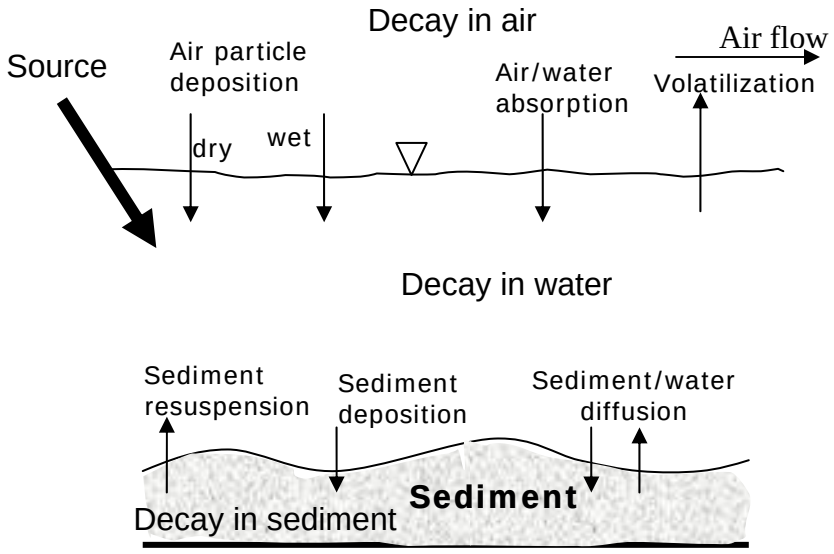

Figure 3.1. A schematic view of the natural processes considered in the fugacity model

The three equations (Equations 3.5 through 3.7) with three unknowns can be solved simultaneously through numerical integration using finite difference approximations. Forward difference approximation is used for time derivatives, and time averaged values are used for the fugacity values of each component on the right-hand side of Equations (3.5), (3.6) and (3.7), as shown below:

$$\left.\begin{aligned} \frac{dF_i}{dt} &= \frac{F_i^{k+1} - F_i^k}{\Delta t} \\ F_i &= \frac{F_i^{k+1} + F_i^k}{2} \end{aligned}\right\} \quad ; \quad i = A, W, S \tag{3.8}$$

Applying this process to governing equations and then collecting all the known values, the final three equations with three unknowns can be written in the following form:

$$\begin{aligned} A_1 F_W^{k+1} + A_2 F_A^{k+1} + A_3 F_S^{k+1} &= B_1 \\ A_4 F_W^{k+1} + A_5 F_A^{k+1} &= B_2 \\ A_6 F_W^{k+1} + A_7 F_S^{k+1} &= B_3 \end{aligned} \tag{3.9}$$

These equations can be written in matrix format as below:

$$\begin{bmatrix} A_1 & A_2 & A_3 \\ A_4 & A_5 & 0 \\ A_6 & 0 & A_7 \end{bmatrix} \begin{bmatrix} F_W \\ F_A \\ F_S \end{bmatrix}^{k+1} = \begin{bmatrix} B_1 \\ B_2 \\ B_3 \end{bmatrix}^k \tag{3.10}$$

Since all the terms on the right-hand side of the above equations are known, the right-hand side terms are simplified and represented as a vector. The ***A*** matrix on the left-hand side can be inverted, or Equation (3.10) can be solved by any matrix solver. An LU decomposition scheme is selected to solve Equation (3.10). The source rate is also introduced into the equations above as a time-dependent initial loading. The source is calculated as the mass of the contaminant per time, which is calculated as a volume ratio of flood waters for the duration of pumping.

The constants in Equation (3.10) represent either the physicochemical properties of the chemicals or the characteristics of the lake. The following section explains information used to calculate these values. The physicochemical properties of the selected chemicals are obtained from reference handbooks (Howard 1989; Mackay et al. 1992) and summarized in Table 3.1.

Table 3.1. Physicochemical Data on Selected Chemicals

Parameter	**C_6H_6 - Benzene**	**$C_8H_{14}ClN_5$ - Atrazine**	**Total PCBs**
Molecular Weight (g/mol)	78.11	215.75	326
Log K_{ow}	2.13	2.75	6.66
Henry's Law Constant (atm-m^3/mole)	5.55×10^{-3}	2.88×10^{-4}	2.9×10^{-5}
Z_{water} (mol/m^3·Pa)	1.78×10^{-3}	3480	0.0818
Z_{air} (mol/m^3·Pa)	4.04×10^{-4}	4.04×10^{-4}	4.04×10^{-4}
$Z_{sediment}$(mol/m^3·Pa)	1.41×10^{-2}	77000	11500
$Z_{bulk\ water}$ (mol/m^3·Pa)	1.8×10^{-3}	3480	0.0951
$Z_{bulk\ air}$ (mol/m^3·Pa)	4.04×10^{-4}	1.62×10^{-3}	4.58×10^{-4}
$Z_{bulk\ sediment}$ (mol/m^3·Pa)	2.96×10^{-3}	14500	1730
Half-life in water (hours)	1700	17000	139000
Half-life in air (hours)	170	5	693
Half-life in sediment (hours)	17000	1700	347000

The amount of flood water pumped into Lake Pontchartrain, information that is used to calculate the loading into the lake, is about 10% of the lake volume, and the draining of the flood waters took about one week. This percentage of the lake volume in one week corresponds to a pumping rate of 3.5×10^6 m^3/h. From this pumping rate, a source rate term is estimated and becomes the key input to the model. Since no measurements were taken prior to the pumping of floodwaters into Lake Pontchartrain, any number of scenarios can be investigated regarding the potential contaminant load in the floodwaters. To reflect the uncertainty in the source rate, a uniform distribution is assigned to the

source rate term. A source rate of 0.01% (by volume) of the inflow floodwaters is used as the lower limit, and a source rate of 1% (by volume) of the floodwaters is used as the upper limit of the distribution. Any source rate between these values is given an equal probability of occurrence. In another scenario, a fixed contaminant loading rate that corresponds to the average of the uniform distribution is used (a contaminant is 0.1% of the total floodwaters is used). This scenario represents the worst case. With this estimation method, the source rate term for benzene becomes 3.84×10^7 mol/h, that for atrazine 1.88×10^7 mol/h, and that for PCB 1.47×10^7 mol/h.

The time of recovery from the contaminant load is calculated as the time it takes to reach concentrations allowable by the EPA according to the 2004 Edition of the Drinking Water Standards and Health Advisories (EPA 2004). The standards, or the regulated values for the aforementioned chemicals, are 0.005 mg/L for benzene, 0.003 mg/L for atrazine, and 0.0005 mg/L for total PCBs.

Also required for the solution of the developed model are transport and transformation parameters such as deposition, resuspension, water outflow, and the wind-induced air flow rate. The water outflow value is the total water output via the tributaries from the system. According to the United States Geological Service (USGS), this value is 1,565,000 m^3/h. Rates from another fugacity-based lake model serve as guidelines for calculating the deposition and resuspension rates in Lake Pontchartrain (Mackay 2001), which, along with the surface area of the lake, were calculated to be 816m^3/h and 1000 m^3/h, respectively.

For the air flow calculations, the USGS (2002) used the annual average wind velocity. An average of 19,900 m/h wind moving in a predominant SE-NW direction is expected above Lake Pontchartrain. In this study, the volumetric air flow rate, from the cross-sectional area of the air compartment in the SW-NE direction and the thickness of the air compartment of 50 cm as the mixing zone, is calculated to be 3.2×10^7 m^3/h. This study mainly focuses on the response time of Lake Pontchartrain to different contaminants that may be present in the floodwaters after Hurricane Katrina. One of the loss mechanisms is volatilization. However, some of the volatilized chemicals can re-enter the system via atmospheric deposition mechanisms. To incorporate this process into the model, this study uses only a small air compartment as a mixing zone or a boundary layer zone with a small thickness to track the contaminant immediately above the lake.

For air-water and sediment-water mass transfer rates, required in the calculation of diffusion between phases, this study uses the two-film theory (Valsaraj 2000):

$$\frac{1}{K_{aw}} = \frac{1}{k_L} + \frac{1}{k_G H}, \tag{3.11}$$

where K_{aw} [L/T] is air-water mass transfer coefficient, k_L [L/T] is the liquid side mass transfer coefficient, k_G [L/T] is the gas side mass transfer coefficient, and H is Henry's law constant. Sediment-water mass transfer coefficients are taken from Reible (Reible 1998), and liquid and gas side mass transfer coefficients from Valsaraj (Valsaraj 2000).

The resulting air-water and sediment-water mass transfer coefficients for benzene, atrazine, and PCBs are presented in Table 3.2:

Table 3.2. Mass Transfer Coefficients

Compound	**Overall Air-Water Mass Transfer Coefficient (m/h)**	**Sediment-water Mass Transfer Coefficient (m/h)**
Benzene	0.00958	0.0006
Atrazine	0.00001	0.0013
PCBs	0.0034	0.0004

Further analysis of the site-specific case of Lake Pontchartrain requires information representing the physical characteristics of Lake Pontchartrain. Forming the northern boundary of the city of New Orleans, Lake Pontchartrain is also bounded by the cities of Mandeville and Madisonville on the north and Slidell on the northeast. It is roughly oval in shape and spans 40 miles (64.4 km) wide from east to west and about 24 miles (38.6 km) from north to south (USGS 2002). This information, as used in the solution of the mass balance model described above, is provided in Table 3.3:

Table 3.3. Physical data on Lake Pontchartrain

Surface Area	1632000000 m^2 (630 mi^2)
Average Depth	3.65 m (12 ft)
Total water outflow	1565000 m^3/h (15350 cfs)
Wind speed on lake	10.75 knots (19910 m/h)
Total air outflow	3.2 x 10^8 m^3/h
Depth of air on lake	0.5 m
Volume of air	816000000 m^3
Depth of sediment	0.05 m
Volume of sediment	81600000 m^3
Density of sediment	2400 kg/m^3

The removal mechanisms from the water column of the lake are first-order decay, transfer into sediments, flow out via tributaries, and transfer into an air compartment, as seen in Equation (3.5). The percentage of each removal mechanism for the three contaminants has been calculated and listed in Table 3.4:

Table 3.4. Removal Percentages of Contaminants from Aqueous Phase

Compound	Decay	Deposition	Outflow	Volatilization
PCBs	0.1 %	73 %	6.7 %	20.2 %
Benzene	20.5 %	0.03 %	7.3 %	72.2 %
Atrazine	13 %	0.45 %	85.8 %	0.9 %

According to Table 3.4, the three contaminants behave very differently. The use of the fugacity approach enables us to follow the removal mechanisms of each contaminant from one compartment to another in the model. The results of the analysis for these three contaminants help to explain and clarify the expected behavior of other potential contaminants in the floodwaters. Thus, if a contaminant were as volatile as benzene, we would expect it to be removed from the lake rapidly; and if a contaminant were hydrophobic, we would expect it to main longer the system.

Table 3.4 shows that the main removal mechanism for benzene is volatilization. A higher value air-water mass transfer coefficient of benzene also enables the transfer of benzene into an air compartment. Once passed into an air compartment, benzene is rapidly removed from the system by wind-induced air flow. Only a negligible percentage of benzene transfers into the sediments. The second most significant removal mechanism for benzene is decay.

As given in Table 3.4, the main removal mechanism for PCBs is deposition onto the sediments, which is expected, as PCBs are the most hydrophobic chemicals among the three contaminants. About three-quarters of the PCBs introduced into the lake system are transferred into the sediment compartment. When a chemical enters the sediments, it remains in the system longer. The loss mechanisms from the sediments are buried and released back into the water column. Hence, PCBs remain in the system longer than other chemicals. This is the main reason why PCBs are still observed in aquatic systems as long as three decades after being legally banned. Sediments then become the source of PCBs by slowly releasing them back into the water column.

Outflow in the tributaries followed by first-order decay in a water column is the main removal mechanism for atrazine, which does not attach onto solid surfaces, nor does it significantly volatilize. Remaining mostly in the aqueous phase, it is removed from the system in its dissolved form. In fact, atrazine has the highest water solubility among the three contaminants selected in this study.

Table 3.4 shows us that our three representative chemicals are indeed representative of very different behaviors in nature. Examining the removal mechanisms of potential contaminants might be a very effective decision tool in any emergency situation, be it a natural disaster or an accidental spill.

3.3. Sensitivity Analysis

After all the constants in Equation (3.10) are calculated, a sensitivity analysis is performed for the model. A sensitivity analysis of the values representing the transport and transformation processes in the lake enable the observation of the parameters with the strongest effect on the self-cleaning capacity of Lake Pontchartrain. Results of the sensitivity analysis show that the most sensitive parameters are the source rate, mass transfer coefficients, and decay rate constants. Decay rate constants directly affect the persistence of a chemical in the lake system. The faster the decay in a specific phase is, the faster the chemical is removed from the system. Mass transfer coefficients are also very important in the recovery time of the system. The faster the chemical attaches to the sediments, the longer it remains in the system. On the other hand, the faster it passes to the air phase, the faster it is removed from the system due to wind-induced advection. However, since the exact amount of a chemical in any flood waters is unknown, it is important that this study consider a probability distribution instead of single, assumed values for the loading of chemicals. The results of sensitivity analysis of the source rate, presented in Table 3.5, show the effect of the source rate on the recovery time of Lake Pontchartrain.

Table 3.5. Sensitivity Analysis Results for Source Rate

	Contaminant Ratio in Floodwaters by volume		
Contaminant	**0.01 %**	**0.1 %**	**1%**
Benzene	0.72 years	0.82 years	0.87 years
Atrazine	1.05 years	1.27 years	1.50 years
PCB	25.49 years	44.09 years	62.7 years

3.4. Monte Carlo Analysis

Mass balance fugacity models, which determine the fate of chemicals, have been increasingly recognized as useful tools for facilitating the management of chemicals released into the environment. However, as models are only an approximation of the actual fate of chemicals, it is crucial that the uncertainties associated with the model be clearly outlined and communicated. The current technique of choice for quantifying uncertainty in environmental models is Monte Carlo analysis. General and unconstrained by the type of model used, Monte Carlo analysis can be applied in numerous fields (MacLeod et al. 2002). With this analysis, the most sensitive parameters recognized during the sensitivity analysis are entered into the fugacity model as random values sampled from a probability distribution.

In the literature, mass transfer coefficients and decay rate constants have been given lognormal distributions (Citra 2004; MacLeod et al. 2002). The choice of a lognormal distribution for many fate and transport model parameters is advantageous, as the lognormal distribution has a positive state space. In addition, it has two parameters, a standard deviation, and a mean, the latter two relating to a corresponding normal distribution.

The pumping rate of flood waters into Lake Pontchartrain is estimated to be 3.5×10^6 m^3/h. An estimate of the source rate term assumes that 0.01% of the floodwaters (by volume) contains a contaminant. A uniform distribution is assigned to the source rate

term. The source rate of 0.01% by volume of the floodwaters is used as the lower limit and that of 1% is used as the upper limit of the distribution. Any source rate between these values has an equal probability of occurrence.

A total of 10,000 trials are performed for Monte Carlo runs and 10,000 random variables created for the overall air-water mass transfer coefficient, the water-sediment mass transfer coefficient, the water decay rate constant, the air decay rate constant, the sediment decay rate constant, and the source rate. The Box-Muller algorithm is used (Gentle 2003; Ronen 1988) to generate random values from a lognormal distribution. The values found in chemical handbooks for these parameters are used as mean values for mass transfer coefficients and decay rate constants (given in Table 3.6). All the coefficients and constants are assigned a standard deviation of 0.5, which renders a confidence factor of about 2.7 (MacLeod et al. 2002), implying that about 95% of all random values lie between $1/2.7$ and 2.7 times the median. The inverse of the cumulative density function of a uniform distribution is used to generate random variables for the source rate. The model (Equation 3.10) is run 10,000 times, each of which chooses a random value for the uncertain parameters used.

Table 3.6. Mean and Standard Deviation Values Used to Generate Random Values for Decay Rate Constants and Mass Transfer Coefficients.

Parameter/Chemical	Benzene		Atrazine		PCBs	
	Mean	**S.D[a]**	**Mean**	**S.D**	**Mean**	**S.D**
Water decay rate constant	0.00077 h^{-1}	0.5	0.00126 h^{-1}	0.5	0.000005 h^{-1}	0.5
Air decay rate constant	0.003316 h^{-1}	0.5	0.386 h^{-1}	0.5	0.0001 h^{-1}	0.5
Sediment decay rate constant	0.0000856 h^{-1}	0.5	0.000199 h^{-1}	0.5	0.000002 h^{-1}	0.5
Overall Air-water mass transfer coefficient	0.00958 m/h	0.5	0.00001 m/h	0.5	0.0034 m/h	0.5
Sediment-water mass transfer coefficient	0.0006 m/h	0.5	0.0013 m/h	0.5	0.0004 m/h	0.5

[a] SD : Standard Deviation

3.5. Results of the Monte Carlo Analysis

Prior to the Monte Carlo Analysis, each contaminant is modeled using fixed values for all the parameters. The mean values for mass transfer coefficients and decay rate constants are used. The source rate is calculated assuming that 0.1% of the floodwaters (by volume) contain the contaminant. Floodwaters are pumped for the duration of one week into the lake. The response of the lake to the introduction of contaminants can be seen in Figure 3.2

During the pumping period, the concentration of each contaminant reaches very high concentrations in the lake. After the pumping stops, depending on the physico-chemical properties, the concentration of contaminants decreases in the aqueous phase. The other compartments follow similar behaviors, so they are not shown.

During the week of pumping, PCB concentration reaches a maximum of about 9 mg/L, which is seven magnitudes larger than the MCL values, which would explain the scene in which the fish were jumping out of the lake in the aftermath of Hurricane Katrina. Similarly, atrazine and benzene also reach a very high concentration, shown in Figure 3.2.

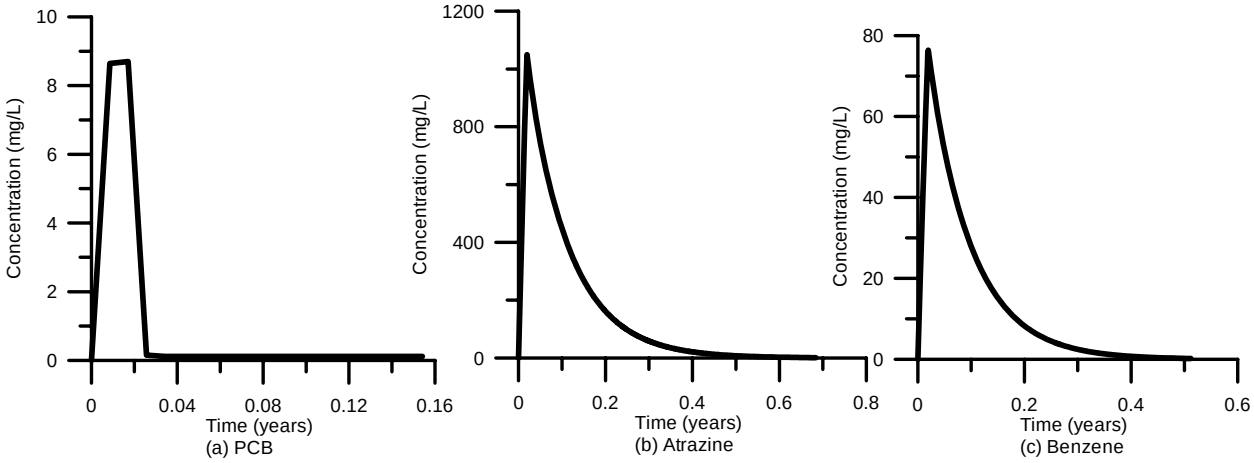

Figure 3.2. Concentration profiles of contaminants in Lake Pontchartrain

While solving the model, two cases have been examined. In the first case, the source rate remains constant at 0.1% by volume of the floodwaters while all the decay rate constants and mass transfer coefficients are sampled from lognormal distributions and randomly used in the model. In the second case, in addition to the mass transfer coefficients and the decay rate constants being sampled from a lognormal distribution, the source rate is also sampled randomly from a uniform distribution.

For each group of randomly-selected model parameters (i.e., mass transfer coefficients, the decay rate coefficients, and the source rates), the time to reach MCL values are recorded. This value reflects the duration of time required for Lake Pontchartrain to recover from the contaminant load by natural processes. In other words, this value is the self-cleansing time of the lake.

The resulting set of 10,000 time values is represented in three plots. The first plot is the frequency of occurrence of a time value. Then cumulative and complementary cumulative probability plots are shown. The complementary cumulative probability plot can be very useful in interpreting the results, as it ascertains the probability of exceeding a certain amount of time to recover from a contaminant load.

Figure 3.3 shows the results of the Monte Carlo simulation for atrazine for the first case, in which the source rate is fixed at 0.1% by volume. Figure 3.4 shows the results for atrazine for the second case, where the source rate is also randomly sampled as well as the mass transfer and decay rate coefficients. Figures 3.5 and 3.6 present the results of cases 1 and 2, respectively, for benzene, while Figures 3.7 and 3.8 present those for total PCBs, respectively.

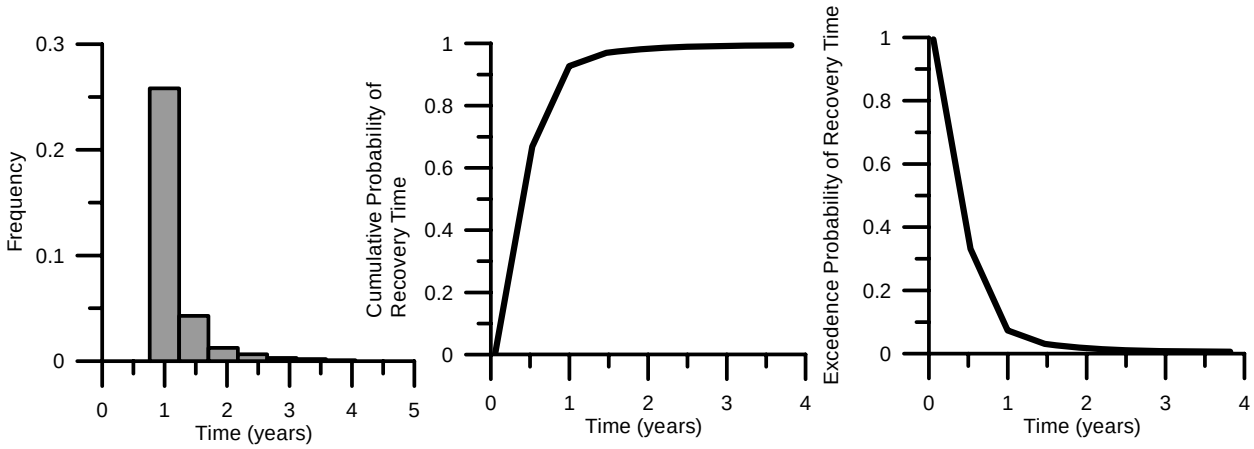

Figure 3.3. Results of the analysis of the recovery of Lake Pontchartrain from atrazine load with the source rate fixed at 0.1%

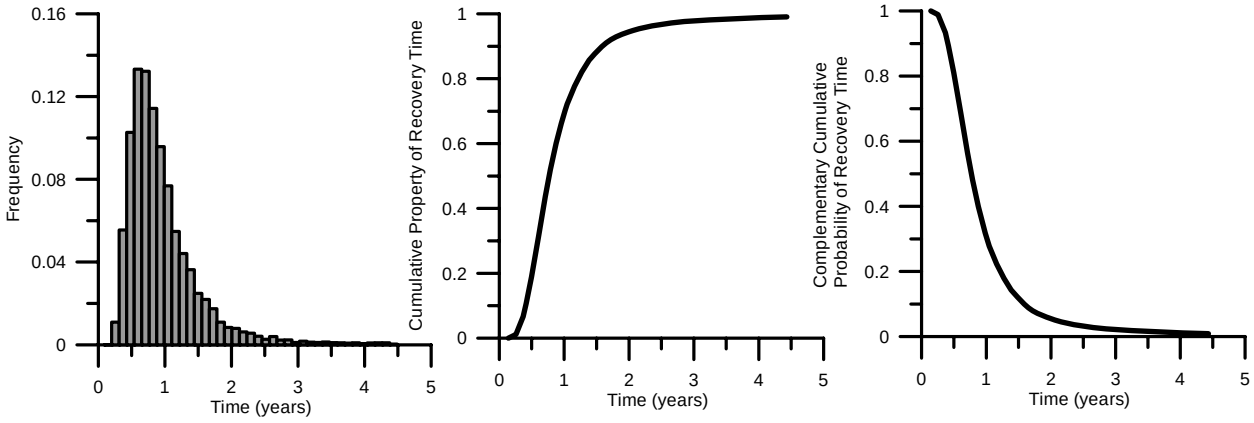

Figure 3.4. Results of the analysis of the recovery of Lake Pontchartrain from atrazine load with an uncertain source rate.

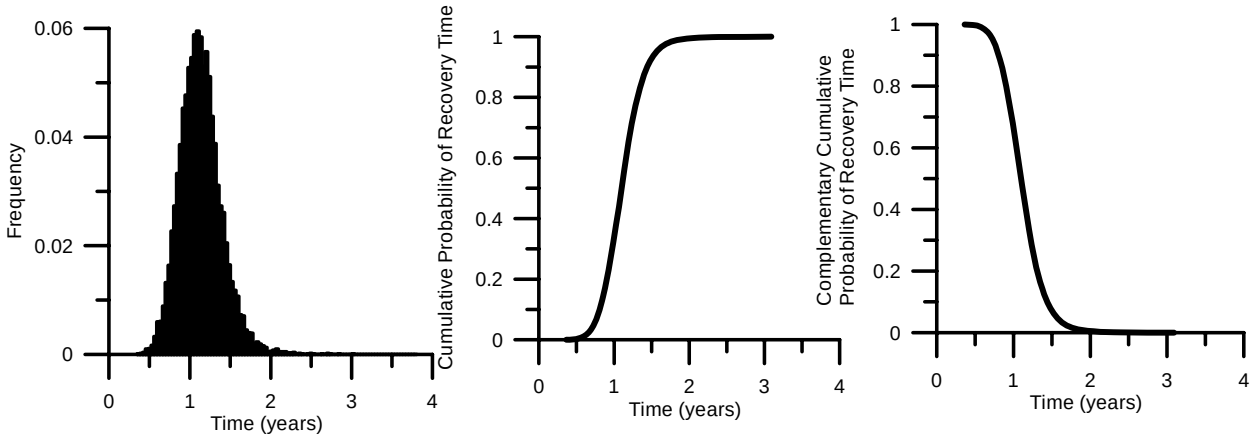

Figure 3.5. Results of the analysis of the recovery of Lake Pontchartrain from benzene load with a source rate fixed at 0.1%

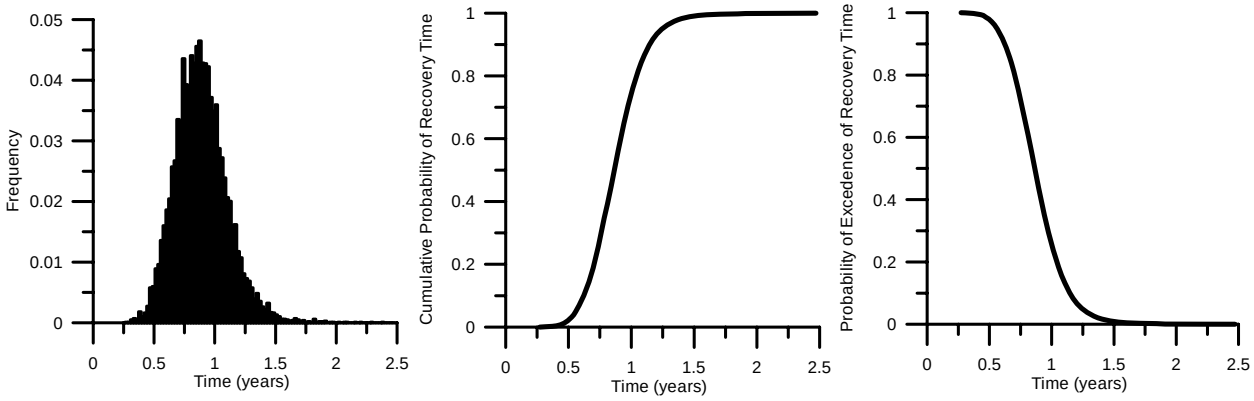

Figure 3.6. Results of the analysis of the recovery of Lake Pontchartrain from benzene load with an uncertain source rate

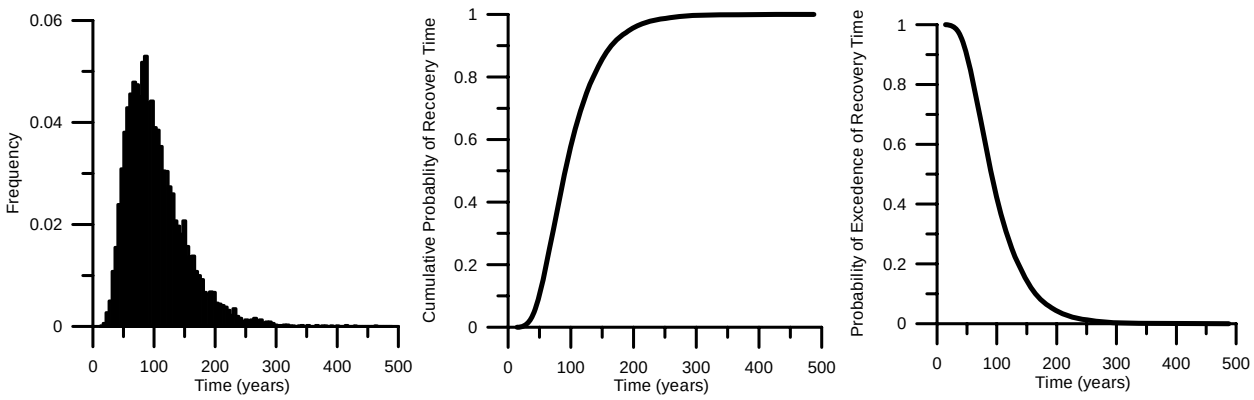

Figure 3.7. Results of the analysis of the recovery of Lake Pontchartrain from PCB load with the source rate fixed at 0.1%

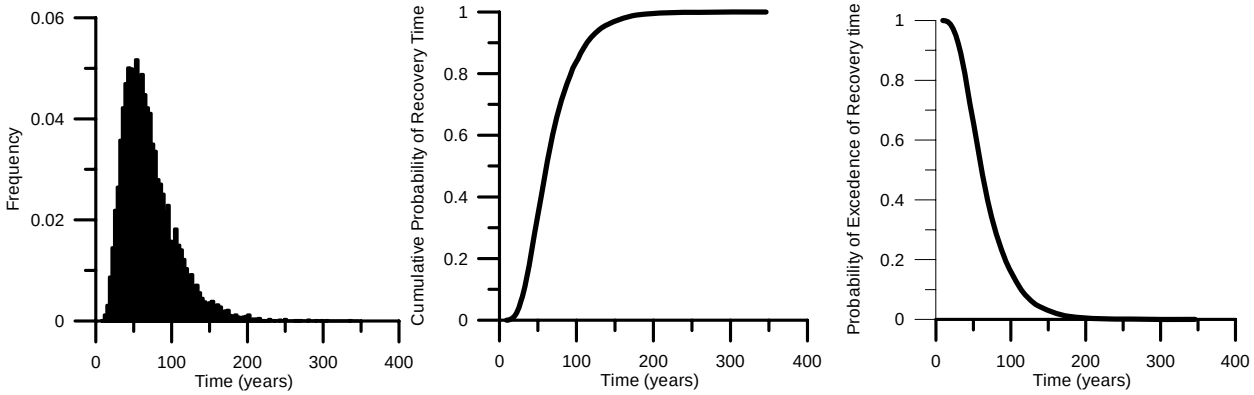

Figure 3.8. Results of the analysis of the recovery of Lake Pontchartrain from PCB load with an uncertain source rate

3.6. Discussion of Results and Conclusion

In the first case, in which the source rate is fixed at 0.1% (by volume), atrazine has a mean recovery time of 1.32 years. The recovery time changes between a half a year to three years. As seen in the complementary cumulative probability plot in Figure 3, Lake

Pontchartrain has a 0.1 probability of cleaning itself in more than a year from the atrazine load calculated in this model.

Since atrazine is the most soluble chemical in water among the three representative contaminants selected in this study, decay within the relatively larger volume of water compartment and outflow with the tributaries enables the more rapid removal of this chemical.

In the second case, in which the source rate is also randomly selected, atrazine has an average recovery time of 0.9 years. In the application of the second case, the source value can take the lower or the higher values with equal probability. The probability of exceeding one year for self-cleansing has a higher value of 0.3 for this case. The cumulative probability plot shows that atrazine will reach MCL values within three years (see Figure 3.4).

In the first case, Figure 3.5 shows that the average time to recover from benzene load is 1.12 years. The same figure also shows that, despite a 50% probability of exceeding one year recovery time, benzene concentrations will reach MCL values within two years. When the source rate is also randomly sampled, the average time of recovery is 0.8 years for benzene as shown in Figure 3.6. The probability that benzene concentrations will still be higher than MCL values after the first year is 0.25. As benzene is the most volatile of the three contaminants, it can be rapidly removed from the Lake Pontchartrain system.

Lake Pontchartrain would recover from a benzene loading of the magnitude calculated in this study within at most two years.

PCBs, the most hydrophobic, are expected to stay the longest in the system. Figures 3.7 and 3.8 show that PCBs are indeed very persistent in nature. In the first case with the fixed source rate, Lake Pontchartrain requires about a century to clean itself from PCB contamination. The recovery time ranges from 15 to 400 years. Figure 3.7 shows that the probability is 0.4 for a recovery time longer than a century. The probability of exceeding the allowable values after 200 years is 0.03. In the second case, the average time of recovery drops to 65 years. However, the probability of recovery in more than 100 years, with a value of 0.2, is still high.

This chapter presented an unsteady state fugacity model to examine the effects of contaminant loads with various physicochemical characteristics. The model provides the fugacities in the water, air, and sediment phases as a function of time, which can be converted to concentrations. This study further includes a Monte Carlo analysis, which serves as a method of determining uncertainties in the parameters used for the solution of the model.

The model developed in this study provides a tool that can be used to explain the behavior of Lake Pontchartrain after Hurricane Katrina. The model can also be used to study the effect of any contaminant load on any shallow lake system. As expected, the more hydrophobic a contaminant is, the longer it will remain in the system, while the

more volatile it is, the shorter time it will remain. The amount of contaminant load introduced into the system is a crucial parameter that determines the time of recovery. Therefore, to evaluate the uncertain terms, Monte Carlo Simulation is an effective tool.

The model developed in this study offers a very simple yet effective procedure to assess the environmental response of surface water systems. Thus, in simulated or real emergency response scenarios in the environment, the model represents a powerful design tool. As it can be generalized, the model can be used for any chemical compound, so decision makers who are forced to find solutions within a short time will find it useful during emergencies such as that which followed Hurricane Katrina.

The time requirements for computation are not long, with single runs taking only a few minutes. Monte Carlo analysis requires more computation time, the longest simulation taking no more than three days. The computations were performed on IBM PC compatible computational platforms. Such an analysis, in turn, could be very effective for decision making and preventing decisions that may lead to long-term pollution of surface water resources. If policymakers had been aware of the results of this study when Hurricane Katrina took place, they would have had alternative solutions at their disposal. For example, they may have applied a primary treatment to flood waters, prior to discharging them into Lake Pontchartrain, using large-scale portable treatment devices that would have significantly reduced the level of pollution rather than leaving the clean-up to natural attenuation alone.

CHAPTER 4

RIVER HYDRODYNAMICS

Rivers and streams are natural open channels with a free surface as a streamline along which the pressure is constant and equal to atmospheric pressure (Sturm 2001). The existence of a free surface means that the flow boundaries are no longer fixed by the channel geometry but adjust themselves to accommodate the flow conditions. Another aspect of open channel flow is the wide variability of the cross-sectional shape and roughness of the channel. Due to the free surface, gravity, instead of pressure, is the driving force, as in closed conduits (Sturm 2001).

The flow of water in natural channels is almost always unsteady (Mahmood and Yevjevich 1975). The unsteady nature of open channel flow causes the complexity of its analysis. The procedure one follows to predict the temporal and spatial variations of a flood wave as it traverses a river reach or reservoir is known as flood routing (Baltas 1988).

Advanced mathematical treatment of unsteady flow in open channels began with the development of two partial differential equations published in the Transactions of the

French Academy of Sciences, Volume 73, July-December 1871, presented by Barre de Saint-Venant. The English title of this document was "Theory of unsteady water flow, with application to river floods and to the propagation of tides in river channels." The second part of this document, titled "Theory and general equations of unsteady flow in open channels," contained two partial differential equations currently known as the Saint-Venant partial differential equations of unsteady flow. These two equations have remained unchanged in their general form since they were first published, during which time many scientists and researchers attempted to modify or improve them. Although these attempts result in more complete and sophisticated versions of the equations, they reduce to the basic Saint-Venant equations upon simplification for practical use (Mahmood and Yevjevich 1975).

Saint-Venant, an engineer as well as a mathematician-physicist, realized that the properties of fluid phenomena, as discovered by observations in nature as well as obtained by experiments, should be the guiding factors in postulating basic hydraulic equations. The fundamental assumptions in the development of Saint-Venant equations can be listed as: (i) hydrostatic pressure distribution along the depth of the flow; (ii) friction losses in the unsteady flow are similar to those in steady flow (so that the Manning or Chezy equations can still be used to calculate the mean shear boundary stress (Sturm, 2001); (iii) velocity distribution does not affect wave propagation; (iv) the flow can be represented in one dimension with negligible transverse velocity and average boundary shear stress applicable to the whole cross-section; and, (v) the bed slope is

small enough so that the sinus of the slope angle can be replaced by the tangent of the angle (Mahmood and Yevjevich 1975; Sturm 2001).

4.1. Derivation of the Saint Venant Equations

The equations required for solving the velocity and depth distribution in any open channel are the conservation of momentum and mass equations, which make up the Saint-Venant equations. These equations can be derived using Reynold's transport theorem for the given cross-section of a river channel in Figure 4.1.

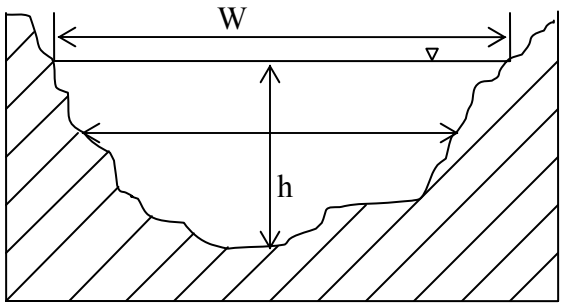

Figure 4.1 Cross-sectional view of a river channel.

The cross-sectional area of the channel as well as the top width of the channel changes with respect to the change in the water depth of the channel. The control volume of the system can be shown as in Figure 4.2.

Total mass and momentum have to be conserved within this control volume. (Streeter and Wylie 1979) present the general form of the conservation law for an arbitrary control volume, shown in Figure 4.2 as

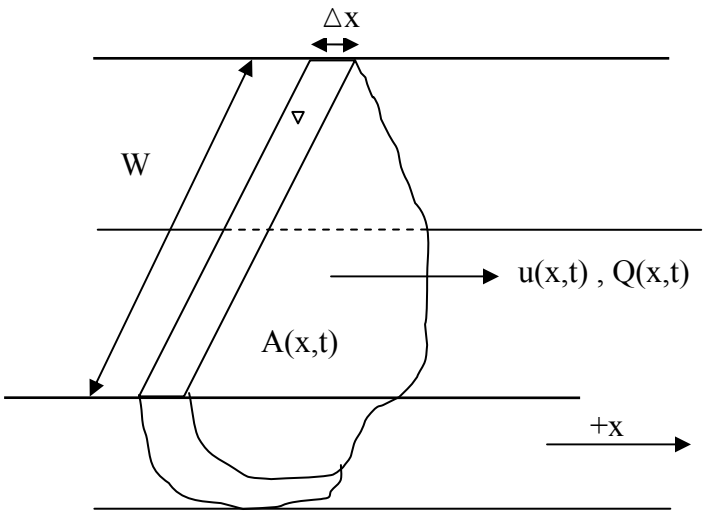

Figure 4.2 Control volume of a river cross-section

$$\frac{dB}{dt} = \iiint_{cv} \frac{\partial b}{\partial t} dV + \iint_{cs} b(\bar{u}\hat{n}) dA \tag{4.1}$$

where B is the system property, b is the intensive value of B per unit mass m, t [T] is time, V [L^3] is the volume of control volume (cv), $\bar{u}$ [L/T] is the velocity vector, $\hat{n}$ is the unit outward normal vector in the flow direction, and A [L^2] is the area of control surface (cs). By introducing different variables for B, one can derive the conservation of mass, momentum, and energy equations using Equation (4.1).

For mass conservation, *B* becomes mass [M] and b becomes the density (ρ) [M/L^3]. As mass cannot be created or destroyed, as stated by the first law of thermodynamics, the rate of change of mass term becomes zero, and the conservation of the mass equation is given as

$$0 = \iiint_{cv} \frac{\partial \rho}{\partial t} dV + \iint_{cs} (\rho \bar{u}.\hat{n}) dA \,. \tag{4.2}$$

For the momentum conservation, the storage term, becomes the total forces acting on the control volume, and the b value becomes the product of the velocity vector and the density as in

$$\overline{F} = \iiint_{cv} \frac{\partial \bar{u} \rho}{\partial t} dV + \iint_{cs} (\rho \bar{u}.\hat{n}) dA \,. \tag{4.3}$$

For incompressible fluids such as water, density does not change with time and through some algebra, Equation (4.2) can be written as Equation (4.4) below:

$$\frac{\partial A}{\partial t} + \frac{\partial Q}{\partial x} = 0 \,. \tag{4.4}$$

At any cross-section, the time rate of the change of the flow area due to the rise and fall of the free surface must be balanced by a spatial gradient of volume flux Q [L^3/T] in the flow direction. Equation (4.4) represents this situation (Sturm 2001).

The momentum equation equates the net force acting on the control volume with the time rate of change of the momentum in the control volume in addition to the rate of efflux of the momentum through the control volume. The resulting equation is given in Equation (4.5):

$$\begin{aligned} &\frac{\partial(Q\Delta x)\rho}{\partial t}+\rho\left\{\left[u(Au)\right]+\frac{\partial}{\partial x}\left[u(Au)\frac{\Delta x}{2}\right]\right\} \\ &-\rho\left\{\left[u(Au)\right]-\frac{\partial}{\partial x}\left[u(Au)\frac{\Delta x}{2}\right]\right\}=\overline{F} \end{aligned}, \tag{4.5}$$

where Q [L^3/T] is the flow rate, Δx [L] is the length of the river reach, ρ [M/L^3] is the water density, u [L/T] is the velocity, A [L^2] is the cross-sectional area, and $\overline{F}$ [L/T^2] is the total force acting on the control volume in the flow direction.

Force vector $\overline{F}$ can be expanded into three subcategories: gravity, shear, and pressure forces.

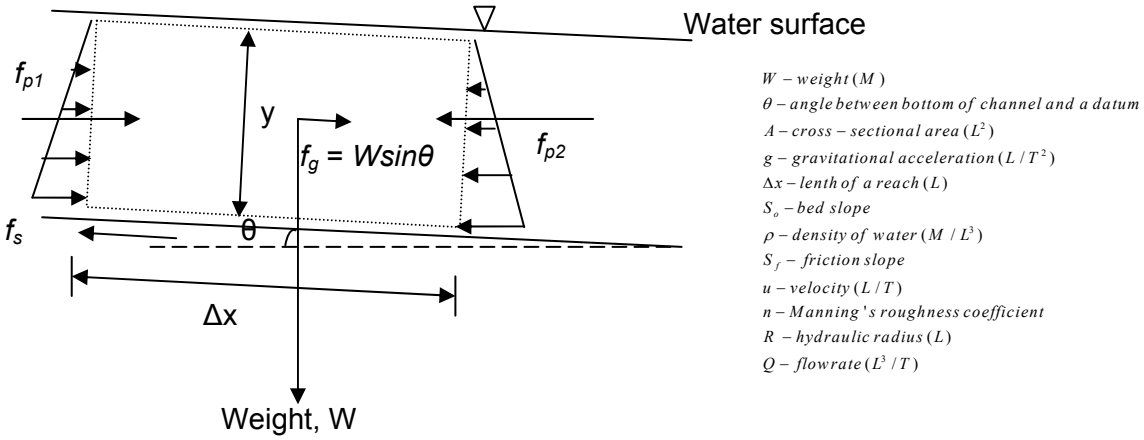

Figure 4.3 Forces acting on the control volume

The forces acting on the control volume are shown in Figure 4.3. Pressure forces act on either side of the control volume. Assuming hydrostatic pressure distribution, the net pressure force would be the difference between these two forces. The resulting difference is caused by the change in surface water elevations at each side of the control volume.

The gravitational force in the x-direction can be calculated using the component of the weight of the water in the x-direction. When angle θ is small enough, the sine and tangent of the angle become identical, and the tangent of the angle is the bed slope (i.e., $\rho g A \Delta x \sin\theta$, in which $\sin\theta$ is the bed slope S_0). Therefore, the gravitational force can be given as

$$f_g = W \sin\theta = \rho A g \Delta x \sin\theta \simeq \rho A g \Delta x S_o , \tag{4.6}$$

where W [ML/T^2] is the weight force, ρ [M/L^3] is the density, A [L^2] is the area, g [L/T^2] is gravitational acceleration, and Δx [L] is the length of the control volume.

Shear force f_S represents the depletion of momentum due to the action of friction on the sides and bottom of the channel. The shear force is mathematically analogous to the gravitational force, so it can be represented very similar to the gravitational force, the only difference between the two force equations is the slope term. In the shear force term, friction slope is used instead of the bed slope used in the gravitational force term:

$$f_S = \rho g A \Delta x S_f , \tag{4.7}$$

where S_f [L/L] is the friction slope, which can take any one of several forms, one of which uses Manning's equation:

$$S_f = \frac{u^2 n^2}{(c.R^{2/3})^2}, \tag{4.8}$$

where u [L/T] is the velocity of water, n is Manning's roughness coefficient, c is a unit system dependent constant (it is 1.0 in the SI unit system, and 1.486 in the British unit system), and R [L] is the hydraulic radius, given as the area divided by the wetted perimeter. When this definition of friction slope is introduced into the shear force in Equation (4.7), the shear force becomes

$$f_S = \rho g A \Delta x \frac{u^2 n^2}{(c.R^{2/3})^2} = \rho g A \Delta x \frac{n^2 |Q| Q}{c^2 . A^2 R^{4/3}} \tag{4.9}$$

Pressure force f_p, the total pressure force acting on the face of the control volume, is directly related to the change in the water depth along the channel:

$$f_p = -\rho g A \frac{\partial h}{\partial x} \Delta x . \tag{4.10}$$

The final form of the conservation of momentum equation becomes

$$\frac{\partial Q}{\partial t} + \frac{\partial}{\partial x}(Qu) + gA\frac{\partial h}{\partial x} = gA(S_0 - S_f), \tag{4.11}$$

where Q [L^3/T] is the flow rate, u [L/T] is the velocity, t [T] is the time, A [L^2] is the area, x [L] is the distance along the river, h [L] is the water surface elevation, g [L/T^2] is gravitational acceleration, S_0 is the bed slope, and S_f is the friction slope.

The continuity and the conservation of momentum equations together form the system of equations representing unsteady flow in channels known as the Saint-Venant equations. They are coupled, non-linear, first-order partial differential equations of the hyperbolic type. Their solution requires one initial and two boundary conditions. These equations have no analytical solution except in a few special cases.

The set of full, non-simplified forms of the original and the modified Saint-Venant equations are known as the dynamic wave model. The first term in Equation (8) is local acceleration, the second term is convective acceleration, the third term is the effect of gravity on the water surface slope, and the last term is frictional resistance.

4.2. Modifications to the Saint Venant Equations

The Saint-Venant equations form the basis of the general mathematical model of the unsteady non-uniform flow in channels; however, they need to be modified for application to natural systems such as rivers, as natural channels are significantly different from man-made channels in terms of channel geometry, channel bed roughness and river form. As a result, several researchers, including Fread (1976) and DeLong (1986 and 1989), have modified the Saint-Venant equations so that they can be applied in

natural channels. They have included the effects of complex channel geometry by adding flood-plains and a meandering pattern in the equations. Once modifications are applied, the Saint-Venant equations can more easily account for the effects of the flood plain, inactive (off-channel or dead) storage, and the meandering ratio (sinuosity factor) of the river (Gunduz and Aral 2004). Below, these modifications and changes in the form of the conservation and momentum equations are described as follows:

i. *Lateral flow.*

The first modification is the addition of lateral flow. In a natural river system, water can enter the system as surface runoff, referred to as *lateral overflow*. Some water in the system can also be lost to groundwater as seepage flow. Such flows affect both the conservation and momentum equations. Additional loss from the system, reflected in the conservation equation in the following form, may also occur:

$$\frac{\partial A}{\partial t} + \frac{\partial Q}{\partial x} = q_L \ , \tag{4.12}$$

where q_L , the lateral flow, can take two different forms:

$$q_L = q_{L_1} + q_{L_2} \, , \tag{4.13}$$

where q_{L1} is lateral overflow and q_{L2} is seepage outflow. As movement is involved in overland inflow and seepage outflow, the momentum equation also requires modification as follows:

$$\frac{\partial Q}{\partial t}+\frac{\partial (Qu)}{\partial x}=-gA\frac{\partial h}{\partial x}+gA(S_o-S_f)+M_L, \tag{4.14}$$

where the momentum effect of the overland flow and seepage flow can be separated again:

$$M_L = M_{L_1} + M_{L_2} \tag{4.15}$$

and each of the terms can be described in terms of flow and area as follows:

$$M_{L1}=\begin{cases} 0 & \text{for seepage inflow} \\ -\dfrac{Qq_{L1}}{2A} & \text{for seepage outflow} \end{cases} \tag{4.16}$$

$$M_{L2}=\begin{cases} -\beta \upsilon_x q_{L2} & \text{for overland inflow} \\ -\dfrac{Qq_{L2}}{A} & \text{for overland outflow} \end{cases} \tag{4.17}$$

where q_{L1} is the lateral seepage flow per channel length (positive for inflow and negative for outflow), q_{L2} is the lateral overland flow per channel length (positive for inflow and negative for outflow), β is the momentum coefficient for velocity distribution, g is gravitational acceleration, h_r is the water surface elevation in the river (i.e., stage), M_{L1} is the momentum flux due to lateral seepage inflow/outflow, and M_{L2} is the momentum flux due to lateral overland inflow/outflow.

ii. *Dead storage.*

In natural rivers, the geometry of the channel is not smooth, as it is in man-made channels. In general, portions of the river, typically near the banks of rivers, contain still water pools called dead storage, as they are not moving. These areas, shown in Figure 4.4, can be represented in Equation (4.18):

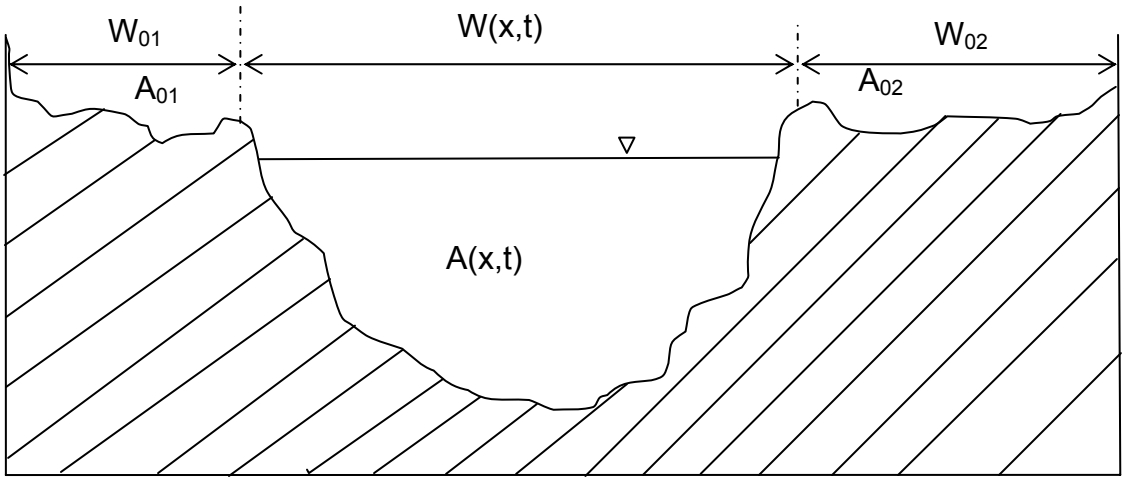

Figure 4.4 Dead storage in natural rivers

$$\frac{\partial(A+A_o)}{\partial t}+\frac{\partial Q}{\partial x}-q_L=0\,. \tag{4.18}$$

Since dead storage zones involve no movement only the mass conservation equation, not the momentum equation, is affected.

iii. *Channel constrictions.*

Natural channels typically experience some constrictions that cause head loss in the flow of water. Thus, head loss needs to be incorporated into the net force balance in the momentum equation. The head loss term is usually given as

$$f_{E/C} = -\rho g \Delta h_E , \tag{4.19}$$

where ρ is the density, g is gravitational acceleration, and Δh_E is head loss, which in turn is defined by the following equation:

$$h_E = \frac{K_E}{2g}\left(\frac{Q}{A}\right)^2 , \tag{4.20}$$

where K_E is the head loss coefficient, g is gravitational acceleration, Q is the flow rate, and A is the area. The head loss caused by constrictions in the river channel can be incorporated into the momentum conservation equation as a slope term, shown in Equation (4.21)

$$S_{E/C} = \frac{K_E \Delta (Q/A)^2}{2g\Delta x} . \tag{4.21}$$

Hence, the momentum equation becomes

$$\frac{\partial Q}{\partial t} + \frac{\partial (Qu)}{\partial x} = -gA\frac{\partial h}{\partial x} + gA(S_o - S_f - S_{E/C}) + M_L . \tag{4.22}$$

Since no additional loss of water from the river occurs, the mass conservation equation remains unaltered.

iv. *Momentum correction factor.*

In natural rivers, the velocity is substantially non-uniform across the width of the river. In order to compensate for the assumption of uniform velocity across the width of the river, a momentum correction factor is used in the convective acceleration term of the momentum equation, shown below:

$$\frac{\partial Q}{\partial t} + \beta \frac{\partial}{\partial x}(Qu) + gA\frac{\partial h}{\partial x} = gA(S_0 - S_{E/C} - S_f) + M_L . \tag{4.23}$$

v. *Meandering form of natural rivers–the addition of a sinuousity factor*

In nature, rivers flow in meandering, curving paths instead of the prismatic, straight pathways that scientists and researchers study. This meandering must be reflected in the Saint-Venant equations, so sinuosity factors are introduced mathematically into the continuity and momentum equations. The sinuosity coefficient, used in the calculation of the sinuosity factor, is the ratio of the straight and real distances between two nodes along the river. The continuity equation area of each reach is calculated with and without using this coefficient, and their ratio is set to S_c.

For the momentum equation, the ratio of conveyances calculated with the real and straight distance between nodes is used to calculate the sinuosity factor S_m. Using the

sinuosity factors and converting the velocity terms into flow terms so that only two unknowns remain, the modified version of the continuity equation of the Saint-Venant equations becomes

$$\frac{\partial s_c (A + A_0)}{\partial t} + \frac{\partial Q}{\partial x} - q_L = 0\,, \tag{4.24}$$

and the momentum equation becomes

$$\frac{\partial s_m Q}{\partial t} + \frac{\partial (\beta Q^2 / A)}{\partial x} + gA\left(\frac{\partial h_r}{\partial x} + S_f + S_{ec}\right) + M_L = 0\,. \tag{4.25}$$

With the above mentioned modifications for the natural, meandering rivers, the final form of the Saint Venant equations becomes

$$\frac{\partial s_c (A + A_0)}{\partial t} + \frac{\partial Q}{\partial x} - q_L = 0 \tag{4.26}$$

$$\frac{\partial s_m Q}{\partial t} + \frac{\partial (\beta Q^2 / A)}{\partial x} + gA\left(\frac{\partial h_r}{\partial x} + S_f + S_{ec}\right) + M_L = 0\,. \tag{4.27}$$

4.3. Initial and Boundary Conditions

4.3.1. Initial Conditions

In order to start the solution, the initial values of the unknowns, which are the discharge and water surface elevation, need to be determined along the one-dimensional river reach.

These initial conditions can be obtained from field data, a previous unsteady model solution, or a solution for a steady and non-uniform flow equation. In any of these cases, the initial conditions are given in the following form:

$$Q(x,0) = Q_0(x) \tag{4.28}$$

$$h_r(x,0) = h_{r0}(x)\,, \tag{4.29}$$

where Q_0 [L^3/T] and h_{r0} [L] represent the discharge and water surface elevation in the channel at the start of the simulation, respectively.

4.3.2. Boundary Conditions

Two different types of boundary conditions, external and internal, are located in the domain. External boundary conditions are located at the most upstream and downstream points of the river system and internal boundary conditions at the junctions where another tributary enters the river system. The model proposed in this study is capable of modeling both a network of river channels and a single channel. However, it does not allow for looped channel networks, only tree-like network structures. The tree-like network structure can accommodate more than one upstream boundary condition and a single downstream boundary condition.

4.3.2.1. External Boundary Conditions

At the upstream boundary, only a discharge or stage hydrograph can be used as the boundary condition. At the downstream boundary, some type of rating curve can also be used as a boundary condition in addition to the discharge or stage hydrograph.

The discharge or stage hydrograph at the upstream can be expressed as

$$Q(0,t) = Q_u(t) \tag{4.30}$$

$$h_r(0,t) = h_u(t), \tag{4.31}$$

where Q_u [L^3/T] and h_u [L] are the upstream boundary discharge and water surface elevation values, respectively. In a similar manner, the discharge or stage hydrograph boundary conditions at the downstream point can be expressed as

$$Q(L_d,t) = Q_d(t) \tag{4.32}$$

$$h_r(L_d,t) = h_d(t), \tag{4.33}$$

where Q_d [L^3/T] and h_d [L] are downstream boundary discharge and water surface elevation values, respectively, and L_d [L] is the total length of the system of rivers.

The downstream boundary condition can be defined as a rating curve as well. Three different types of rating curves can be used as a boundary condition. A single-valued rating curve uses a stage-discharge data set and linear interpolation, as shown below:

$$Q(L_d,t) = Q^k + \frac{Q^{k+1} - Q^k}{h_r^{k+1} - h_r^k}(h_d - h_r^k), \tag{4.34}$$

where Q^k [L^3/T], Q^{k+1} [L^3/T], h_r^k [L] and h_r^{k+1} [L] are tabular data sets of the discharge and stage values consecutively on the rating curve and h_d [L] is the stage at the downstream boundary.

A looped rating curve describes the stage value according to several possible discharge values, depending on the hydraulic conditions of the channel. It can be expressed using Manning's equation:

$$Q(L_d,t) = \frac{c_1}{n_r} A R_h^{2/3} S_f^{1/2}, \tag{4.35}$$

where the friction slope S_f is derived from the modified momentum equation as

$$S_f = -\frac{1}{gA}\frac{\partial Q}{\partial t} - \frac{1}{gA}\frac{\partial (Q^2/A)}{\partial x} - \frac{\partial h_r}{\partial x}. \tag{4.36}$$

Critical depth can also be used as the downstream boundary condition when the most downstream point of the modeling domain is a controlling structure such as a weir. In such a case, the critical depth is defined by the critical discharge:

$$Q(L_d, t) = \sqrt{\frac{g}{W}} A^{3/2}, \tag{4.37}$$

where W is the cross-sectional top width of the channel.

4.3.2.2. Internal Boundary Conditions

At the junctions where two or more rivers intersect in a river network, internal boundary conditions must satisfy the mass and energy balance. The water depth has to be equated at each of the rivers coming into or out of the junction through the mass balance equation. The mass balance equation at a junction is given as

$$\sum_{k=1}^{m} Q_k - Q_0 = \frac{dS}{dt}, \tag{4.38}$$

where m is the total number of rivers entering the junction. Only one outgoing river from the junction is allowed in this model. Q_k [L^3/T] is the discharge at the end of the k^{th} inflowing river into the junction; Q_0 [L^3/T] represents the discharge at the beginning of the outflowing river from the junction. dS/dt [M/T] denotes the change in the storage of mass within the junction. The change in storage is believed to be negligible with respect

to the change in storage within a river (Fread 1976; Gunduz 2004). Hence, the mass balance equation becomes a continuity equation. The energy conservation equation at the junction can be written as

$$(h_r)_k + \frac{V_k^2}{2g} = (h_r)_0 + \frac{V_o^2}{2g} + h_T \quad k = 1, 2, ..., m\,, \tag{4.39}$$

where $(h_r)_k$ [L] and V_k [L/T] are the stage and flow velocity at the end of the kth inflowing channel into the junction, respectively, and $(h_r)_0$ and V_o are the stage and flow velocity at the beginning of the outflowing channel from the junction, respectively. h_T [L] is the total head loss in the junction. In the case in which all the flows associated with one junction are subcritical and the head loss in the junction is negligible, Equation (4.39) simplifies to

$$(h_r)_k = (h_r)_0 \quad k = 1, 2, ..., m\,, \tag{4.40}$$

which is commonly used in the modeling of river networks (Fread 1976; Gunduz 2004).

4.4 Numerical Solution Scheme–The Preissmann Weighted Four-Point Scheme

These two equations together form the system of equations representing unsteady flow in channels, also known as the Saint-Venant equations. These two equations are coupled, nonlinear, first-order partial differential equations of the hyperbolic type whose solutions

require one initial and two boundary conditions (Baltas 1988). These equations have no analytical solution except for a few special cases (Gunduz and Aral 2004). However, several numerical methods that solve Saint-Venant equations have been developed. They can be classified into i) the method of characteristics, ii) the method of finite differences, and iii) the method of finite elements. Each of these methods can further be classified as explicit or implicit, depending on the solution.

Among these three numerical solution procedures, the method of finite elements is less likely to be selected to solve the Saint-Venant equations of unsteady flow (Blandford and Ormsbee 1993; Cooley and Moin 1976; Szymkiewicz 1991). Even though method of finite elements offers many advantages over other numerical solution procedures in a general setting, these advantages become somewhat less viable in a one-dimensional setting such as rivers. The power of the finite element method is much more apparent in two- and three-dimensional problems.

The method of characteristics has been the first technique successfully applied to solving Saint-Venant equations. The application of this method requires the transformation of the original partial differential equations into their characteristic forms, thus having ordinary differential equations, which are easier to deal with. Liggett and Woolhiser (1967) and Streeter and Wylie (1967) developed explicit solution techniques to characteristic forms of the Saint-Venant equations while Amein (1966) and Wylie (1970) formulated some implicit solution methods for the same characteristic forms of the original equations.

The method of characteristics is applied to either a characteristic (curvilinear) grid, which is not suitable for natural pathways with irregular geometry, or to a rectangular grid in the x-t solution plane, which requires interpolation within a finite difference solution procedure (Fread 1985; Gunduz 2004). These restrictions limit the application of the method of characteristics to flood routing (Fread 1985).

The method of finite differences involves the transformation of the governing differential equations into algebraic equations through approximation of the derivative in terms of difference equations. Using an explicit finite difference method, the solution is advanced from point to point along one time line until all the unknown values in that particular time line have been calculated. Afterwards, the same principle is applied in the next time step. In an implicit finite difference method, the solution from one time line to the next is performed simultaneously on all the points of unknown values. Explicit methods are straightforward and easily programmed, but they are restricted by conditions for stability. However, the solution of implicit methods is more complex and difficult to program, but most are unconditionally stable (Fread 1985).

The first explicit technique for the solution of flood routing problems was developed by Stoker in 1953, followed by Liggett and Woolhiser in 1967 and later by Strelkoff in 1970. The restrictions inflicted on the size of the computational time step by explicit methods drove the need to develop implicit methods, which were first formulated by Preismann in 1961 and followed by the work of Amein and Chu in 1975. Amein and

Fang (1969) showed that implicit schemes are the only ones suited to handling large variations in flow characteristics. Today, the Preismann method has become the most implemented method due to its flexibility in using large time steps and its unconditional stability (Gunduz 2004). The numerical grid for this method is below:

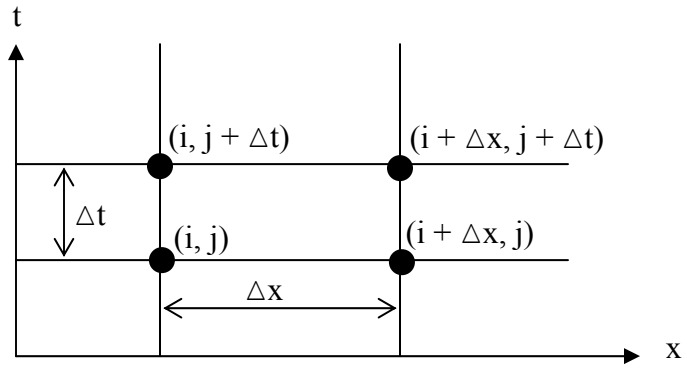

Figure 4.5 The numerical grid for the weighted four-point scheme.

The Preissmann four-point method is weighted implicitly at each time level and unconditionally stable for weighing factor θ between 0.5 and 1.0. It permits the use of unequal space and time steps. This scheme has second-order accuracy when θ is 0.5 and first-order accuracy when θ is 1.0.

If ϕ is a variable that changes with respect to time and space, the finite difference representation is the average of the forward difference in time between four corners given as

$$\frac{\partial \phi}{\partial t} = \frac{\left(\frac{\phi_x^{t+\Delta t} + \phi_{x+\Delta x}^{t+\Delta t}}{2} - \frac{\phi_x^t + \phi_{x+\Delta x}^t}{2} \right)}{\Delta t} \tag{4.41}$$

$$\frac{\partial \phi}{\partial x} = \frac{(1-\theta)\left(\phi^{t}_{x+\Delta x} - \phi^{t}_{x}\right) + \theta\left(\phi^{t+\Delta t}_{x+\Delta x} - \phi^{t+\Delta t}_{x}\right)}{\Delta x}, \tag{4.42}$$

and the ϕ itself can be represented using a similar finite difference representation:

$$\phi = (1-\theta)\left(\frac{\phi^{t}_{x+\Delta x} + \phi^{t}_{x}}{2}\right) + \theta\left(\frac{\phi^{t+\Delta t}_{x+\Delta x} + \phi^{t+\Delta t}_{x}}{2}\right). \tag{4.43}$$

With Equations (4.42) to (4.43) as guidelines, both the continuity and momentum equations can be written in terms of these representations. Thus, the finite difference representation of the continuity equation becomes

$$\begin{aligned}
&\frac{\Delta x_i}{2\Delta t^{j}}\left[s^{j+1}_{c_{i+1/2}} (A + A_0)^{j+1}_{i+1} + s^{j}_{c_{i+1/2}} (A + A_0)^{j+1}_{i} - s^{j}_{c_{i+1/2}} (A + A_0)^{j}_{i+1} - s^{j}_{c_{i+1/2}} (A + A_0)^{j}_{i} \right] \\
&+\theta_f \left[Q^{j+1}_{i+1} - Q^{j+1}_{i} - \Delta x_i \left[\left(-\frac{K_r w_r}{m_r} \right)^{j+1}_{i+1/2} \left(h^{j+1}_{r_{i+1/2}} - h^{j+1}_{g_{i+1/2}} \right) \right] - \Delta x_i (q_{L2})^{j+1}_{i+1/2} \right] \\
&+(1-\theta_f) \left[Q^{j}_{i+1} - Q^{j}_{i} - \Delta x_i \left[\left(-\frac{K_r w_r}{m_r} \right)^{j}_{i+1/2} \left(h^{j}_{r_{i+1/2}} - h^{j}_{g_{i+1/2}} \right) \right] - \Delta x_i (q_{L2})^{j}_{i+1/2} \right] = 0
\end{aligned} \tag{4.44}$$

Similarly, the momentum equation can be written as

$$\frac{\Delta x_i}{2\Delta t^j}\left[s^{j+1}_{m_{i+1/2}} Q^{j+1}_{i+1} + s^{j}_{m_{i+1/2}} Q^{j+1}_{i} - s^{j}_{m_{i+1/2}} Q^{j}_{i+1} - s^{j}_{m_{i+1/2}} Q^{j}_{i} \right]$$
$$+\theta_f \left[\begin{array}{l} (\beta Q^2 / A)^{j+1}_{i+1} - (\beta Q^2 / A)^{j+1}_{i} + g A^{j+1}_{i+1/2}\left[h^{j+1}_{r_{i+1}} - h^{j+1}_{r_i} + \Delta x_i S^{j+1}_{f_{i+1/2}} + \Delta x_i S^{j+1}_{ec_{i+1/2}} \right] \\ +\Delta x_i (M_{L1})^{j+1}_{i+1/2} + \Delta x_i (M_{L2})^{j+1}_{i+1/2} \end{array} \right] \quad . \quad (4.45)$$
$$+(1-\theta_f) \left[\begin{array}{l} (\beta Q^2 / A)^{j}_{i+1} - (\beta Q^2 / A)^{j}_{i} + g A^{j}_{i+1/2}\left[h^{j}_{r_{i+1}} - h^{j}_{r_i} + \Delta x_i S^{j}_{f_{i+1/2}} + \Delta x_i S^{j}_{ec_{i+1/2}} \right] \\ +\Delta x_i (M_{L1})^{j}_{i+1/2} + \Delta x_i (M_{L2})^{j}_{i+1/2} \end{array} \right] = 0$$

The definitions developed for the slope terms S_f and S_{ec}, and the lateral flow terms M_{L1} and M_{L2} are included in the above representation. Subscripts *i* and *j* represent the spatial and temporal indices, respectively. The terms with subscript j are known either from initial conditions or from the solution of the Saint-Venant equations at the previous time line. As the cross-sectional area and the top width of the river are functions of water surface elevation, the only unknown terms in these equations are the discharge and water surface elevation at the $(j+1)^{th}$ time line at nodes *(i)* and *(i+1)*. Therefore, these equations contain only four unknowns. The remaining terms are either known constants or functions of the unknowns. The algebraic equations (4.44) and (4.45) are nonlinear, requiring an iterative solution technique.

When the system is derived using the above guidelines, 2(N-1) equations are formed for one time-line between the upstream and downstream boundaries of a channel of N nodes. At this point, there are 2N unknowns for each time line with 2(N-1) equations to solve them. Hence, two more equations are needed to close the system and solve it. These two equations are supplied by the upstream and downstream boundary conditions of the channel. The system of 2N equations with 2N unknowns is non-linear and solved by a matrix solution algorithm.

To demonstrate the solution of scheme, two functions, F and G, can be defined as F being the residual of the continuity equation, and G being the residual of the momentum equation. Both F and G are functions of four dependent variables, S_1, S_2, S_3, and S_4 which represent the to represent the unknowns, $Q_x^{t+\Delta t}$, $A_x^{t+\Delta t}$, Q_x^t, and A_x^t, respectively, which are the flow and area at the present and future time steps.

This solution matrix is formed by the application of Taylor's series for these two equations, F and G as follows:

$$F(S_1, S_2, S_3, S_4) = 0 \tag{4.47}$$

$$G(S_1, S_2, S_3, S_4) = 0\,. \tag{4.48}$$

If the exact solution to the unknows were known as $S_{1,r}$, $S_{2,r}$, $S_{3,r}$, and $S_{4,r}$ as

$$\begin{aligned} S_1 &= S_{1,r} \\ S_2 &= S_{2,r} \\ S_3 &= S_{3,r} \\ S_4 &= S_{4,r} \end{aligned}\quad, \tag{4.49}$$

then the exact solution can be approximated by the following equation using Taylor's series expansion:

$$F(S_{1,r}, S_{2,r}, S_{3,r}, S_{4,r}) \approx F(S_{1,\xi}, S_{2,\xi}, S_{3,\xi}, S_{4,\xi}) + \frac{\partial F}{\partial S_1} dS_1\Big|_{\xi} + \frac{\partial F}{\partial S_2} dS_2\Big|_{\xi} + \frac{\partial F}{\partial S_3} dS_3\Big|_{\xi} + \frac{\partial F}{\partial S_4} dS_4\Big|_{\xi} = 0 \tag{4.50}$$

and

$$G(S_{1,r}, S_{2,r}, S_{3,r}, S_{4,r}) \approx G(S_{1,\xi}, S_{2,\xi}, S_{3,\xi}, S_{4,\xi}) + \frac{\partial G}{\partial S_1} dS_1\Big|_{\xi} + \frac{\partial G}{\partial S_2} dS_2\Big|_{\xi} + \frac{\partial G}{\partial S_3} dS_3\Big|_{\xi} + \frac{\partial G}{\partial S_4} dS_4\Big|_{\xi} = 0, \tag{4.51}$$

where the higher-order terms of the Taylor's series expansion can be neglected. Then the solution can be approximated by

$$\begin{aligned} S_{1,r} &\approx S_{1,\xi} + dS_1 \\ S_{2,r} &\approx S_{2,\xi} + dS_2 \\ S_{3,r} &\approx S_{3,\xi} + dS_3 \\ S_{4,r} &\approx S_{4,\xi} + dS_4 \end{aligned}. \tag{4.52}$$

The Equation (4.52) is only an approximate of the true solution; however, this approximation can be improved through iterations in which each interation estimates a solution better than the previous one until there is not much room for improvement (a preset tolerance value can determine this condition):

$$\begin{aligned} S_1^{\xi+1} &\approx S_1^{\xi} + dS_1^{\xi} \\ S_2^{\xi+1} &\approx S_2^{\xi} + dS_2^{\xi} \\ S_3^{\xi+1} &\approx S_3^{\xi} + dS_3^{\xi} \\ S_4^{\xi+1} &\approx S_4^{\xi} + dS_4^{\xi} \end{aligned} \tag{4.53}$$

The estimates from a previous iteration improve with each step further in time and finally converge on a solution, which can be performed by setting the equations in matrix form:

$$\mathbf{J}(X^{\xi})\Delta X = -\mathbf{R}(X^{\xi}), \tag{4.54}$$

where X^{ξ} is a vector of estimated values of the unknowns from the ξ^{th} step or iteration, and the coefficient matrix $\mathbf{J}(X^{\xi})$, also known as the Jacobian, contains the partial derivatives with the values evaluated at the ξ^{th} iteration. ΔX is a vector of unknowns (dS_1, …, dS_4), as given in this example. $\mathbf{R}(X^{\xi})$ is a vector of residuals, the values of which should approach zero as the solution converges to an exact solution. The solution can be obtained using one of the various numerical methods such as Gauss Elimination or LU decomposition for the simultaneous solution of the given equations.

The Jacobian matrix, made up of the partial derivatives of the continuity and momentum equation, must be set up to start the solution. The resulting matrix form is given as

$$\begin{bmatrix}
\frac{\partial G_0}{\partial A_1} & \frac{\partial G_0}{\partial Q_1} & 0 & 0 & 0 & 0 & 0 & . & . & . & 0 & 0 \\
\frac{\partial F_1}{\partial A_1} & \frac{\partial F_1}{\partial Q_1} & \frac{\partial F_1}{\partial A_2} & \frac{\partial F_1}{\partial Q_2} & 0 & 0 & 0 & . & . & . & 0 & 0 \\
. & . & . & . & . & . & . & . & . & . & . & . \\
. & . & . & . & . & . & . & . & . & . & . & . \\
. & . & . & . & . & . & . & . & . & . & . & . \\
0 & . & . & . & \frac{\partial F_i}{\partial A_i} & \frac{\partial F_i}{\partial Q_i} & \frac{\partial F_i}{\partial A_{i+1}} & \frac{\partial F_i}{\partial Q_{i+1}} & . & . & . & 0 \\
0 & . & . & . & \frac{\partial G_i}{\partial A_i} & \frac{\partial G_i}{\partial Q_i} & \frac{\partial G_i}{\partial A_{i+1}} & \frac{\partial G_i}{\partial Q_{i+1}} & . & . & . & 0 \\
. & . & . & . & . & . & . & . & . & . & . & . \\
. & . & . & . & . & . & . & . & . & . & . & . \\
. & . & . & . & . & . & . & . & . & . & . & . \\
0 & 0 & . & . & . & 0 & 0 & 0 & \frac{\partial G_{N-1}}{\partial A_{N-1}} & \frac{\partial G_{N-1}}{\partial Q_{N-1}} & \frac{\partial G_{N-1}}{\partial A_N} & \frac{\partial G_{N-1}}{\partial Q_N} \\
0 & 0 & . & . & . & 0 & 0 & 0 & 0 & 0 & \frac{\partial G_N}{\partial A_N} & \frac{\partial G_N}{\partial Q_N}
\end{bmatrix}_{NxN}
\begin{bmatrix}
dA_1^{\xi} \\ dQ_1^{\xi} \\ dA_2^{\xi} \\ dQ_2^{\xi} \\ . \\ . \\ . \\ dQ_{N-2}^{\xi} \\ dA_{N-1}^{\xi} \\ dQ_{N-1}^{\xi} \\ dA_N^{\xi} \\ dQ_N^{\xi}
\end{bmatrix}_{Nx1}
=
\begin{bmatrix}
R_{2,0}^{\xi} \\ R_{1,1}^{\xi} \\ R_{2,1}^{\xi} \\ R_{1,2}^{\xi} \\ . \\ . \\ . \\ R_{2,N-2}^{\xi} \\ R_{2,N-2}^{\xi} \\ R_{1,N-1}^{\xi} \\ R_{2,N-1}^{\xi} \\ R_{2,N}^{\xi}
\end{bmatrix}_{Nx1} \quad (4.55)$$

When all the equations are written for a system with N_k number of nodes, $2(N_k\text{-}1)$ equations are formed for one time-line between the upstream and downstream boundaries of channel k. At this point, we have $2N_k$ unknowns for each time line with $2(N_k\text{-}1)$ equations to solve them. Hence, we need two more equations to close the system and solve it. These two equations are supplied by the upstream and downstream boundary conditions of the channel. When this procedure is repeated for each river tributary in the network, a total of $\sum(2N_k) = 2N$ equations are formed. k is the number of rivers in the network, and N is the total number of nodes in the entire system. The system of 2N equations with 2N unknowns is non-linear and solved by the matrix solution algorithm explained above.

Newton-Raphson is the most common iterative technique used for solving a system of non-linear equations. When a sufficiently accurate first estimate is provided, the Newton-

Raphson method converges efficiently to a root. The basic steps in this solution follow (EnvironmentalLaboratory 1995):

1. Assume Q and A are known from either of the previous time steps of the initial conditions.
2. Insert Q and A into the equations for F and G and form the first vector of residuals by evaluating the continuity and momentum equations.
3. After the residuals are formed, the gradients should be formed and the estimates used to calculate the residuals (either the initial conditions or the estimates obtained from the previous iteration)
4. Using the matrix form, solve the system of equations.
5. The ΔX^{ξ}, the solution of the matrix form, is the departure vector from the old estimates. Using this departure vector, evaluate new estimates:

$$\begin{aligned} Q_x^{t+\Delta t,\xi+1} &= Q_x^{t+\Delta t,\xi} + dQ_x^{\xi} \\ A_x^{t+\Delta t,\xi+1} &= A_x^{t+\Delta t,\xi} + dA_x^{\xi} \end{aligned} \tag{4.56}$$

6. Check to see how close the new estimates match the previous ones. If the new estimates are within some specified tolerance, then proceed to the next time step beginning at step 1. If they are not within the specified tolerance, repeat the process beginning at step 2.

4.5 Verification of the Hydrodynamics Solution

The solution procedure has been applied to some simple hypothetical cases for testing and verification purposes. These example applications are also used to verify the solution technique used in this thesis. In Figure 4.6 below, one of these example cases is depicted. The set of non-linear, coupled partial differential equations, which comprise the so-called Saint Venant equations, are applied to a single, trapezoidal channel that is 10 km long with a bed slope of 0.001 m/m and a Manning roughness coefficient of 0.020. The sides of the trapezoidal cross-section of the channel, with a width of 20 m., have a 2:1 ratio

A triangular hydrograph is used as the upper boundary condition, and a constant depth of 1.44 m is used as the downstream boundary condition.

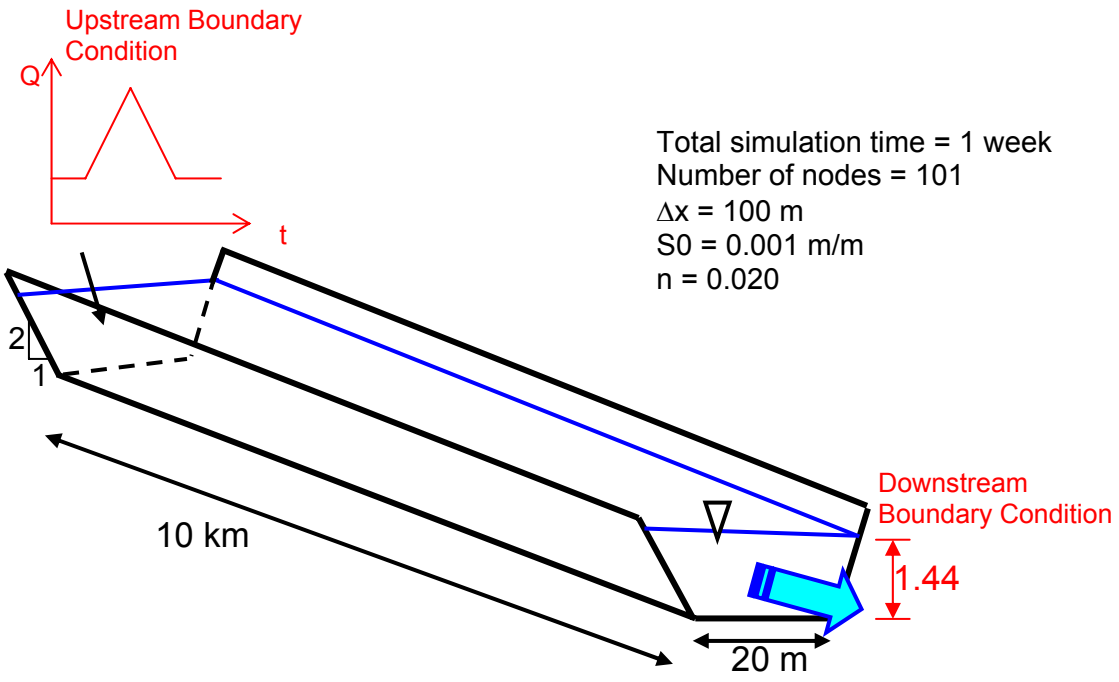

Figure 4.6 A schematic view of a single, trapezoidal channel

HEC-RAS, a well-known and widely-used flood routing model developed by the USGS is used to verify the model developed in this study. Different example cases are used for comparison between the model in this study and HEC-RAS, Figures 4.7 and 4.8 below show the results from the application of the single, trapezoidal channel explained above.

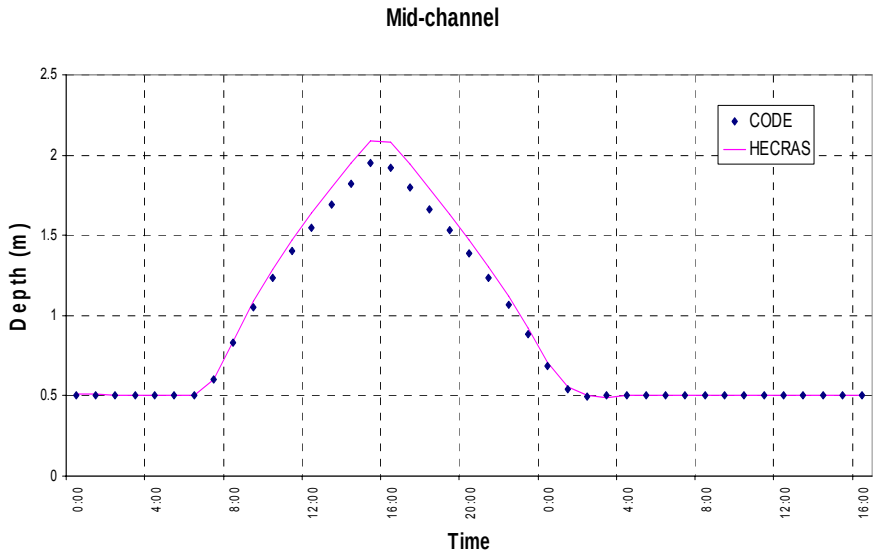

Figure 4.7 A comparison between this model and HEC-RAS at mid-channel

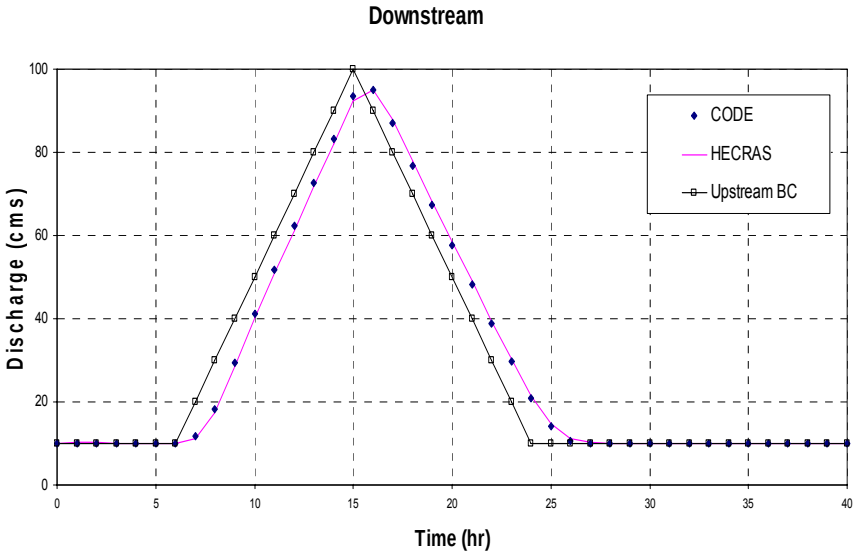

Figure 4.8 A comparison between this model and HEC-RAS at the downstream boundary condition.

Based on the results from both the model described and developed in this study and HEC-RAS, which has been run under the same conditions, the developed model, these figures exhibit confidence in the developed model.

4.6. Channel Network Example

A second example application involves the existence of a junction and more than one channel entering the junction. In this example case, straight, trapezoidal channels make up the configuration given in Figure 4.9 below

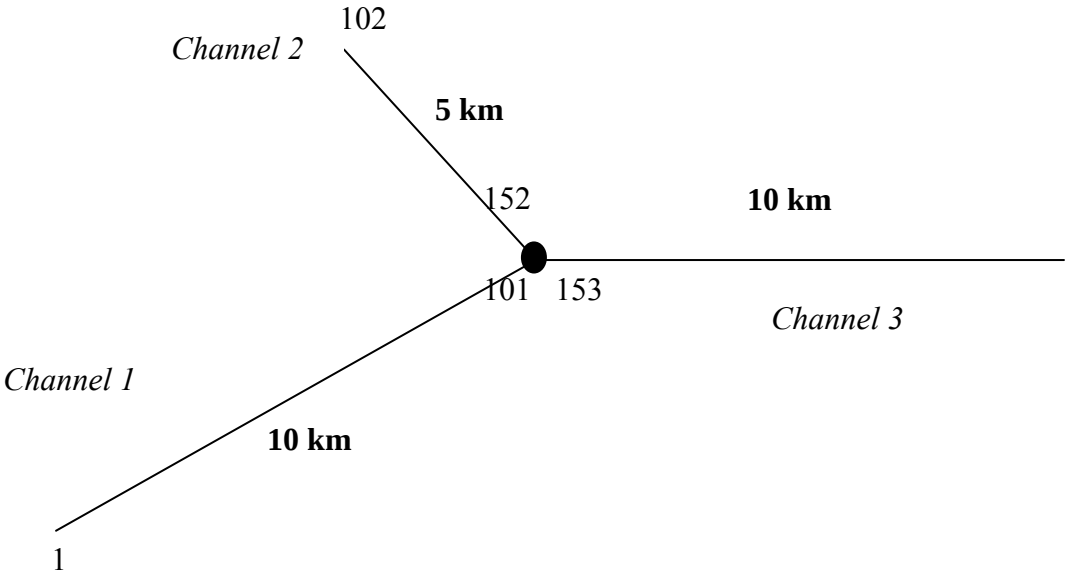

Figure 4.9 An example river network

In this case of a river network application, a total of three rivers with one junction is examined. Two of the rivers enter the junction while a third one exits. The figure (which figure), which illustrates the set up of the river network, shows that the two rivers are 10 km long and 5 km long. All the nodes are separated by 100 m with a total of 253 nodes in the system. The figure also depicts the node numbers at the beginning and end of each river channel.

All the rivers have a constant bed slope of 0.001 m/m and a Mannings' roughness coefficient of 0.030 in the main channel. The cross-sections of all three rivers are trapezoids with a 10 m bottom width and side slopes of a 2:1 ratio. No lateral overland or seepage flow occurs. The total length of the run was for 50 hours at one-hour intervals.

The upstream boundary condition for the 5 km river is a discharge time series composed of two sequential triangular hydrographs, and the upstream boundary condition for the 10 km river entering the junction is a triangular discharge hydrograph. The downstream condition of the outflowing river is a depth of 2 m.

The results of the application of the same model to a river system network are presented in Figure 4.10 below. Channel 1, a triangular hydrograph, and Channel 2, a double triangular hydrograph, form a confluence at the junction and combine their flow patterns. This new flood pattern is routed in Channel 3, which has a 2 m constant depth downstream boundary condition.

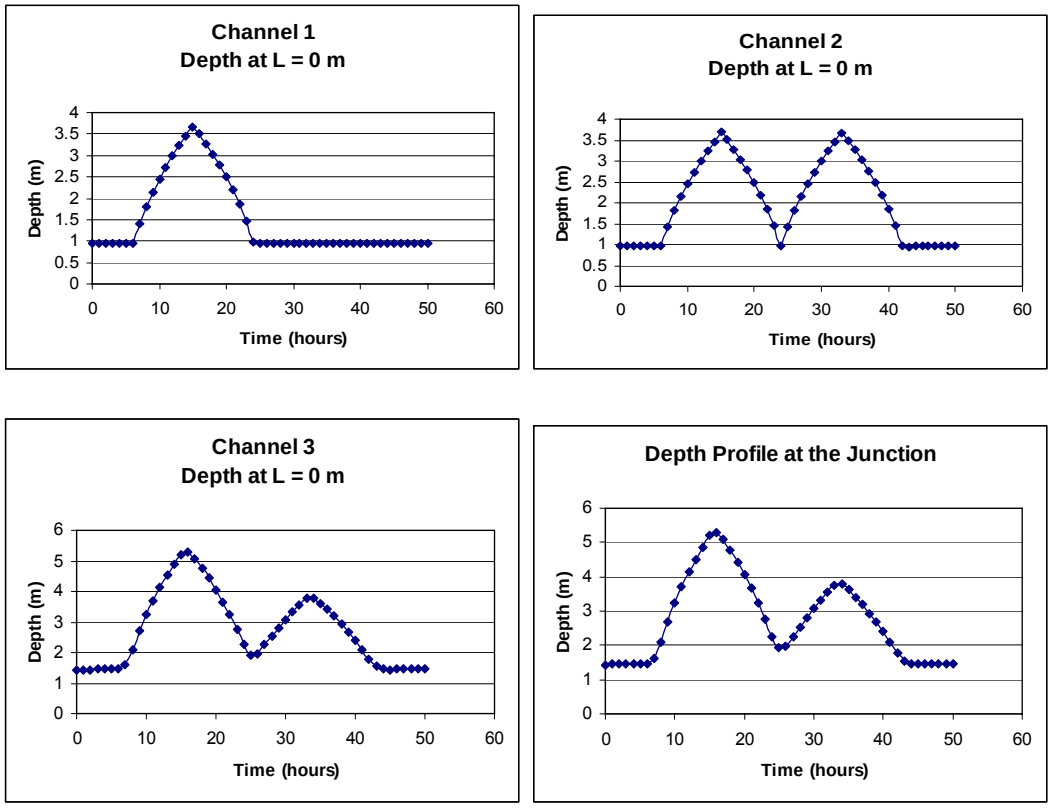

Figure 4.10 Results of a river network application

4.7 Altamaha River Application

The Lower Altamaha River basin, formed by the confluence of the Ocmulgee and Oconee Rivers, is the largest watershed in Georgia. The confluence of the two rivers then forms the Altamaha River, which flows into the Atlantic Ocean about 137 miles from the confluence. Approximately 100,000 gallons of fresh water per second is expelled into the Atlantic Ocean from this system, which is home to 120 species of rare or endangered plants and animals. A plan view of the Altamaha River system can be seen in Figure 4.11 below.

Figure 4.11 The Altamaha River system

In order to model the river network, a simplified, conceptual version of the network is depicted in Figure 4.12 below. This version illustrates the differences in the real versus linear length between the upstream and the downstream of the channels, with real distances in blue and linear distances in black. These values are used to calculate the sinuosity factors of the rivers, which help modify the model for the meandering nature of rivers. The three channels in the Altamaha River network are called Altamaha River Main 1, Altamaha River Main 2, and the Ohopee River, which acts as a tributary entering the main stream divided by this junction. The channels are divided into small reaches at 394 cross-sections. The required data at these nodes are obtained by using measurements taken at three gaging stations by USGS, and the topographic maps of the region. Each node corresponds to a USGS gage, so geometric information as well as the flow and water elevation at the start of the model is known. The geometric information, which is actually the depth versus width information at each node, is known from the gages and entered into the model. One such cross-section is shown in Figure 4.13 below. For the

application of this model, each cross-section if described with 10 sets of elevation-top width pairs.

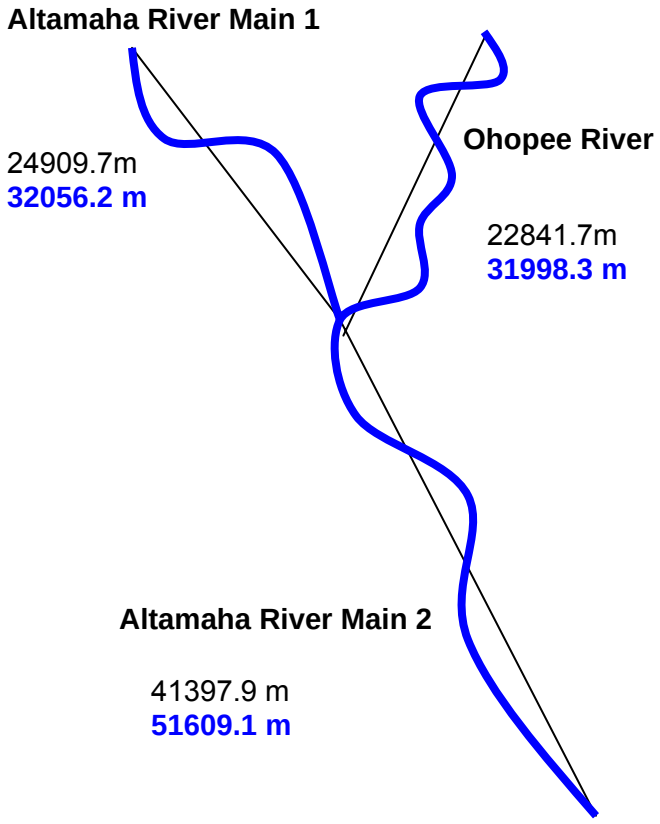

Figure 4.12 Conceptual drawing of the Altamaha River network

From previous modeling studies in the same area, Manning's roughness coefficients have been selected and have values between 0.020 to 0.030 within the main channel and 0.030 to 0.070 along the floodplain (Gunduz and Aral 2004).

Three boundary conditions are specified for the application of Altamaha River system for the river flow model. The upstream boundary conditions at both the Altamaha River as well as Ohoopee River is taken to be discharge-time series obtained from Baxley and Reidsville river stream gages operated by U.S. Geological Survey. The most downstream boundary condition is a rating curve obtained from the Doctortown gauging station, developed by the U.S. Geological Survey staff for use in their modeling studies.

The initial discharge and stage conditions in the river network are based on previous studies in the same domain (Gunduz and Aral 2004).

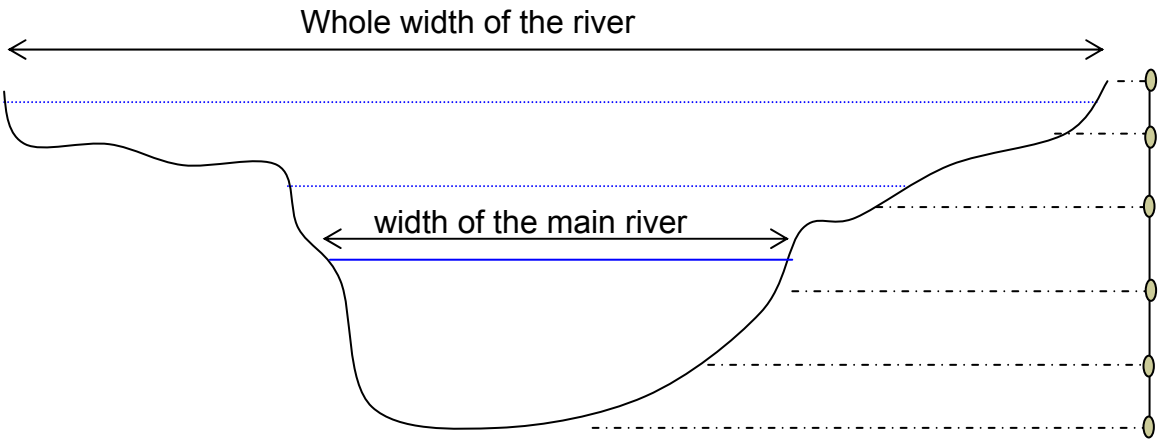

Figure 4.13 Cross section view of a node.

The results of the Altamaha River applications will be used directly and indirectly as input for the contaminant transport model, which will be explained in detail in the next chapter. The results of this application include a velocity distribution in the river network over the simulation time as well as depth and width values at each node at each time step.

Width is used to calculate the surface area of each element together with the distance between nodes. Depth will then be used to calculate the volume of water in each element using the previously calculated surface area information. Velocities at each node will be used in the advection portion of the contaminant transport equation as well as in the calculation of a longitudinal dispersion coefficient for each element, using an empirical formula. All these results will be prepared as an array input in a small program developed to handle output and then to use the output of the hydrodynamic portion and convert it into input files to be used by the contaminant transport model.

As these results are intermediate steps in the solution of totally dynamic fugacity-based water quality model, they are not shown here. Just as an example, the velocity distribution in the Altamaha River network is given below:

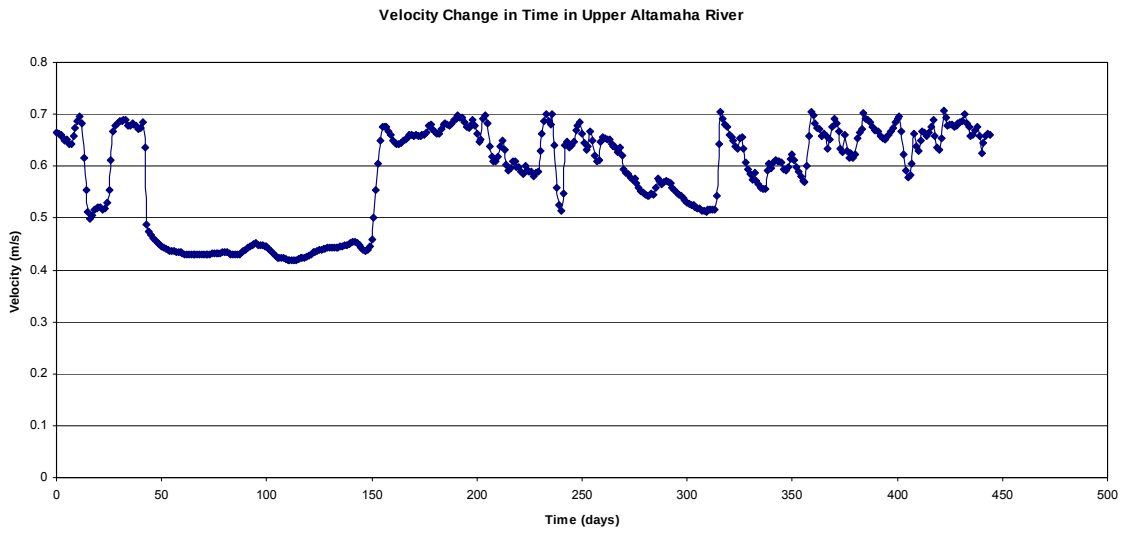

Figure 4.14 Velocity time series at location 5 km from upstream in the Altamaha River system

The velocity distribution follows the rise and fall of water levels due to rain events, water intake, and other activities performed in a channel, so it does not follow a smooth curve. The real USGS stream gage readings are input into the solution of the model as initial and boundary conditions, and the results reflect changes in the river elevations and flow rate fluctuations due to natural and artificial reasons. The velocity time series is illustrated in Figure 4.14 and the width and depth distribution at each cross-section are used as input information into the contaminant transport model developed in Chapter 5.

CHAPTER 5

CONTAMINANT TRANSPORT MODELING IN RIVERS

One of the most studied aspects of the general mass transport process in the environment has been contaminant transport in rivers. Since most cities have arisen along rivers and streams carrying fresh water, contaminants and the fate and transport of contaminants are very important to humans. Thus, many models that simulate the migration of contaminants along a river have been developed. However, because of their predictive capabilities as well as cost-effectiveness, only mathematical models can be used to predict the response of rivers to an external pollution load.

Rivers are usually faced with two major water quality issues: eutrophication (algal bloom due to nutrient enrichment) and contamination by hazardous substances. So far, the purpose of most river water quality models is to assess eutrophication. Eutrophication models follow the fate of algae (phytoplankton) and green plants and their effect on the dissolved oxygen and nutrient concentration of a river.

In this thesis, interest is not in the modeling of eutrophication but in the fate and transport of hazardous substances in a river. Contamination by hazardous substances in rivers is

usually examined under the heading of contaminant fate models that describe the fate and transport of contaminants in the environment.

5.1 The Advection-Dispersion Equation

The river water quality models are based on the conservation of mass within a finite volume of water. In quantitative terms, mass-balance equations in this finite volume account for all transfer of matter across the boundaries of the system and all transformations occurring within the system.

The mass-balance of pollutants in a river is usually described by the advection-dispersion equation, based on the conservation of mass and Fick's law:

$$\frac{\partial C}{\partial t} + \frac{\partial (Cu)}{\partial x} - \frac{\partial}{\partial x}\left(D_H \frac{\partial C}{\partial x} \right) = \sum \text{Reaction} + \text{interactions}, \tag{5.1}$$

where C [M/L^3] is the concentration of the contaminant, t [T] is time, u [L/T] is velocity, x [L] is the direction of the flow, and D_H [L^2/T] is the dispersion coefficient.

The velocity term in the advection-dispersion equation will come from the solution of the Saint Venant equations, representing river hydrodynamics. The longitudinal dispersion coefficient is calculated empirically using river geometry and velocity distribution.

The longitudinal dispersion coefficient D_H is a parameter that is dependent on the velocity of the river and can be estimated from the local velocity. The longitudinal dispersion coefficient is a very important parameter in the overall distribution of contaminants within a river system. In mildly moving or stagnant sections of rivers, it becomes the only means of transport mechanism. The ideal way to determine the longitudinal dispersion coefficient is to perform tracer studies in the river system under study; however, such a study is not always feasible. Therefore, water quality models often rely on empirical or semi-empirical formulations for the estimation of the longitudinal dispersion coefficient. Many researchers have developed methods for estimating the longitudinal dispersion coefficient, starting with (Taylor, 1954), (Elder, 1959) and (Fisher, 1966; Fisher, 1968; Fisher et al., 1979). Their research was followed by (Aral et al., 1980; Liu, 1977; McQuivey and Keefer, 1974) and later by (Deng et al., 2001; Iwasa and Aya, 1991; Kashefipour and Falconer, 2002; Koussis and Rodriguez-Mirasol, 1998; Magazine et al., 1988; Seo and Cheong, 1998). In spite of the vast amount of published research on the prediction of the longitudinal dispersion coefficient, no globally accepted equation has yet been formulated. Therefore, in this study, Fisher's formula, below, has been used for the estimation of a longitudinal dispersion coefficient:

$$D_L = \frac{0.011 U^2 W^2}{H U_*} \quad , \tag{5.2}$$

where D_L [L^2/T] is the longitudinal dispersion coefficient, U [L/T] is the velocity in the river, W [L] is the width of the river, H [L] is the depth of flow, and U_* [L/T] is the bed shear velocity.

The reaction and interactions term, on the right hand side of Equation (5.1), incorporates all transformation processes and inter-compartmental transport occurring in a river environment. As the contaminants are distributed among all the possible phases, such as suspended particles, fish, aerosols, sediments, and air, in the vicinity or within the water column, , an environmental model that examines only aqueous phase transport cannot accurately predict the fate of these contaminants. Thus, an evaluation of the interactions among all the possible phases in surface waters is necessary.

In all natural rivers, a dynamic interaction among all available phases occurs. After all, chemical compounds are continuously dissolving, attaching to suspended particles, resuspending due to diagenesis (bioturbation on the active surface of sediments) or due to the shear force of the flowing water on top of the sediments, reacting, diffusing, and advecting with bulk water movement. Due to the complexity of building these interactions into a model, the use of fugacity instead of concentration facilitates the modeling between phases. Fugacity, which is the pressure or chemical potential a compound exerts wherever it exists, can also be described as “the escaping tendency of a chemical from a phase.” The fugacity values of a chemical in water, sediments, and air tell us the direction of the movement a chemical. As proposed here, this study aims to incorporate, with the use of the fugacity concept for tracking the fate of contaminants in rivers, this thermodynamic information into the classical contaminant fate and transport models.

5.2. Contaminant Transport Modeling with a Fugacity Approach

Fugacity, an equilibrium criterion, is linearly related to concentration at low concentrations. Therefore, these two variables can be used interchangeably in the advection-dispersion Equation 5.1. In this case, the partitioning among phases can also be represented using the reaction terms and fugacity. Fugacity is a better chemical property than concentration to follow the movements of a contaminant between phases. A contaminant can partition into solid phases, such as sediments and suspended particles in a water column as well as various biota in the water column. In addition, it can partition into air phases such as aerosols in the atmosphere and volatilize into the air in the gas phase.

Similarly, a mass balance equation can be written for the sediment phase. Assuming that the sediment phase is immobile, the accumulation of a contaminant in sediments is a function of reactions within the sediment phase and the interactions with the water column just above it:

$$\frac{\partial C_{sed}}{\partial t} = \sum (\text{Reactions} + \text{interactions with water}). \tag{5.3}$$

Each of the terms representing one process in the reaction can be defined using fugacity:

$$\begin{aligned} C_{water} &= F_{water} Z_{water} \\ C_{sediment} &= F_{sediment} Z_{sediment} \end{aligned}, \tag{5.4}$$

where C_{water} and $C_{sediment}$ [M/L^3] are concentration in water and sediment compartments, respectively; F_{water} and $F_{sediment}$ [Pa] values are fugacities in water and sediment compartments; Z_{water} and $Z_{sediment}$ [M/Pa.L^3] values are fugacity capacities in water and sediment compartments, respectively. Fugacity capacities (Z-values) are constant for specific compounds in a particular medium, and thus, concentration and fugacity change proportionally.

5.3. Derivation of the Contaminant Fate and Transport Model

In this section, a dynamic, continuous, fugacity-based advection-dispersion equation is derived to represent the fate and transport of contaminants in the water column and sediment compartments of a river. The advection-dispersion equation is modified with the reaction and interaction terms used in the multimedia environmental fugacity models. The reactions and interactions, which have a significant effect on the fate of a contaminant are described using the unsteady-state Level IV fugacity model, developed by (Mackay, 2001). The processes affecting the fate of a contaminant in a river can be classified under three headings: (i) diffusive flux terms; (ii) material flux terms; and (iii) reactive processes.

All the processes included in the reaction and interactions term on the right hand side of the advection dispersion equation are illustrated in the schematic diagram given in Figure 1.

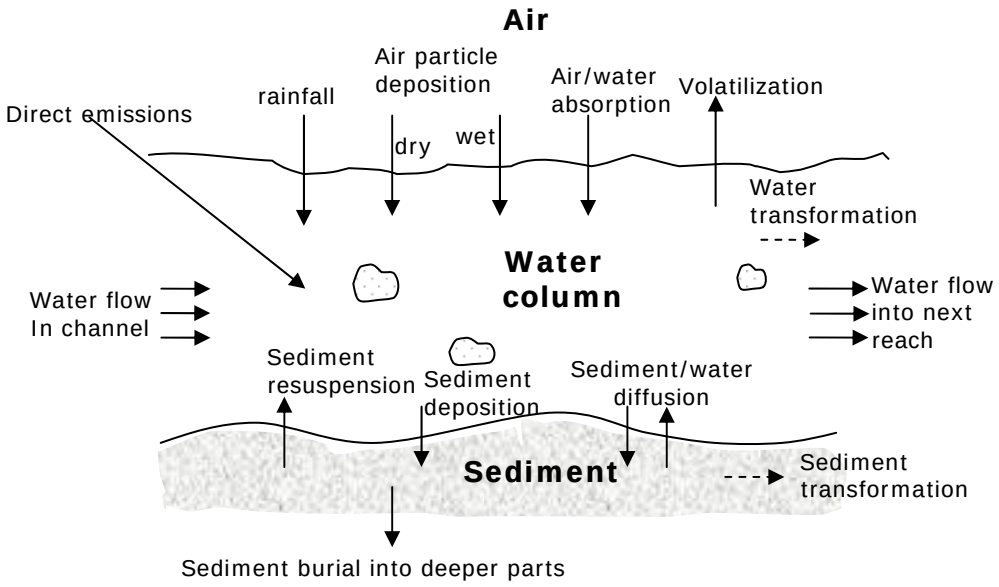

Figure 5.1 Processes in a river reach

The major processes/reactions include dry and wet particle deposition from the air, sediment deposition and resuspension, sediment burial, diffusion between the air and water, and diffusion between sediment and water as well as transformations occurring in each compartment. These transformations include chemical hydrolysis, oxidation/reduction, decay, photodegradation, and sorption onto particles. Abiotic transformations (photolysis, hydrolysis, oxidation, and reduction) can be lumped together and denoted with a first-order reaction rate constant derived from the half life of the contaminant.

Diffusive fluxes between air-water and water-sediment are represented with Whitman's two-film theory. Deposition of the particles is represented by Stoke's formulation for the settling velocity of particles. Resuspension is denoted using shear velocity at the bottom. Air-to-water interaction involves diffusion, rain dissolution, or dry and wet deposition. Water-to-air interaction involves only volatilization. Water-to-sediment interaction can be listed as diffusion and deposition; and sediment to water interaction can be listed as diffusion and resuspension.

All of these interactions can be classified into diffusive flux processes, material transport processes, and reactive processes. Diffusive flux processes involve the transport of a chemical between two phases due to a gradient and may occur in both directions while material transport involves the transport of a bulk amount of a chemical from one phase to another in strictly one direction.

The process in which a chemical spreads is called "diffusion." The fundamental mechanism of diffusion is the random action of molecules on a very small scale, primarily by Brownian motion (Chin, 2000). The diffusion between a water and a gas phase has been the most frequently investigated process, but the same principles apply to diffusion from sediment to water, soil to air or water, and even biota to water (Mackay, 2001). Traditionally, mass transfer between two phases has been explained by the Whitman two-resistance mass transfer coefficient approach, simply known as the two-film theory, which Whitman developed for industry in 1923. The theory has been adapted to environmental systems by Lisa and Slater in 1974 (Chuco, 2004). In this

approach, two films of very small thickness lie on each side of the interface separating the two phases, forming boundary layers in each phase. The flux through each film must be equal and the concentrations at the interface in equilibrium. The two-film theory can be expressed in the Equation 5.5 below:

$$\frac{1}{K_w} = \frac{1}{k_w} + \frac{RT}{Hk_g}, \tag{5.5}$$

where K_w [L/T] is the overall water-air mass transfer coefficient, k_w [L/T] is the water film resistance, k_g is the gas film resistance, H [J/mol] is Henry's law constant, R [J/mol.K] is universal gas constant, and T [K] is the temperature. The overall mass transfer coefficient between water and air is the sum of the total resistances in the two films that occur on both sides of the water-air interface.

In the fugacity based multimedia environmental fate and transport models, the diffusive flux is represented by the product of overall mass transfer coefficient between the two compartments, the surface area between the two compartments, and the fugacity capacity of the contaminant in the compartment from which the diffusive flux occurs:

$$\text{Diffusive flux from water to air} = K_{aw} A_w Z_w, \tag{5.6}$$

where K_{aw} [L/T] is the overall mass transfer coefficient between air and water compartments, A_w [L^2] is surface area of water in interaction with air, and Z_w [M/Pa. L^3]

is the fugacity capacity of the contaminant in water column. All diffusive flux terms can be written in a similar manner.

Similarly, the air-side diffusive flux and the sediment-side diffusive fluxes can be represented as follows:

$$\text{Diffusive flux from air to water} = K_{aw} A_w Z_a , \tag{5.7}$$

$$\text{Diffusive flux from water to sediment} = K_{sw} A_s Z_w , \tag{5.8}$$

where K_{sw} [L/T] is the mass transfer coefficient between water and sediment, A_s [L^2] is the surface area between sediment and water, and Z_a [mol/Pa.L^3] is the fugacity capacity in the air compartments. Between the water column and sediments, diffusive flux occurs between the dissolved portions of the chemical in the sediment matrix. Sediment is made of solid particles and water in between solid particles. Hence, the water fugacity capacity of the chemical is used to describe the diffusive flux between the sediment and the water column.

Material transport involves the transport of a chemical in bulk form from one phase to another. Two examples are the deposition of particles to the bottom of a lake or a river and the resuspension of particles from sediment into the water column. Also listed among the material transport processes are the atmospheric depositions onto water or soil. These processes, which are dependent on a velocity of the flow rate, can be

described by the velocity or the flow rate value and the appropriate fugacity capacity for the contaminant, in the generic form:

$$\text{Material flux from compartment i to compartment j} = Q_{transport} Z_i \ , \qquad (5.9)$$

where $Q_{transport}$ [L^3/T] can represent any of the material flux terms in Figure 1 and Z_i [mol/Pa.L^3] is the fugacity capacity of the contaminant that is being transported.

Atmospheric deposition consists of wet and dry deposition from the air. Wet deposition of a compound from the atmosphere occurs when that compound is scavenged from the atmosphere by rain, snow, or fog. The efficiency of wet deposition of a compound is directly related to its water solubility and vapor pressure. For wet deposition to occur, the compound should dissolve in rain water or snow and be scavenged.

Rain dissolution can be calculated by simply multiplying the rain rate (given as $m^3 \text{rain} / m^2 \text{area}.h$) with the volume fraction of aerosols (very small particles in the air that hold the contaminant) with the area of air in contact with the compartment into which rain dissolution will occur as follows:

$$\mathrm{Q_{rain}} = A_w U_R v_Q \ , \qquad (5.10)$$

where Q_{rain} [L^3/T] is the rain deposition rate, A_w [L^2] is the surface area of water (in the case of an air-water interaction), U_R [L/T] is the rain rate, and v_Q [L^3/L^3] is the volume fraction of aerosols.

Wet deposition incorporates the scavenging of the contaminant into the medium by rain or snow. The same simple approach used in rain dissolution can be used with the incorporation of a scavenging ratio. In the case of an air-water interaction, the equation would be

$$Q_{wet} = A_w U_R Q v_Q \ , \tag{5.11}$$

where Q_{wet} [L^3/T] is the wet deposition rate, A_w [L^2] is the surface area of water, U_R [L/T] is the rain rate, Q is the scavenging ratio, and v_Q [L^3/L^3] is the volume fraction of aerosols.

Dry particle deposition of particle-bound chemicals in a water body depends on the deposition layer, particle size, and macro and micrometeorology. In the simplest case, dry depositional flux can be described by the area of the compartment into which the deposition would occur, the dry deposition rate, and the volume fraction of a contaminant in the aerosol phase:

$$Q_{dry} = A_w U_Q v_Q \ , \tag{5.12}$$

where Q_{dry} [L^3/T] is the dry deposition rate, A_w [L^2] is the surface area of water, U_D [L/T] is the dry deposition rate, and v_Q [L^3/L^3] is the volume fraction of aerosols.

Sediment deposition can be explained in terms of the fall velocity of particles onto which a contaminant is sorbed. The velocity of a settling particle is given by the well-known equation of the fall velocity:

$$V_{fall} = \sqrt{\frac{4(\rho_s - \rho)gd}{3\rho C_D}} \ , \tag{5.13}$$

where g [L/T^2] is gravitational acceleration, d [L] is the effective particle diameter, and C_D is the drag coefficient. Although the particle diameter is a variable, the average particle diameter can be used as the effective diameter of the particles. Hence, a constant average settling velocity can be described for the flow domain. When possible, sediment traps can be used to check the reliability of this equation.

The deposition rate onto the sediments is the result of the multiplication of this settling velocity and the area onto which the particles (contaminant) will fall.

$$Q_{dep} = V_{fall}.A_{sed} = A_{sed}\frac{gd^2}{18}\left(\frac{\rho_s - \rho}{\mu}\right). \tag{5.14}$$

When the shear stress on the bottom of the water column exceeds a critical value, the resuspension of settled sediments occurs. The resuspension rate is directly proportional to the excess shear stress on the surface of the sediments. Several different expressions, all complicated, have been used to describe the resuspension process. Thus, for the

purpose of simplification, an average resuspension rate for the whole water body can be used to estimate the resuspension process. Mackay (2001) suggests an average value for the resuspension of contaminants from a small lake as $1.1x10^{-8}\ m^3/m^2h$ $(0.0001\ m/year)$. Resuspension occurs throughout the entire area of the sediments, so resuspension flow rate Q_{res} $[L^3/T]$ is estimated by multiplying the resuspension rate by the area from which the resuspension occurs:

$$Q_{res} = U_{resuspension}.A_{sed} \ . \tag{5.15}$$

Reactions of a chemical, which can occur in any compartment (i.e., water, soil, sediments, or air) usually involve the degradation of the chemical into other forms, or self-decay. For simplification, first-order decay is assumed for the non-reactive contaminants in this thesis. If we substitute the concentration with fugacity, we have the following equation to represent the reaction terms in our equations:

$$\frac{dF_i}{dt} = kZ_iF_i \qquad i = W, S, A \ . \tag{5.16}$$

The first-order reaction rate constant is the calculated half-life of a chemical in a certain medium.

Combining all of the terms that cause an interaction between the water, air, and sediment phases, the mass balance equation can be written as follows:

$$\frac{\partial(F_W Z_{BW} V_W)}{\partial t} = -\frac{\partial(F_W Z_{BW} V_W u)}{\partial x} + \frac{\partial}{\partial x}\left(D_{Hx} \frac{\partial F_W Z_{BW} V_W}{\partial x}\right) + \left(K_{sw} A_s Z_w + Q_{res} Z_p\right) F_S + \left(K_{aw} A_w Z_w + Q_{dry} Z_{aerosol} + Q_{wet} Z_{aerosol} s\right) F_A - \left(k_w Z_w V_v + Q_{dep} Z_p + K_{aw} A_w Z_w + K_{sw} A_s Z_w\right) F_W \quad , \qquad (5.17)$$

$$V_s Z_{bs} \frac{dF_S}{dt} = (Q_{dep} Z_p + K_{sw} A_s Z_w) F_W - (k_s V_s Z_s + Q_{res} Z_s + K_{sw} A_s Z_w) F_S \quad , \qquad (5.18)$$

where all the transport and transformation processes described so far are combined and substituted for the reactions and interactions term of Equation 5.1. The concentration is written in terms of fugacity, and the transformation is performed through the use of the appropriate fugacity capacity. Equation 5.17 is written for the water compartment and Equation 5.18 for the sediment compartment. The only difference is that the sediments are immobile; therefore, advection or dispersion is not included in the sediment mass-balance equations. The interactions are expressed as a collection of transport and transformation processes. These equations are not only temporally dynamic but also spatially dynamic. Since the surface area and the surface area of sediments as well as their volumes are changing with respect to both time and space, these values change at every node at every time step of the solution.

5.4 Solution to the Contaminant Fate and Transport Equations

Advection-dispersion equations are excessively used in the mathematical models of contaminant transport and water quality within rivers. Unfortunately, with all the advances achieved in the numerical modeling of partial differential equations, an efficient globally-accepted algorithm that solves this advection-dispersion equation has still not been formulated. The equation looks simple; however, mathematically, it exhibits dual behavior. When advection dominates, the equation shows the characteristics of a hyperbolic equation, but when dispersion dominates, it exhibits the characteristics of a parabolic partial differential equation (Holly and Preissman, 1978). Because this changing behavior of the transport phenomenon could occur in a time- and space-dependent fashion, the numerical solution becomes an extremely challenging task. Hence, the solution to advection-dispersion equations has been the target of many researchers in the field of computational fluid mechanics.

The numerous numerical techniques developed and implemented to solve advection-dispersion equation can be divided into three major categories. The first includes Eularian methods, the second Langrangian methods, and the third a combination of both, namely, Eularian-Langrangian hybrid methods. Eularian methods typically use fixed-grid structures whereas Langrangian methods use moving coordinates. Since most major problems in the solution of the equation arise from the advection operator, most studies have focused on the numerical solutions which handle advection. It has been found that

the remaining terms in the equation such as dispersion, decay, or sink/source terms do not pose any additional difficulties for the numerical solution.

Among the numerical schemes developed for the solution of the advection-dispersion equation, the **Q**uadratic **U**pstream **I**nterpolation for **C**onvective **K**inematics with **E**stimated **S**treaming **T**erms (QUICKEST) algorithm has been deemed the best, as it is highly accurate (Manson and Walllis, 1995). This algorithm, a new approach also referred to as the "split-operator," was introduced to overcome the problem of duality in the solution of advection-dispersion equations. The application involves the separation of advection and dispersion operators, and performance of them in a sequential manner. This method effectively handles the stability problems caused by the nature of the equation. The advection equation can be discretized into the form below:

$$(F_w Z_{bw} V_w)_i^{j+1} = (F_w Z_{bw} V_w)_i^j + \Delta t\left(-\frac{\partial}{\partial x}\left(V_w F_w Z_{bw} u\right)\right)^j + \Delta t\left(\frac{\partial}{\partial x}\left(Z_{bw} V_w D_L\left(\frac{\partial F_w}{\partial x}\right)\right)\right)^{j+1} - \Delta t\left(g_w(x,t) Z_{bw} F_w + g_s(x,t) Z_{bs} F_s + g_a(x,t) Z_{ba} F_A\right)^{j+1}, \quad (5.19)$$

which produces cell-averaged values of mass $(F_w Z_{bw} V_w)$ in each control volume, i for the time step, and $j+1$ based on the cell-averaged value at the current time step, j. g_w is the function representing all water column losses, g_s is the function representing all the additions into the water column from sediment phase, and g_a is the function representing all the additions into the water column from the air phase. As the advection operator is

solved explicitly, Equation 5.19 can be separated without altering its mathematical integrity:

$$(F_w Z_{bw} V_w)_i^{j+1} = (F_w Z_{bw} V_w)_i^* + \Delta t\left(\frac{\partial}{\partial x}\left(Z_{bw} V_w D_L\left(\frac{\partial F_w}{\partial x}\right)\right)\right)^{j+1} - \Delta t\left(g_w(x,t) Z_{bw} F_w + g_s(x,t) Z_{bs} F_s + g_a(x,t) Z_{ba} F_A\right)^{j+1} \tag{5.20}$$

$$(F_w Z_{bw} V_w)_i^* = (F_w Z_{bw} V_w)_i^j + \Delta t\left(-\frac{\partial}{\partial x}\left(V_w Z_{bw} F_w u\right)\right)^j \tag{5.21}$$

The procedure for splitting operators, in fact, allows the fluid first to advect for one time step and then to disperse and react (including all transformation and transport processes) in the new advected location. The control volume for the application of QUICKEST algorithm is given in Figure 2 below.

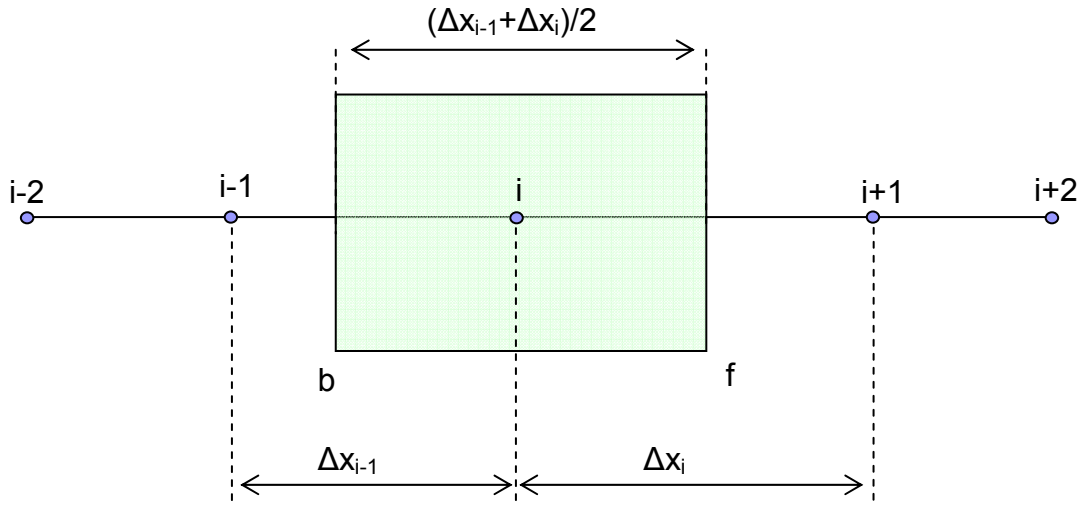

Figure 5.2. The element in the application of the QUICKEST scheme.

The solution procedure can be summarized in Equations 5.22 through 5.26.

$$(F_w Z_{bw} V)_i^{j+1} = (F_w Z_{bw} V)_i^{*} + \Delta t(-g_w(x,t) Z_{bw} F_{wi}^{j+1} + g_s(x,t) Z_{bs} F_{si}^{j+1} + g_a(x,t) Z_{ba} F_{Ai}^{j+1}) + \frac{\Delta t}{0.5(\Delta x_{i-1} + \Delta x_i)} \times \left[\left(V_f^{j+1} Z_{bw} (D_H)_f \frac{(F_{wi+1}^{j+1} - F_{wi}^{j+1})}{\Delta x_i} \right) - \left(V_b^{j+1} Z_{bw} (D_H)_b \frac{(F_{wi}^{j+1} - F_{wi-1}^{j+1})}{\Delta x_{i-1}} \right) \right], \quad (5.22)$$

where the subscript *f* stands for the forward face of the control volume and *b* for the backward face of the control volume. $(F_w Z_{bw} V)_i^{*}$ can be calculated in the current time step for each element *i* as shown in Equation 5.23 below.

$$(F_w Z_{bw} V)_i^{*} = (F_w Z_{bw} V)_i^{j} + \frac{\Delta t}{0.5(\Delta x_{i-1} + \Delta x_i)} \left[F_{wf}^{\ j} Z_{bw} u_f^j V_f^j - F_{wb}^{\ j} Z_{bw} u_b^j V_b^j \right]. \quad (5.23)$$

The velocity and volume at the forward and backward faces of the control volume can be calculated as averages of the nearest two nodes. The calculation of fugacity at the forward and backward faces involves the use of a Courant number (Equation 5.26) and Taylor's series expansion around center node *i* of the control volume.

$$F_{wf}^{\ *} = \frac{1}{2}((F_w)_{i+1} + (F_w)_i) - \frac{c}{2}\left((F_{wi+1} - F_{wi}) - \frac{1}{6}((1-c^2)(F_{wi+1} - 2F_{wi} + F_{wi-1}) \right) \quad (5.24)$$

$$F_{wb}^{\ *} = \frac{1}{2}((F_w)_i + (F_w)_{i-1}) - \frac{c}{2}\left((F_{wi} - F_{wi-1}) - \frac{1}{6}((1-c^2)(F_{wi} - 2F_{wi-1} + F_{wi-2}) \right), \quad (5.25)$$

where c is the Courant number,

$$c = \frac{u\Delta t}{\Delta x} \tag{5.26}$$

5.4.1. Initial Conditions

In the solution for unsteady-state models, initial values of contaminant fugacity need to be specified along the one-dimensional river domain. These values can be given for both the water column as well as the sediment compartment in the following form:

$$\begin{aligned} F_w(x,0) &= F_{w0}(x) \\ F_s(x,0) &= F_{s0}(x) \end{aligned}, \tag{5.27}$$

where F_{w0} and F_{s0} [Pa] represent the initial fugacity distribution along the river network.

5.4.2. Boundary Conditions

Similar to the hydrodynamic model, the contaminant transport model also requires two types of boundary conditions specified at i) external boundaries and ii) internal boundaries of the river system. External boundary conditions are specified at the upstream and downstream points of the river network, and internal boundary conditions are specified at the junction points where a tributary enters the river system.

A constant fugacity value or a fugacity time series can be used as upstream boundary conditions in this model. A no-flux boundary condition, used for the downstream boundary condition, is usually the type of boundary condition where the downstream boundary is far away from the contaminant zone.

$$V_w Z_{bw} \left. \frac{\partial F_W}{\partial x} \right|_{x=L} = 0, \tag{5.28}$$

where L [L] is the total length at the downstream point of the domain. A mass balance equation at the junction points is used for the internal boundary condition as follows:

$$\sum_{k=1}^{m} A_k J_k - A_o J_o = \frac{dM}{dt}, \tag{5.29}$$

where m is the total number of inflowing channels entering a junction, J_k [M/L^2.T] and A_k [L^2] are the total mass flux and area, respectively, at the end of the kth inflowing channel; J_o [M/L^2.T] and A_o [L^2] are the total mass flux and area, respectively, at the beginning of the outflowing channel from the junction; and dM/dt [M/T] represents the change in mass within the junction. In the application of this model, it is assumed that mass change in the junctions is negligible, so the mass balance can be written in the following form:

$$\sum_{k=1}^{m} A_k J_k - A_o J_o = 0. \tag{5.30}$$

5.5 Verification of the Model

In the absence of a fully dynamic, continuous fugacity model, this study modeled a simple hypothetical case using a concentration-based model to verify the developed contaminant transport model. The results of the model developed in this thesis have been converted to concentration and the results compared with those obtained from the performance in the **W**ater Quality **A**nalysis **S**imulation **P**rogram (WASP). The primary purpose of WASP, a program developed by the EPA to evaluate water quality in river networks, is to examine eutrophication in rivers. However, it can also solve for simple toxicants. The example application of this study involved the simple case of a 10 km rectangular channel with constant hydrodynamics, that is, the velocity and river geometry remain constant throughout the entire domain. A simple toxicant, atrazine, was selected as the contaminant because atrazine, being water soluble, did not interfere with other phases around the water column, so it was a good candidate for comparison. Simple linear sorption was selected to account for sediment involvement. All possible transformations were represented with a lumped first-order decay rate. The simulation period was one week.

In the model of this study, all the parameters were similar to those used in the application of the WASP model. A continuous source of 8 ppb atrazine was introduced at the upstream boundary of the channel. The results, shown in Figure 5.3, indicate a very similar trend in the performance of the model. The results were expected to deviate from each other when complications, such as hydrophobic characteristics and river

hydrodynamics, were introduced. Nevertheless, the similarity in the results of this simple case increases the confidence in the developed model.

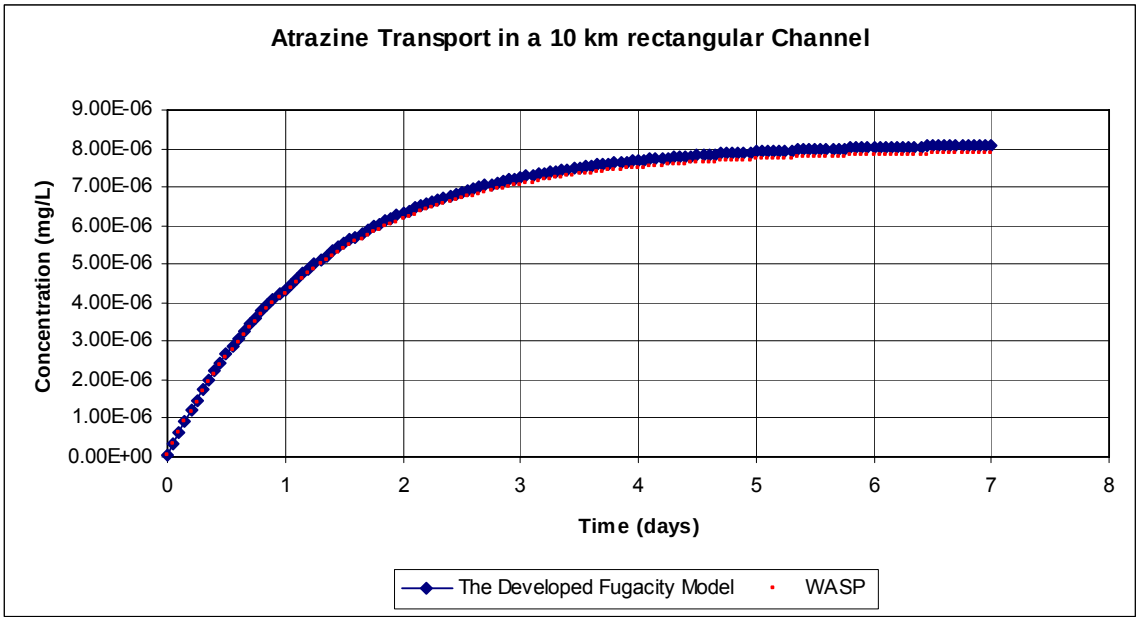

Figure 5.3 A comparison of the results from this model and the WASP model

5.6 Application of the Developed Model to the Altamaha River System

In this research study, a totally dynamic, continuous, fugacity-based contaminant fate and transport model is developed. The Lower Altamaha River system has been chosen as the application of the contaminant transport model as well as the hydrodynamic model. Actually, the same discretization is used for both of the applications.

This portion of the model incorporates the solution of the full form of the Saint Venant equations discussed in Chapter 4 in order to calculate the velocity distribution in a river.

Then the contaminant fate and transport portion developed in this chapter is applied to determine the contaminant distribution in the water column and the sediment compartment of the Altamaha River system.

The contaminants atrazine and PCBs were selected for this part of the thesis as well, as most PCBs enter and stay in the sediments whereas atrazine is mostly in dissolved form in the water column, which will be observed in the results of the application later on.

This model involves the application of fugacity in a continuous model for the first time. Furthermore, for the first time, a fugacity-based fate and contaminant model is linked with the solution of the full form of the Saint Venant equations, which reflect the hydrodynamics of the river.

Depth, width, and velocity values obtained from the application of the hydrodynamic model were used for the water quality portion. The width of the river is used to calculate the surface area of water, together with the length of the element (from one cross-section to the next). The bottom width of the river, which is a constant parameter in the model, is used to calculate the surface area of the sediment compartment in each element. The depth at each cross-section is used to calculate the volume of the water in each element. The depth of the sediment compartment is taken as the active depth of the sediments and kept constant throughout the mode. The velocity at each cross-section is the other output to be used in the application of the water quality portion of the model.

The Altamaha River is the largest river in the state of Georgia as well as a habitat for many species, some of which are in the list of endangered species. The Altamaha River has been designated as a bioreserve in 1991 by the Nature Conservancy of Georgia. Hence, it is extremely important to keep the Altamaha River clean and to have a thorough understanding of the river system to be well prepared in case of contamination. Figure 5.4 depicts a schematic of the Lower Altamaha River system, modeled in this study. The river is composed of a main river and a tributary, the Ohoopee River, which enters the main river. A single junction exists in the river system. Both the hydrodynamics and the contaminant fate and transport models can solve river networks which have a junction.

The model developed is applied to Lower Altamaha River system for different cases that demonstrates the purpose of this effort. These cases examine the effect of contaminant source location with regard to a junction; and the effect of physicochemical characteristics of the contaminant.

In the first application, the contaminant source is introduced into the system at the upstream point of Altamaha River, shown as Altamaha River Main1 in Figure 5.4. In this case the contaminant magnitudes become negligibly small within the 3 km reach of the river. The results in Figures 5.5 through 5.8 show the 30 km of the Altamaha River system (Main 1) before the junction. In the second case of the Altamaha River application, the source is introduced about 4 km upstream of junction where Ohoopee river confluences, also shown in Figure 5.4. The river waters flowing in Ohoopee River are assumed to be uncontaminated, which causes a decrease in the contaminant

concentration after the junction due to dilution. The results of this second application are illustrated in Figure 5.11.

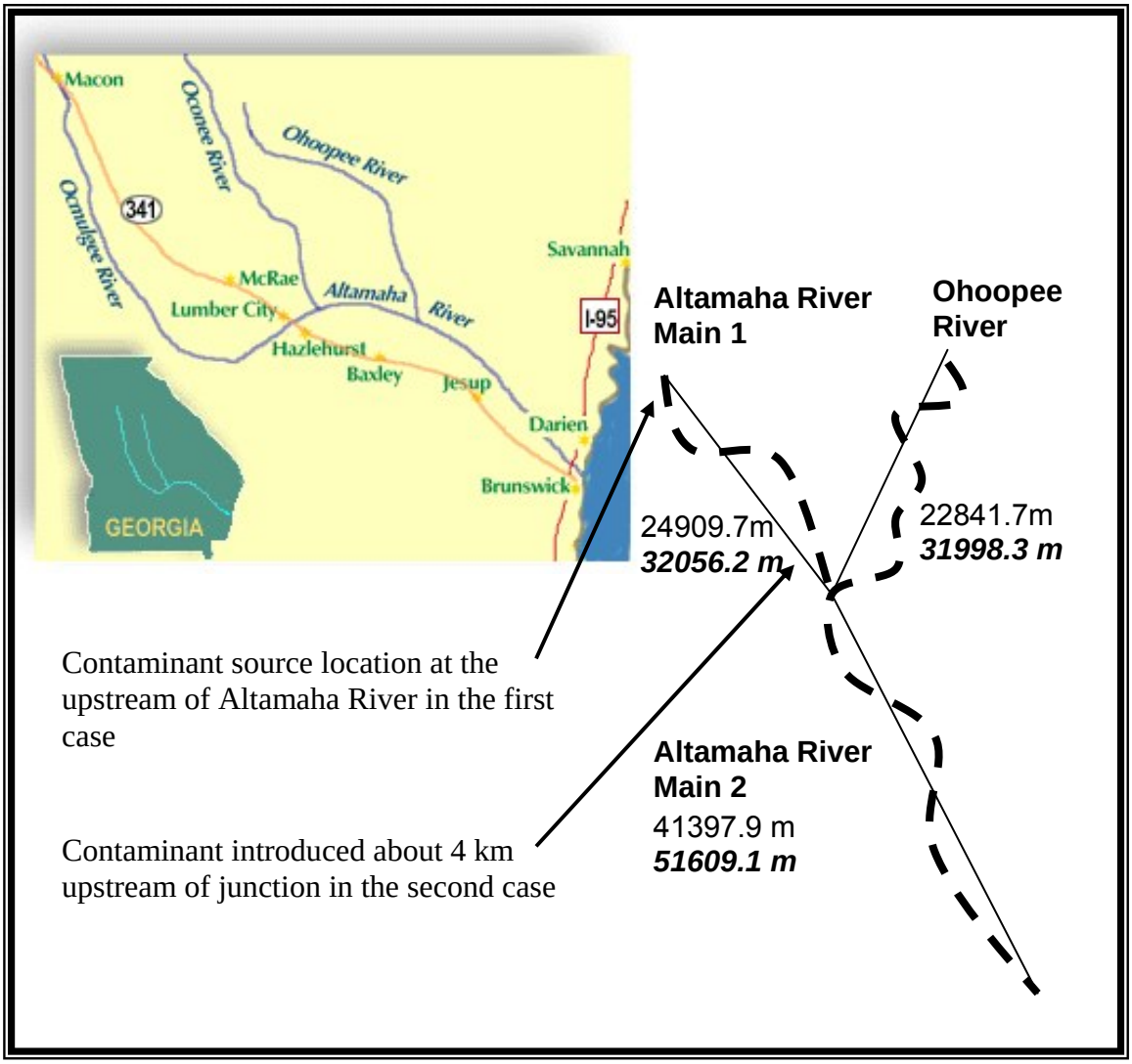

Figure 5.4. Schematic view of the Altamaha River system

In Figure 5.4, the dashed black line shows the meandering natural river, and the black solid line shows the linear distance. The distance between each node, or cross-section, is entered in two different forms, real distance and linear distance. The model calculates the sinuosity factors using these different distance information so that the meandering nature of the Lower Altamaha River system is represented in the model. For the solution of the advection-dispersion equation, linear distances between adjacent nodes are used. The velocity and geometry information already reflects the meandering nature of the solution as sinuosity factors are calculated and used in the solution of the hydrodynamics.

Altamaha River Main 1 has been used in the first part of the application. The nodes are placed where a USGS stream gage exists; the information in each node allows a cross-section of the river to be plotted at each node. Height vs. width information and the elevation and flow values at the start of the modeling are entered at each node.

After the application of the hydrodynamics portion, area and volume values for each element are calculated. The same finite difference grid is used for both the solution of hydrodynamic and contaminant transport equations of the model so as to avoid interpolation, and to run the simulations continuously without a need for transformation. The QUICKEST algorithm, described previously, is applied in the solution of the contaminant transport equation.

A relatively hydrophobic contaminant is chosen to examine the consequences of a hypothetical pollution occurring in Altamaha River, so that the partitioning between water column and sediment phases can more easily be distinguished easily. To

demonstrate the effect of the physicochemical properties of the contaminant, an application with a more water soluble contaminant is also performed. The two contaminants chosen for the demonstration of the model developed in this study are polychlorinated biphenyls (PCBs) and atrazine. Both chemicals are known to be toxic and abundant in nature. Atrazine is the most commonly used agricultural pesticide in the United States. PCBs, although banned in the 1970s, still exist in nature, especially in river sediments, due to their persistent characteristics.

The contaminant is introduced into the river system as a result of a spill or as a result of some dredging activity. As the use of PCBs has been abandoned during 1970s, PCB contamination due to dredging is more plausible for PCBs. During dredging, a small amount of PCBs was released from sediments into water column at a rate of 3×10^{-7} mols/hr. PCB release from sediments continues for a day, and then it ceases. So the source is introduced into water column of the river system. In Figure 5.5, the concentration distribution of PCBs in the 30 km portion of the Main Altamaha River is given when PCBs are released from the deeper bottom sediments due to dredging. As PCBs are released from the sediments, its concentration increases and then decreases in water column. PCBs in the water phase move downstream with the bulk flow as well as volatilize and decay. As PCBs move downstream in the river, their concentration decreases significantly.

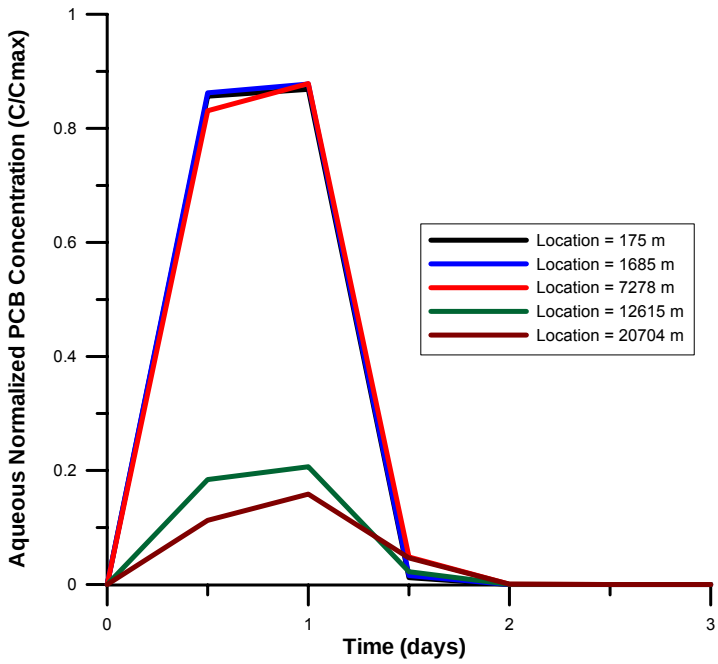

Figure 5.5 Aqueous PCB concentrations in Altamaha River with sediment input

In Figure 5.6, the concentration of PCBs in sediment compartment is given in terms of concentration versus time at different locations in the river. As sediments are immobile, the only reason for PCB concentration to change along the river is due to advection of PCB in the water phase above the sediments and re-entry of PCBs back into the sediment phase as the water flows over sediments. That is, as PCBs are released from sediments into water column, they travel with water, and settle onto sediments in the downstream of the source location. Since PCBs are highly hydrophobic, the partitioning of PCBs into sediment compartment occurs fast. The concentration in sediments increases proportional to the concentration in water column, and then decreases due to chemical processes in the sediment column. After about 10 km, the concentration in water column is significantly lower and this decrease is also reflected in the concentration in sediments.

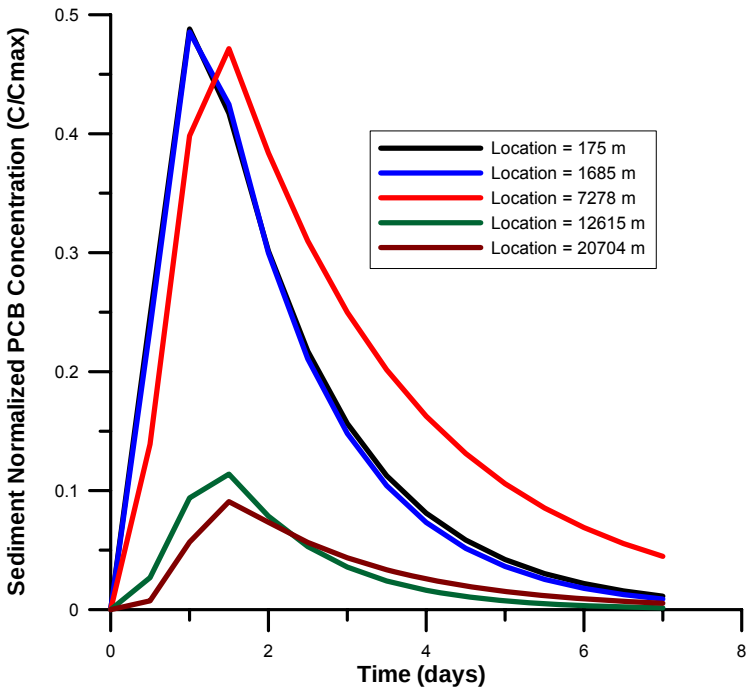

Figure 5.6 PCB concentrations in sediments in Altamaha River

In Figure 5.7, the aqueous and sediment concentrations of PCBs in Main Altamaha River are illustrated in terms of concentration versus location in the river in a non-dimensional form. Immediately after the release of PCBs, the concentration of PCBs in the river is higher in the whole river, although decreasing away from the source. As time continues, and release of PCBs into the water column stops, the aqueous concentration decreases significantly. The irregularities in the shape of cross-sections of a natural river cause the shape concentration change along the channel. There are many factors such as the change in the geometry of the river, rise and fall of the water levels, the velocity in the channel affecting the transport of a contaminant; it is very hard to identify the reasons for the sudden changes in the concentration along the river.

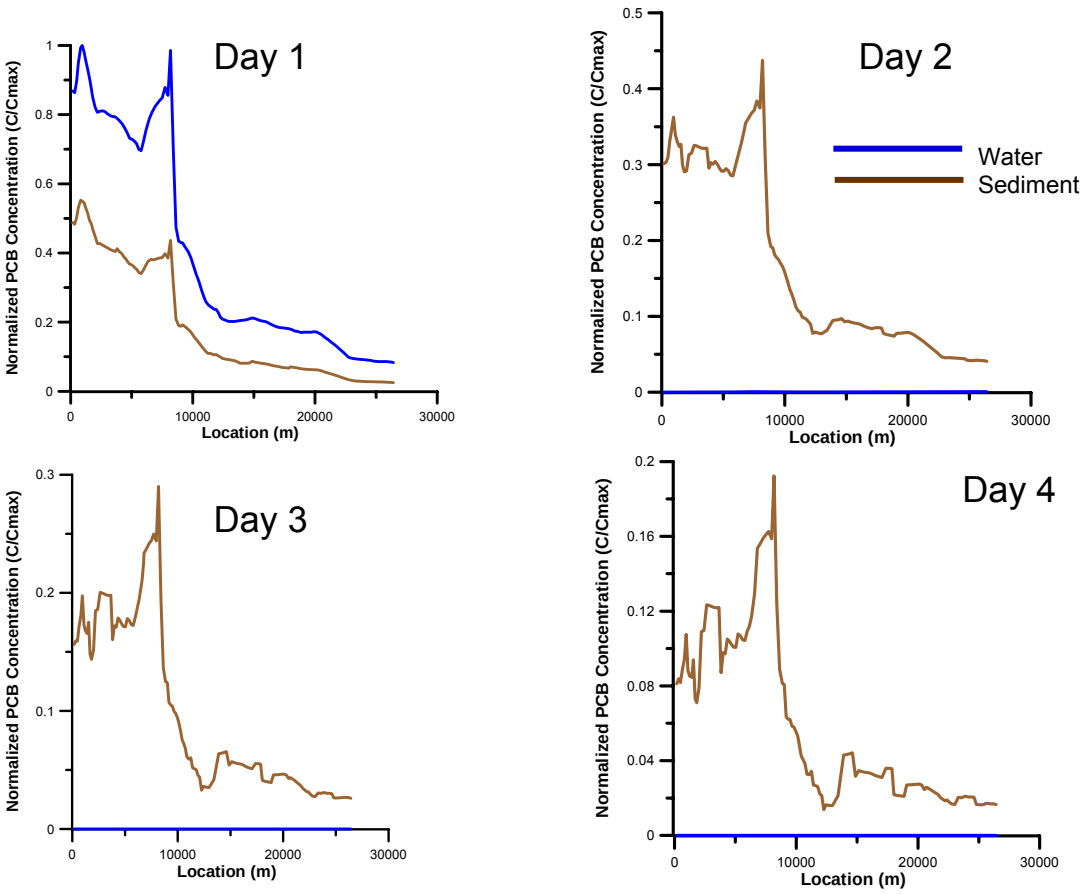

Figure 5.7 Aqueous and sediment PCB concentrations along Altamaha River

As Figure 5.7 demonstrates, during the first day, both the PCBs in water column and the sediments can be observed. However, starting from the second day, the PCBs that can be observed are in the sediment phase alone.

Figure 5.8 shows the total PCB concentration in both the aqueous and sediment phases. The concentration rises and then falls rapidly in water phase, while PCB partitions into sediments slowly and releases back into the water again slowly.

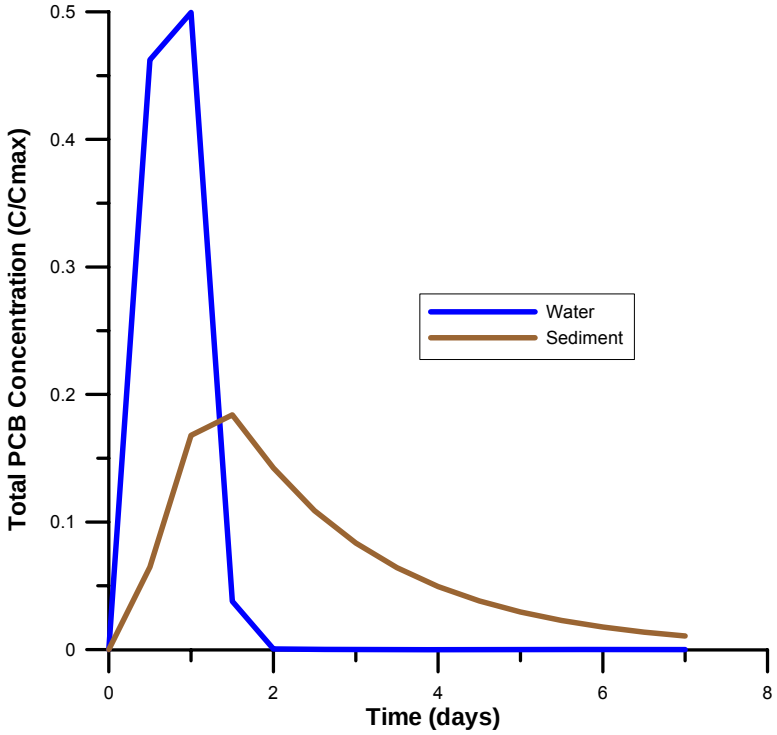

Figure 5.8 Total PCB concentration in Altamaha River

The model was also applied to a more water soluble contaminant to compare the results between two contaminants with distinctly different physicochemical properties. In Figures 5.9 and 5.10 we show the results of the model simulation with atrazine and PCBs at three different locations in the river. The concentrations of atrazine in water column and sediment phases are shown in Figure 5.9. Comparing Figure 5.9 (a) and (b), atrazine concentration in sediments seems negligible compared to aqueous atrazine concentration. Atrazine in water column moves with water very rapidly without being distributed among different phases. The movement is almost like a plug through the river reach. As atrazine moves downstream, a small portion partitions into the sediments and then immediately releases back into the water column. PCBs, on the other hand, are almost negligible in

water column compared to the PCB concentrations in sediment phase. Water column concentrations are about 4 magnitudes lower than sediment concentrations as seen in Figure 5.10. PCBs partition to solid phases almost immediately, and PCBs are then released from the sediments into the water column slowly. A residual PCB concentration stays in the sediment particles, and a corresponding concentration of PCBs in water column is observed which is in equilibrium with this residual concentration. Figures 5.9 and 5.10 show that the fate of a contaminant depends on its physicochemical characteristics significantly and this is reflected in the way it behaves in nature.

Furthermore, the observations in Figures 5.9 and 5.10 emphasize the importance of including all available phases in a river system in the solution of contaminant fate and transport models. If only aqueous phase was considered, we would have missed the PCB accumulation in sediment compartment, and the results would have been misleading.

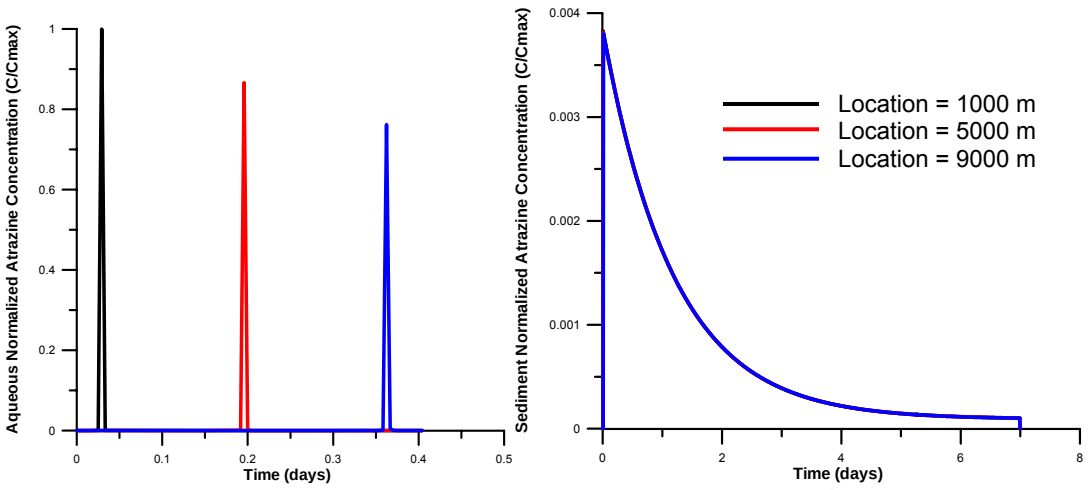

Figure 5.9 (a) atrazine concentration in water column (b) atrazine concentration in sediment compartment

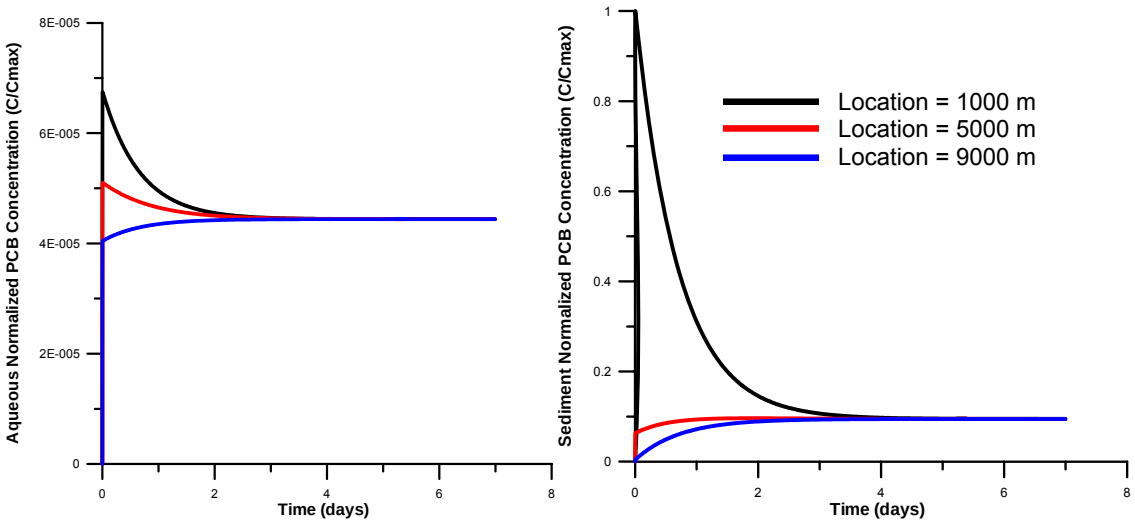

(a) (b)

Figure 5.10 (a) PCB concentration in water column (b) PCB concentration in sediment compartment

The model developed is very versatile; it can be used both with single reach river application as well as river networks. As mentioned before, the model is also applied to a case, where the contaminant is introdced into the main Altamaha River about 4 km above the junction of Ohoopee River. Since it is assumed that clean water is flowing in Ohopee River, the concentration of PCB in the main river decreases after the junction. The results of this application are shown in Figure 5.11 below. After the confluence of Ohoopee River with its clean waters, the PCB concentration both in water column and sediment compartments decrease due to dilution effects.

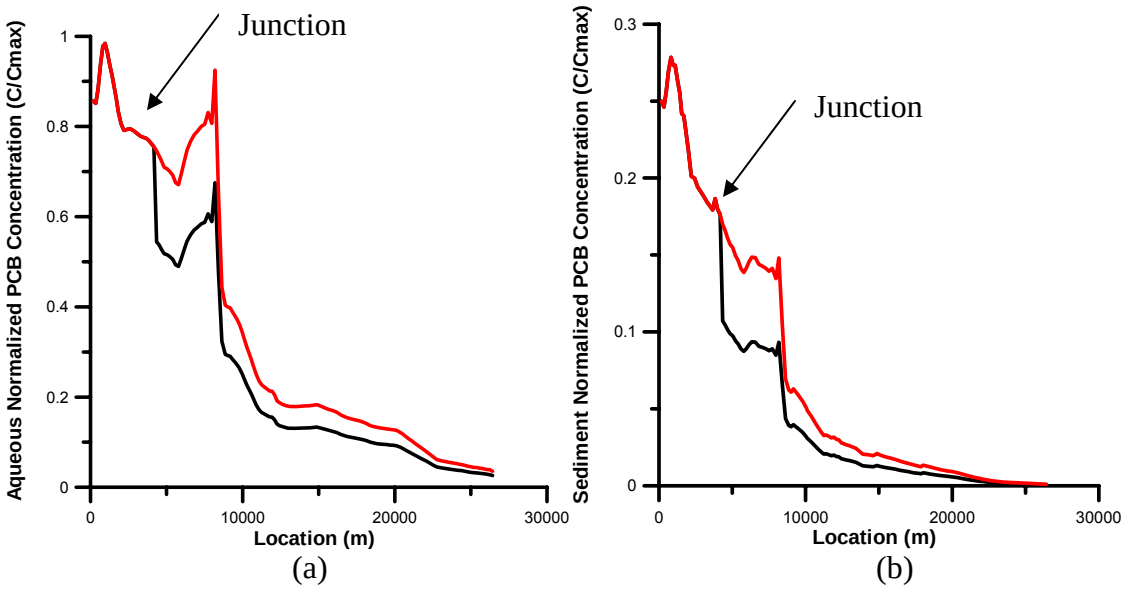

Figure 5.11 (a) Aqueous PCB concentration and (b) sediment PCB concentration in the river network where there is a junction at 4336 m and contaminant is input into water column

In order to evaluate the effect of a junction on contaminant concentrations, the Lower Altamaha River system simulation discussed above is repeated this time as a single river reach application. In this case the contaminant is again introduced to the river 4 km before the junction. For the single river channel case Ohoopee River was excluded and only Altamaha River Main 1 and 2 reaches are used in the simulation. The results obtained are shown separately for the aqueous and sediment phase concentrations of PCBs in the river both with and without the presence of the junction in Figure 5.11. If Ohoopee River did not confluence with the Altamaha River, the concentration of PCBs would have been higher in the river. As can be seen the existence of Ohoopee River decreases the contaminant concentration in Altamaha River. When the waters flowing in Ohoopee River, which are free from PCB contamination, combine with contaminated

waters of Altamaha River, the amount of contamination in the water column reduces due to dilution.

In the solution procedure, a junction is treated as an internal boundary condition. At the junction, a mass balance condition is used to ensure the conservation of mass. As mass can neither be created nor can be lost, the mass of the contaminant stays same before and after the junction. However, volume of the water flowing in the river system increases when the tributary is combined with the main channel. Hence the concentration of the contaminant decreases. When the PCB concentration in water column decreases, a shift occurs in the equilibrium of the phases of the system, and more contaminant is released from the sediments to attain the equilibrium once more. Therefore, the concentration of PCBs in the sediment phase also decreases as a result of the presence of the junction. This observation is important and reflects the dynamic behavior of phase equilibrium within the system which needs to be considered.

In this thesis, a dynamic and continuous model has been developed. First, the Saint Venant equations are solved to determine the velocity, depth and width variables along the river at each node at each time step. Then, this information is used in the solution of contaminant fate and transport model. Fugacity, a thermodynamic equilibrium criterion, is used as its use makes it easier to follow a chemical from one phase to another within the system.

In past, the use of dynamic fugacity analysis only referred to unsteady-state solution of a series of mass-balance equations in a well-mixed setting. In this study, dynamic fugacity application refers to the solution of a totally continuous and dynamic system, spatially as well as temporally. For the first time, an advection-dispersion equation has been developed and used with fugacity as the unknown variable instead of the concentration. Coupling the advection-dispersion equation with a mass-balance equation developed for the sediment phase, we have a dynamic, continuous fate and transport model in rivers. With this model, a river system does not need to be solved in a discreet manner as it is done using "reactors in series" approach, but instead continuous solutions along the river reach can be represented.

By applying the model to two contaminants with different physico-chemical characteristics, the importance of the presence of phases in an environmental setting and the dynamic equilibrium conditions among phases has been emphasized. For more hydrophobic contaminants, a model examining only aqueous phase transport would not capture the true fate of the chemical in a river system. PCBs, the more hydrophobic contaminant, partition into the sediments and prefer to stay in the sediments. Atrazine, the more water soluble contaminant, prefers to stay in the water column, and flow in the river, almost as a plug flow. It is easy to observe these differences with the model developed in this paper.

In another numerical experiment demonstrated in this study, the consequences of a dredging activity at the head waters of Altamaha River and at a point 4 km upstream of

Ohoopee river confluence are examined. The use of PCBs has been banned in 1970s; their hydrophobicity enables them to be still abundant in the sediments of many rivers. PCBs are released from sediments for a period of a day in the application of the model developed in this study. First, the solution of Saint Venants equations yields the velocity, depth, and width of Lower Altamaha River at each cross-section at all time steps. The depth and width are used to calculate the volume and surface area of each element of the river.

Lower Altamaha River is a river network with three channels and one junction. The model developed is versatile in its application. It can be applied to a river network as well as a single river. In the first solution, the contaminant source is placed about 32 km upstream of the junction; therefore, the contaminant does not reach the junction in significant concentrations. The solution is similar to a single river solution. In the second application, the source is located 4 km above the junction, hence the effect of the junction on the solution can be observed.

The water quality model, developed in this paper, is not only novel but also brings with it the accuracy of using velocity patterns that is obtained from a hydrodynamics model instead of averages or constant values for each element as well as using more than one phase in the analysis to represent the partitioning of the contaminants. This approach can be expanded to account for other phases as well based on the objective of the modeling activity. One addition can be towards the inclusion of biological activity in the system. The transport and transformation processes can be modeled more or less rigorously

according to the model requirements, giving the user a lot of flexibility. Our ongoing studies on this subject are directed towards that goal.

CHAPTER 6

INCORPORATION OF A BIOFILM COMPARTMENT FOR THE MULTI-SPECIES FATE AND TRANSPORT MODEL

One of the most essential aspects of modeling is the transformation of a chemical in a water body. Such a transformation includes processes such as hydrolysis or photosynthesis, which do not require any microbial involvement. However, in nature, particularly in aquatic environments, many microorganisms live and interact with chemicals. In the earlier parts of this thesis, all possible processes, including hydrolysis, photosynthesis, decay, and even biodegradation, are lumped together as one single parameter called the "decay rate constant." This parameter is derived using the half-life of a chemical in a certain compartment given in reference books. Although this approach simplifies the modeling efforts and creates reasonable results, it cannot be applied to all chemicals. For chemicals that undergo a decidedly biological transformation, the biotic processes that take place must be modeled.

One such case is the modeling of the fate and transport of a multi-species compound such as trichloroethylene (TCE), which definitely undergoes biological reactions. TCE, an abundant contaminant, can produce other harmful chemicals under certain conditions.

Depending on the dissolved oxygen concentration, TCE can undergo both aerobic and anaerobic transformations, but each produces different results. In the case of aerobic transformations, TCE is totally mineralized, producing carbon dioxide and water. In the case of anaerobic transformations, however, TCE yields daughter products, that is, by-products. Daughter products are even more harmful to humans than TCE itself. Therefore, although TCE may disappear from an aquatic system, a model must account for the formation of more toxic chemicals in the form of daughter products.

In this chapter, biological transformations are added to the developed model, which is modified so that it allows for the modeling of the fate and transport of more than one chemical. This study has selected TCE and its daughter products for incorporation into the model.

Biological transformation, or simply biotransformation, is the transformation of organic chemicals through microbial activities. Such biological transformations can occur under both aerobic and anaerobic conditions. In biodegradation, microorganisms can decompose not only conventional organic material but also anthropogenic contaminants such as industrial solvents and pesticides to obtain carbon or energy. Unlike biodegradation, biotransformation reactions do not produce a carbon or energy source for the microorganisms. Still, they are important processes, as they can change toxic chemicals into either non-toxic or more toxic compounds.

When TCE undergoes anaerobic transformation, called reductive dechlorination, it loses its chlorine atoms one by one. With the removal of one chlorine atom, dichloroethylene (DCE) is produced. Removal of a second chlorine atom produces vinyl chloride (VC). The removal of the only remaining chlorine atom causes the production of ethane, the harmless end product.

6.1. Biofilm Compartment

The microbial population in aquatic environments is generally condensed on the sediment-water interface, where they form a biofilm. The occurrence of a biofilm has been proven in many experiments. In one such experiment, the scientists inserted a glass plate into a river and observed the formation of microbial populations on the surface of the plate. By the end of a day, the researchers identified various species of microorganisms living in communities on the glass plate (Costerton et al., 1987; Marshall, 1992). These microbial communities form biofilms in the aquatic environments. The formation of biofilms is, in fact, a survival mechanism, as microorganisms that have better access to nutrients are protected from scouring and are able to form symbiotic relationships. Many scientists have proven attached biofilms more effective in removing organic carbon in shallow streams and lakes compared to suspended biomass (Chuco, 2004).

This thin layer on top of sediments is where all the biological action occurs. If TCE is introduced into an aquatic environment, it undergoes microbial transformation and yields

product intermediates such as DCE and VC in this thin layer. Hence, it is advisable that this portion of the sediments be treated separately in the model and that all biotransformations are dealt with here. Several modelers accounted for the aerobic portion of sediments; however, they did not treat it separately, but instead acknowledged the existence of aerobic bacteria on the very top of the sediments. QUAL2E, a commonly used software developed by the U.S. Army Corps of Engineers, accounts for a 1 mm thick layer of aerobic microorganisms. Nevertheless, this acknowledgement is the extent of their attention.

By including the top of sediments, the biofilm layer, as a separate compartment in the water quality model, this model realistically accounts for all the transformation processes, including not only the aerobic activities of microorganisms but also the anaerobic activities and cometabolic processes. "Cometabolism" is the transformation of a substrate that cannot be used as a carbon or energy source but that can be degraded in the presence of other chemicals. Through cometabolic activities, the mixture of microorganisms existing in the top portion of sediments can degrade TCE and its daughter products.

Typically, a mixture of heterotrophic and autotrophic bacteria as well as aerobic and anaerobic bacteria live in the biofilm. The dynamics of the biofilm are dependent on nutrient penetration. Since organic materials are usually abundant in rivers and lakes, the main determining parameter becomes oxygen. The oxidation state in the biofilm changes with depth as oxygen cannot penetrate the biofilm thickness. Oxygen is also the main

separator of aerobic and anaerobic microorganisms. However, oxygen is very rapidly consumed in most lakes due to the high rate of mineralization. Thus, the oxygen penetration depth is generally less than 10 mm and results in the formation of anoxic environments in sediments. In aerobic sediments, heterotrophic bacteria can completely mineralize organic matter to carbon dioxide. In anaerobic sediments, organic matter is decomposed in more complex and less energy efficient pathways that require colonies of physiologically different microorganisms. Each of the microbial groups participates in the decomposition process, forming an end product that another group of microbes uses until the decomposition is complete (Holmer and Storkholm, 2001; Tank and Dodds, 2003).

The aerobic and anaerobic portion of the biofilm can be determined using the oxygen penetration depth. The number of microorganisms present in the biofilm can also be divided into aerobic and anaerobic groups using the oxygen penetration depth.

Biofilms, so far, have not been used as part of a big scale water quality model such as the one in this study. In the literature, they have been used in a water treatment unit process, called a biofilm reactor, the purpose of which was to clean TCE contamination in an engineered environment. These reactors have been designed based on the operating principles of biofilms observed in nature (Gerritse J et al., 1995; Rauch et al., 1999; Tartakovsky et al., 2005). In this study, biofilm reactor models have been used to determine the fundamental activities taking place in a biofilm environment.

A mixed culture of bacteria grows in a biofilm that forms between the liquid phase and the underlying solid phase. An ideal biofilm system is depicted in Figure 6.1 below.

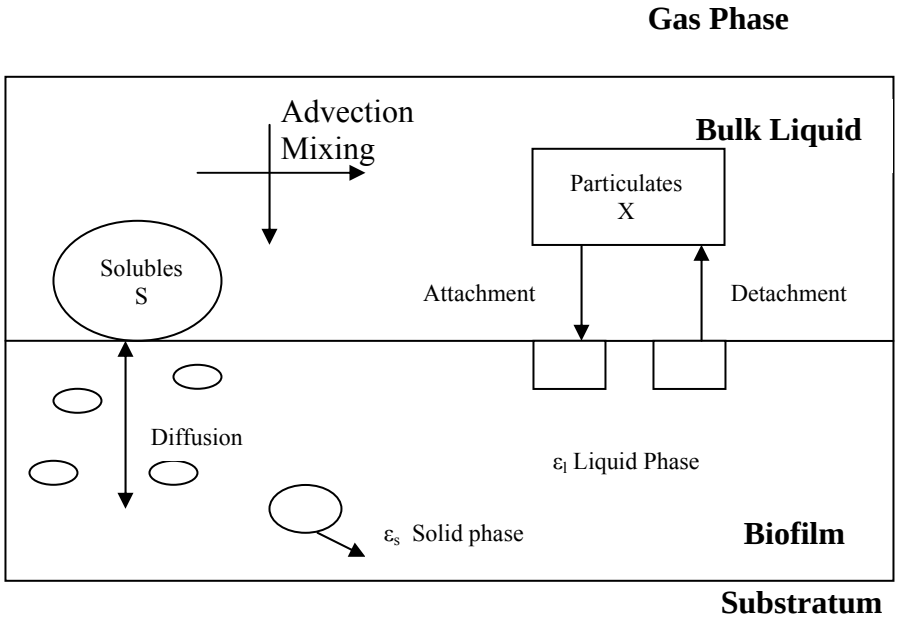

Figure 6.1. Transport processes in a biofilm.

In the biofilm seen above, dissolved substances are transferred from the bulk liquid into the biofilm and then transported by molecular diffusion. Particulate components cannot be transferred inside the biofilm, but they will be adsorbed onto the biofilm (denoted as attachment). The reverse phenomenon of the displacement of particulate components from the biofilm is consequently termed detachment. Detachment is calculated using a detachment rate together with the velocity of the biofilm surface movement perpendicular to the substratum. (It corresponds to the resuspension of sediments in our system.)

The biofilm consists of two phases: 1) a liquid phase in which the dissolved substances are transported, and 2) a solid matrix that consists of several species of bacteria as well as particulate substrate and inert material. The basic consideration is whether the substrate fully penetrates the length of the biofilm or not. If the biofilm is fully penetrated, the reaction occurs throughout the entire length of the biofilm. However, if the substrate can penetrate partially (called substrate limitation), the reaction takes place only over a certain depth of the biofilm (Rauch et al., 1999), which becomes an important issue for oxygen penetration. Whereas the upper part of the biofilm, where oxygen penetrates, becomes an oxidized environment in which aerobic bacterial activities prevail, the lower part of the biofilm, where oxygen cannot penetrate, becomes reduced and anaerobic. A number of studies have demonstrated the co-existence of aerobic and anaerobic populations in a biofilm under oxygen-limited conditions (Gerritse J et al., 1995).

According to the model proposed by Tartakovsky (2005), oxygen consumption by aerobic bacteria leads to a steep oxygen gradient across the biofilm. Therefore, the interior parts of a sufficiently thick biofilm become anoxic and provide a suitable environment for the growth of anaerobic methanogenic bacteria. Simultaneously, methane production by methanogens in the presence of oxygen provides a suitable environment for the growth of aerobic methanotrophic bacteria in the outer layer of the biofilm. Thus, both aerobic and anaerobic populations coexist in the same reactor system. Although both methanogens and methanotrophs from these populations are capable of degrading TCE, they follow different degradation mechanisms. Therefore, three different

populations of bacteria—anaerobic bacteria, aerobic heterotrophic bacteria, and aerobic methanotrophic bacteria—coexist in the biofilm.

The three bacteria populations require a primary carbon source that needs to be transformed into methane for anaerobic bacteria to survive. The anaerobic degradation of TCE results in the sequential formation of dichloroethylenes (DCEs) and vinyl chloride (VC). Aerobic degradation of TCE, DCEs, and VC by methanotrophic bacteria proceeds co-metabolically. The intermediates of aerobic degradation are readily consumed by heterotrophic bacteria, thus resulting in complete mineralization to carbon dioxide.

The biofilm is divided into aerobic and anaerobic fractions according to the depth of oxygen penetration. Each fraction is assumed to have constant substrate concentrations. The depth of oxygen penetration is determined according to the following formula (Tartakovsky et al., 2005):

$$\delta = \sqrt{\frac{2D_e C_{O_2}}{q_{\max} X_{\max}}} \tag{6.1}$$

where δ [L] is the oxygen penetration depth, D_e [L^2/T] is the effective diffusivity of oxygen in the biofilm, C_{O2} [M/L^3] is the concentration of oxygen, q_{max} is the maximal specific rate of oxygen uptake, and X_{max} [M/L^3] is the biofilm density.

In the biofilm compartment, a constant bacterial population is assumed as a result of steady-state conditions in the aquatic environment with respect to microorganisms. In the

aquatic system, a constant and abundant primary carbon source is assumed to exist, so all bacterial activities can occur. Another assumption used for the model is a constant dissolved oxygen concentration in the water column of the aquatic system, a lake or a river. The dissolved oxygen distribution typically varies seasonally in water bodies due to temperature variations.

The biofilm compartment, with its liquid phase and solid matrix, is an extension of the sediment compartment, so it has the same physical characteristics. Hence, the same density, porosity, and fugacity capacity information of the sediment compartment can be used for the biofilm compartment.

6.2. TCE Biotransformations

Biodegradation of TCE occurs both aerobically and anaerobically. Reductive dechlorination of TCE under anaerobic conditions causes the formation of less chlorinated species such as dichloroethylenes (DCE) and vinyl chloride (VC) as intermediates. These transformations occur in considerably reduced conditions and the dechlorination rate decreases as the number of chlorine atoms in the compounds decreases, causing the accumulation of intermediates. On the other hand, both TCE and its intermediates can biodegrade aerobically, and degradation increases as the number of chlorine atoms per molecule decreases, especially in the co-metabolic transformation of TCE, DCE, and VC by methanotrophic bacteria. Thus, a combination of aerobic and anaerobic pathways can result in the total degradation of TCE and its intermediates

(Rauch et al., 1999; Tartakovsky et al., 2005). These pathways can be seen in Figure 6.2 below:

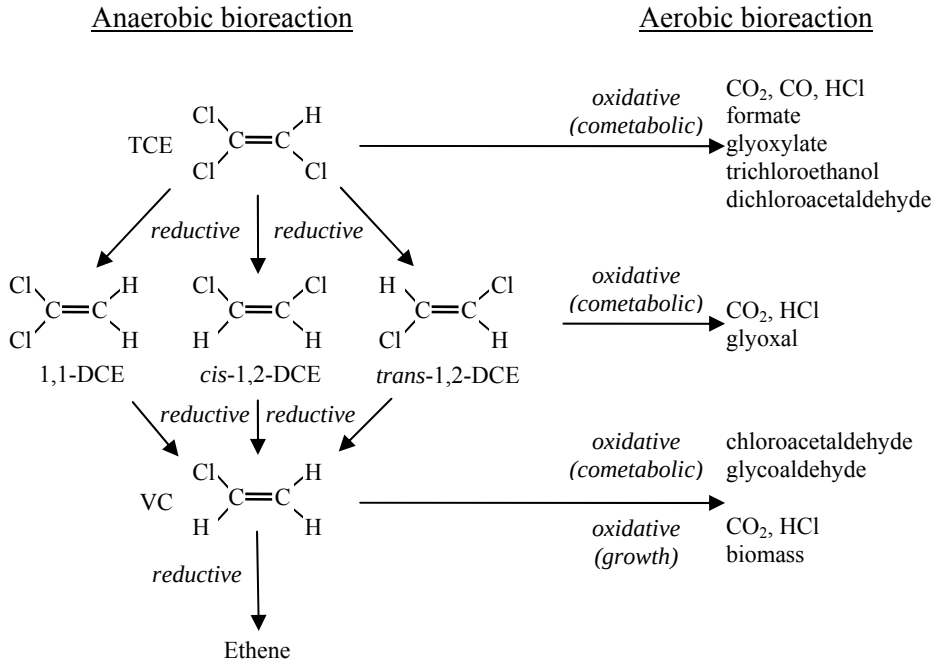

Figure 6.2. Aerobic and anaerobic pathways of TCE biodegradation

In another representation, the reactions in the biofilm compartment and the formation of aerobic and anaerobic zones in the compartment due to limited oxygen penetration can be seen in Figure 6.3 below:

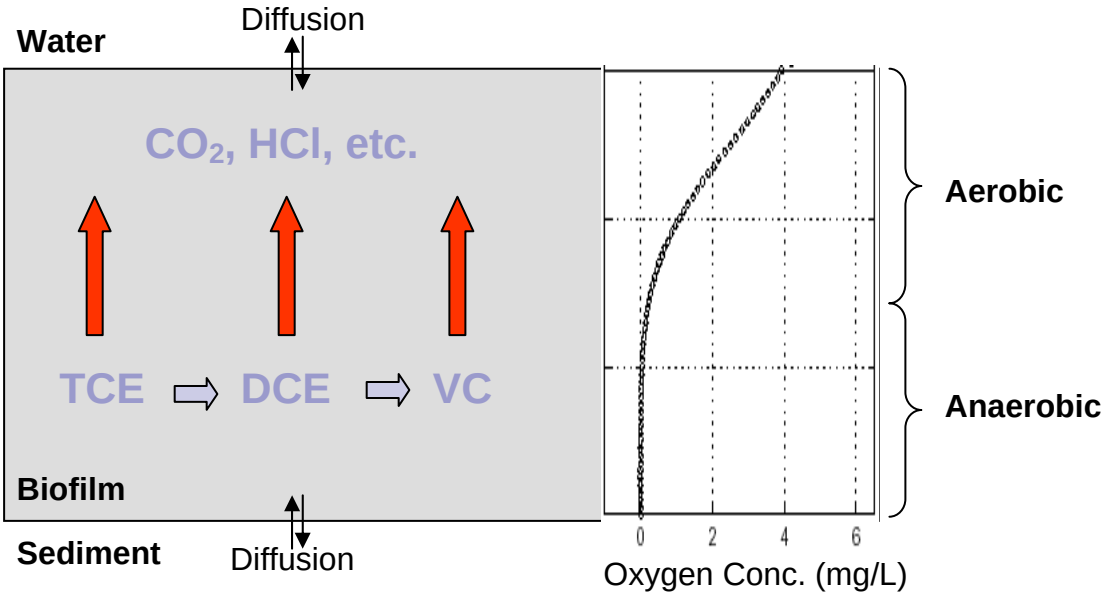

Figure 6.3. TCE biotransformation processes and oxygen penetration in a biofilm

Then, the reactions in the biofilm compartment for the biotransformation of TCE and its daughter products, DCE and VC can be developed. These are the reaction rates, r_{TCE}, r_{DCE}, and r_{VC} [M/T], can be written in the following form:

$$
\begin{aligned}
r_{TCE} &= -k_{TCE}^{anaerobic} V_{b_{an}} Z_{TCE} F_B^{TCE} - k_{TCE}^{aerobic} V_{b_a} Z_{TCE} F_B^{TCE} \\
r_{DCE} &= k_{TCE}^{anaerobic} V_{b_{an}} Z_{TCE} F_B^{TCE} - k_{DCE}^{anaerobic} V_{b_{an}} Z_{DCE} F_B^{DCE} - k_{DCE}^{aerobic} V_{b_a} Z_{DCE} F_B^{DCE} \\
r_{VC} &= k_{DCE}^{anaerobic} V_{b_{an}} Z_{DCE} F_B^{DCE} - k_{VC}^{anaerobic} V_{b_{an}} Z_{VC} F_B^{VC} - k_{VC}^{aerobic} V_{b_a} Z_{VC} F_B^{VC}
\end{aligned}
\qquad (6.2)
$$

Where $k_{TCE,}$ k_{DCE} *and* k_{VC} [1/T] are the first order reaction rate constants for biodegradation of TCE, DCE, and VC in bioiflm, V_b [L^3] is the volume of the biofilm compartment and F_B^{TCE}, F_B^{DCE}, *and* F_B^{VC} [Pa] are the fugacities of TCE, DCE, and VC in biofilm compartment; and $Z_{TCE,}$ Z_{DCE} ,*and* Z_{VC} [M/Pa.L^3] are the fugacity capacities of TCE, DCE, and VC in the biofilm compartment.

6.3 The Governing Equations for the Fate and Transport of TCE and its Daughter Products in a Lake

A lake system consists of different phases which are in dynamic interaction with each other. These interactions play an important role in the persistence of chemicals in each phase. Air, water, and sediment phases make up the major three compartments of a lake system. In addition to these three compartments, in this study we also include a thin biofilm layer on top of the sediments to model the microbial activities as the forth compartment.

All four compartments are assumed to be well mixed. The interactions between the air and water compartments involve wet and dry deposition from air to water and diffusive flux at the air and water interface. The interactions between the biofilm and water compartments involve diffusive flux at the water-sediment boundary, deposition of water particles onto biofilm, and resuspension of particles from biofilm. Between biofilm and sediment compartments, diffusive flux is the main interaction. In addition, water outflows from the lake via tributaries and chemicals are removed through wind-induced air flow just above the lake. All the microbial activities occur in the biofilm compartment. Further, in air, water, and sediment compartments chemicals may follow first-order decay reactions, based on their their half-lives. This also causes removal of the compound from the overall system. All of these interactions and processes represented in the developed model are illustrated in Figure 6.4 below.

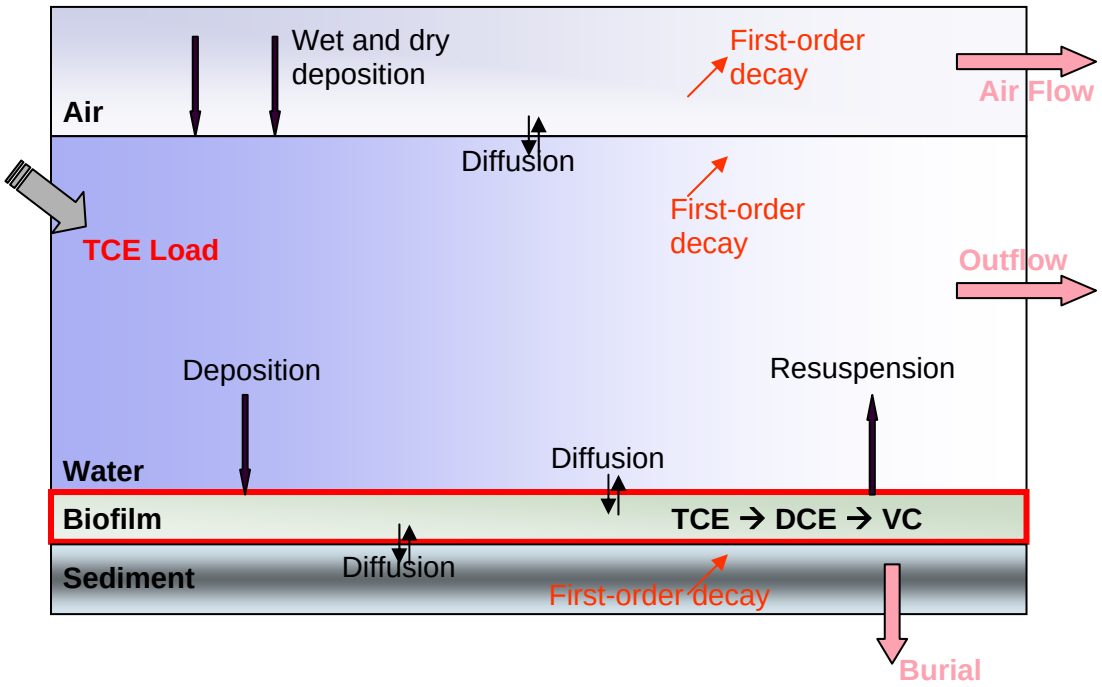

Figure 6.4 The four compartments and processes and interactions in the lake system

Assuming that TCE is introduced into the water column as a source rate, the mass-balance equation for the TCE in the water column would be as follows:

$$V_w Z_{bw} \frac{dF_W^{TCE}}{dt} = S_{TCE} + (K_{aw} A_w Z_w + Q_{dry} Z_{aerosol} + Q_{wet} Z_{aerosol}) F_A^{TCE} + (Q_{res} Z_p + K_{bw} A_s Z_w) F_B^{TCE} - (k_w V_w Z_w + Q_{dep} Z_p + Q_{out} Z_{bw} + K_{aw} A_w Z_w) F_W^{TCE} \quad (6.3)$$

where F_W,, F_A,, and F_B [Pa] are the fugacities in water, air, and biofilm, respectively. V_w [L^3] is the volume of the water column, V_b [L^3] is the volume of the biofilm compartment, A_w [L^2] is the surface area of the water column, A_s [L^2] is the surface area of the biofilm and sediment compartments (the biofilm compartment is the top 10 mm of sediments and have the same surface area). K_{bw} [L/T] is the mass transfer coefficient between the

biofilm and the water column, and K_{aw} [L/T] is the mass transfer coefficient between the water and the air. Z_w [M/L^3.Pa] is the water fugacity capacity, Z_a [M/L^3.Pa] is the air fugacity capacity, Z_p [M/L^3.Pa] is the suspended particle fugacity capacity, Z_{bw} [M/L^3.Pa] is the bulk water fugacity capacity, and $Z_{aerosol}$ [M/L^3.Pa] is the aerosol fugacity capacity. Q_{dry} [L^3/T] is the dry deposition rate, Q_{wet} [L^3/T] is the wet deposition rate, Q_{res} [L^3/T] is the resuspension rate, and Q_{out} [L^3/T] is the rate of water flow out of the lake through tributaries.

When introduced into the system, TCE will partition onto sediments in the water phase, volatilize, advect out of the system, and biodegrade with the reactions discussed in the biofilm model (r_{TCE}), resulting in the production of intermediates, DCE, and VC. In turn, they will also partition in the system and continue biodegradation. Equation (6.4) below shows the mass-balance equation of TCE in the biofilm compartment, where it produces DCE

$$\begin{aligned} V_b Z_{bb}^{TCE} \frac{dF_B^{TCE}}{dt} = & (K_{sw} A_s Z_w^{TCE}) F_S^{TCE} \\ & + (Q_{dep} Z_p^{TCE} + K_{bw} A_w Z_w^{TCE}) F_W^{TCE} \\ & - (K_{bw} A_w Z_w^{TCE} + K_{bs} A_s Z_s^{TCE}) F_B^{TCE} - r_{TCE} \end{aligned} , \qquad (6.4)$$

where F_W,, F_S,, and F_B [Pa] are the fugacities in water, sediment, and biofilm respectively. A_w [L^2] is the surface area of the water column, A_s [L^2] is the surface area of the biofilm and sediment compartments K_{bw} [L/T] is the mass transfer coefficient between the biofilm and the water column, Z_w [M/L^3.Pa] is the water fugacity capacity,

Z_{bs} [M/L^3.Pa] is the bulk sediment fugacity capacity, Z_p [M/L^3.Pa] is the suspended particle fugacity capacity, and Z_{bb} [M/L^3.Pa] is the bulk biofilm fugacity capacity. Q_{dep} [L^3/T] is the deposition rate of suspended particles. r_{TCE} is the reaction term that produces DCE through microbial reductive dechlorination as described previously. In turn, DCE goes through reductive dechlorination in the biofilm and produces VC. The same equation can be written for DCE and VC as follows:

$$\begin{aligned} V_b Z_{bb}^{DCE} \frac{dF_B^{DCE}}{dt} &= (Q_{dep} Z_p^{DCE} + K_{bw} A_w Z_w^{DCE}) F_W^{DCE} \\ &+ (K_{sb} A_s Z_b^{DCE}) F_S^{DCE} \\ &- (Q_{dep} Z_p^{DCE} + K_{bw} A_w Z_w^{DCE} + K_{bs} A_s Z_b^{DCE}) F_B^{DCE} - r_{DCE} \end{aligned} \quad (6.5)$$

$$\begin{aligned} V_b Z_{bb}^{VC} \frac{dF_B^{VC}}{dt} &= (Q_{dep} Z_p^{VC} + K_{bw} A_w Z_w^{VC}) F_W^{VC} \\ &+ (K_{sb} A_s Z_b^{VC}) F_S^{VC} \\ &- (Q_{dep} Z_p^{VC} + K_{bw} A_w Z_w^{VC} + K_{bs} A_s Z_b^{VC}) F_B^{VC} - r_{VC} \end{aligned} , \quad (6.6)$$

where r_{DCE} is the reaction term through which DCE produces VC and r_{VC} is the reaction rate through which ethane is produced with the removal of a chlorine atom from vinyl chloride. After DCE and VC are produced in the biofilm compartment, they, too, partition into the water column and the sediments below, and volatilize to air from the water column. These equations can be written as follows for the water column:

$$V_w Z_{bw}^{TCE} \frac{dF_W^{TCE}}{dt} = S_{TCE} + (K_{aw} A_w Z_w^{TCE} + Q_{dry} Z_{aerosol}^{TCE} + Q_{wet} Z_{aerosol}^{TCE}) F_A^{TCE}$$
$$+ (Q_{res} Z_s^{TCE} + K_{sw} A_s Z_w^{TCE}) F_B^{TCE} \quad (6.7)$$
$$- (k_{TCEdecay} V_w Z_w^{TCE} + Q_{dep} Z_p^{TCE} + Q_{out} Z_{bw}^{TCE} + K_{aw} A_w Z_w^{TCE}) F_W^{TCE}$$

$$V_w Z_{bw}^{DCE} \frac{dF_W^{DCE}}{dt} = (K_{aw} A_w Z_w^{DCE} + Q_{dry} Z_{aerosol}^{DCE} + Q_{wet} Z_{aerosol}^{DCE}) F_A^{DCE}$$
$$+ (Q_{res} Z_s^{DCE} + K_{sw} A_s Z_w^{DCE}) F_B^{DCE} \quad (6.8)$$
$$- (k_{DCEdecay} V_w Z_w^{DCE} + Q_{dep} Z_p^{DCE} + Q_{out} Z_{bw}^{DCE} + K_{aw} A_w Z_w^{DCE}) F_W^{DCE}$$

$$V_w Z_{bw}^{VC} \frac{dF_W^{VC}}{dt} = (K_{aw} A_w Z_w^{VC} + Q_{dry} Z_{aerosol}^{VC} + Q_{wet} Z_{aerosol}^{VC}) F_A^{VC}$$
$$+ (Q_{res} Z_s^{VC} + K_{sw} A_s Z_w^{VC}) F_S^{VC} \quad . \quad (6.9)$$
$$- (k_{VCdecay} V_w Z_w^{VC} + Q_{dep} Z_p^{VC} + Q_{out} Z_{bw}^{VC} + K_{aw} A_w Z_w^{VC}) F_W^{VC}$$

The mass-balance equations for the three chemicals, TCE, DCE, and VC, are given as Equations 6.10 through 6.12 in the sediment compartment

$$V_s Z_{bs}^{TCE} \frac{dF_S^{TCE}}{dt} = (Q_{dep} Z_p^{TCE} + K_{sb} A_s Z_b^{TCE}) F_B^{TCE}$$
$$- (K_{sb} A_s Z_s^{TCE} + Q_{bury} Z_s^{TCE} + k_{TCEdecay} V Z_s^{TCE}) F_S^{TCE} \quad (6.10)$$

$$V_s Z_{bs}^{DCE} \frac{dF_S^{DCE}}{dt} = (Q_{dep} Z_p^{DCE} + K_{sb} A_s Z_b^{DCE}) F_B^{DCE}$$
$$- (K_{sb} A_s Z_s^{DCE} + Q_{bury} Z_s^{DCE} + k_{DCEdecay} V Z_s^{DCE}) F_S^{DCE} \quad (6.11)$$

$$V_s Z_{bs}^{VC} \frac{dF_S^{VC}}{dt} = (Q_{dep} Z_p^{VC} + K_{sb} A_s Z_b^{VC}) F_B^{VC} - (K_{sb} A_s Z_s^{VC} + Q_{bury} Z_s^{VC} + k_{VCdecay} V Z_s^{VC}) F_S^{VC} \quad . \tag{6.12}$$

Similarly, mass-balance equations for the three chemicals in the air compartment can be written as

$$V_a Z_{aw}^{TCE} \frac{dF^{TCE}{}_A}{dt} = (K_{aw} A_w Z_w^{TCE}) F_W^{TCE} - (Q_{dry} Z_{aerosol}^{TCE} + Q_{wet} Z_{aerosol}^{TCE} + Q_{air} Z_{ba}^{TCE} + K_{aw} A_w Z_w^{TCE} + k_{TCEdecay} V Z_a^{TCE}) F_A^{TCE} \tag{6.13}$$

$$V_a Z_{aw}^{DCE} \frac{dF^{DCE}{}_A}{dt} = (K_{aw} A_w Z_w^{DCE}) F_W^{DCE} - (Q_{dry} Z_{aerosol}^{DCE} + Q_{wet} Z_{aerosol}^{DCE} + Q_{air} Z_{ba}^{DCE} + K_{aw} A_w Z_w^{DCE} + k_{DCEdecay} V Z_a^{DCE}) F_A^{DCE} \tag{6.14}$$

$$V_a Z_{aw}^{VC} \frac{dF^{VC}{}_A}{dt} = (K_{aw} A_w Z_w^{VC}) F_W^{VC} - (Q_{dry} Z_{aerosol}^{VC} + Q_{wet} Z_{aerosol}^{VC} + Q_{air} Z_{ba}^{VC} + K_{aw} A_w Z_w^{VC} + k_{VCdecay} V Z_a^{VC}) F_A^{VC} \quad . \tag{6.15}$$

As a result, the model for the fate and transport of TCE and its daughter products requires nine equations that need to be solved simultaneously. The fugacity capacities for each chemical have been calculated and the half life of each of the chemicals in water, air, and

sediment are found from reference chemical handbooks. These values are listed in Table 6.1 below:

Table 6.1 The fugacity capacities of TCE and its daughter products

Parameter	TCE	DCE	VC
Z_w (mol/m^3.Pa)	1.00×10^{-3}	2.93×10^{-3}	3.55×10^{-4}
Z_a (mol/m^3.Pa)	4.04×10^{-4}	4.04×10^{-4}	4.04×10^{-4}
Z_s (mol/m^3.Pa)	1.11×10^{-4}	2.38×10^{-4}	3.39×10^{-5}
Z_b (mol/m^3.Pa)	5.53×10^{-5}	1.19×10^{-4}	1.70×10^{-5}
Z_{bw} (mol/m^3.Pa)	1.00×10^{-3}	2.93×10^{-3}	3.55×10^{-4}
Z_{ba} (mol/m^3.Pa)	4.04×10^{-4}	4.04×10^{-4}	4.04×10^{-4}
Z_{bs} (mol/m^3.Pa)	8.68×10^{-4}	2.52×10^{-3}	3.07×10^{-4}
Z_{bb} (mol/m^3.Pa)	9.07×10^{-4}	2.65×10^{-3}	3.21×10^{-4}
Z_p (mol/m^3.Pa)	1.11×10^{-4}	2.38×10^{-4}	3.39×10^{-5}
$Z_{aerosol}$ (mol/m^3.Pa)	0.246	0.101	7.19
k_w (h^{-1})	0.00077	0.001925	0.00077
k_a (h^{-1})	0.0064	0.0194	0.214
k_s (h^{-1})	8.56×10^{-5}	0.000214	8.56×10^{-5}

This model, derived for the examination of the behavior of TCE and its daughter products in a lake environment, is applied to Lake Pontchartrain. The fate of contaminants with abiotic reactions and all information about the lake were already analyzed in Chapter 3. However, other information required for the solution is the oxygen penetration depth. This depth is also used to identify the ratio of aerobic to anaerobic portions of the biofilm as well as the ratio of the aerobic to anaerobic microbial population.

The dissolved oxygen concentration close to the bottom of Lake Pontchartrain is about 4.5 mg/L (Stoeckel et al., 2005). Biomass density can be taken to be 8 g/L (the value used in the biofilm reactors) (Rauch et al., 1998; Rauch et al., 1999). If the biofilm layer is 10 mm thick and Equation 6.1 is applied, the oxygen penetration depth is 3.2 mm. Hence,

32% of the bacteria are aerobic, and the rest is anaerobic. 32% of the biofilm volume is also deduced to be aerobic whereas the remaining 68% is anaerobic.

6.4. Results of Lake Application

The derived model, with its twelve simultaneous, linear equations, provides a very useful tool for analyzing the fate and transport of a parent compound and its daughter products in a lake system because it allows one to follow the amount of byproduct formation as well as amount of each chemical in each compartment. Such information can be extremely useful in emergency situations as well as in the general management of the water quality of a lake system.

Table 6.2 below presents the removal values, given as percentages, of TCE, DCE and VC from each of the compartments. For example, if a total amount of 100 units of TCE is introduced into the water column, about 61% of it will be lost to decay, about 21% will partition into the biofilm compartment by settling, 9% will diffuse into the biofilm compartment, 9% will volatilize, and the remaining, almost negligible amount will stay in water column and be removed with outflowing tributaries. The information supplied in Table 6.2 is crucial to the understanding of the behavior of a certain chemical in a lake environment.

Table 6.2 The types of removal from TCE, DCE, and VC (in percentages) from each compartment of the system

	Water Column				
	Decay	Outflow	Deposition	Volatilization	Diffusion to Biofilm
TCE	60.68	0.0012	21.43	8.95	8.95
DCE	80.93	0.0005	11.43	5.97	1.67
VC	61.78	0.001	21.82	13.67	2.73
	Biofilm compartment				
	Reaction to Another Chemical	Diffusion to Water	Diffusion to Sediments	Resuspension	
TCE	0.0044	94.71	5.24	0.043	
DCE	0.03	96.06	3.90	0.034	
VC	0.06	95.38	4.57	0.05	
	Sediment Compartment				
	Diffusion to Biofilm		Decay	Burial	
TCE	2.42		97.58	0.0004	
DCE	6.17		93.83	0.0004	
VC	2.99		97.01	0.0005	
	Air Compartment				
	Diffusion to Water		Decay	Air flow	
TCE	13.79		1.72	84.5	
DCE	32.54		1.68	65.78	
VC	84.11		0.47	15.41	

A considerable amount of information, such as the fact that VC seldom enters the air phase, can be derived from Table 6.2 The main mechanism between the more solid compartment, primarily the sediment and biofilm compartments, is diffusion. When daughter products occur in biofilm, they immediately partition into the water column through diffusive fluxes.

Figure 6.5 illustrates the change of total TCE, DCE, and VC concentrations in the whole system. Upon partitioning into the biofilm compartment, TCE immediately starts to produce daughter products.

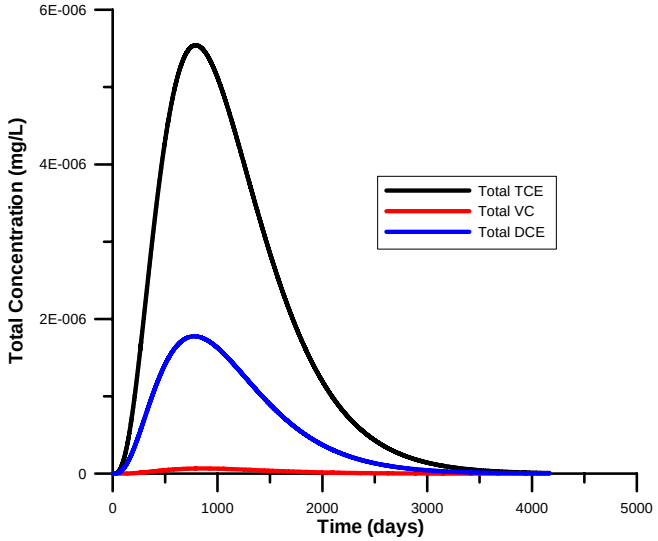

Figure 6.5 Total TCE, DCE, and VC concentrations

Results of the model showing the TCE concentrations in each compartment are summarized in Figure 6.6, briefly followed by a discussion. The figure shows that TCE is introduced into the water column for a period of one week and then stopped. As can be seen in Figure 6.6 (b), the concentration of TCE in the water initially rises and then decreases. According to the interactions among the compartments, some concentration of TCE occurs in each compartment. As TCE is not very hydrophobic and thus, avoids the solid phase, the concentration of TCE in neither the biofilm compartment nor the sediment compartment reaches very high values. Furthermore, TCE produces daughter products, DCE and VC, in the biofilm compartment due to microbial activity. According to Table 6.2, TCE, as expected, prefers to enter the air, so its concentration in the air compartment reaches higher values than its concentration in other compartments. Despite the wind-induced air flow that removes TCE from the system, it remains longer in the air phase. TCE concentrations in four different

Figures 6.7 and 6.8 show the concentration of DCE and VC, respectively, in each of the compartments. Unlike TCE, DCE neither stays in the air compartment long nor reaches higher concentrations. While DCE reaches its highest concentrations in the water column and has more affinity to solid phases compared to TCE, VC reaches its highest concentrations in the sediment compartment and reaches significant concentrations in the air and exits the water column more rapidly.

Figure 6.9 shows the concentration of all three chemicals together in one plot for each compartment.

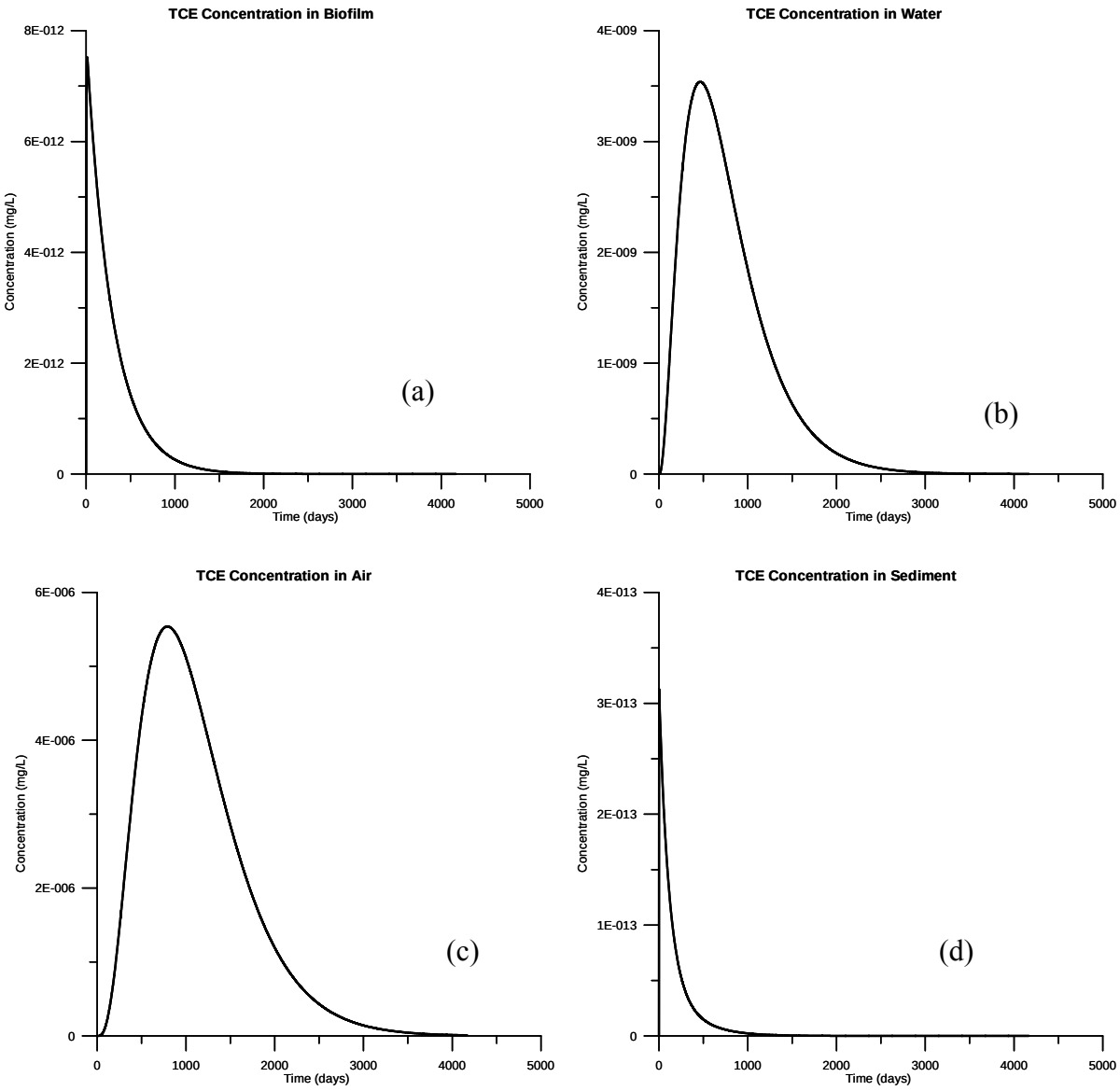

Figure 6.6 TCE concentration in (a) the biofilm compartment, (b) the water column, (c) the air, and (d) sediment

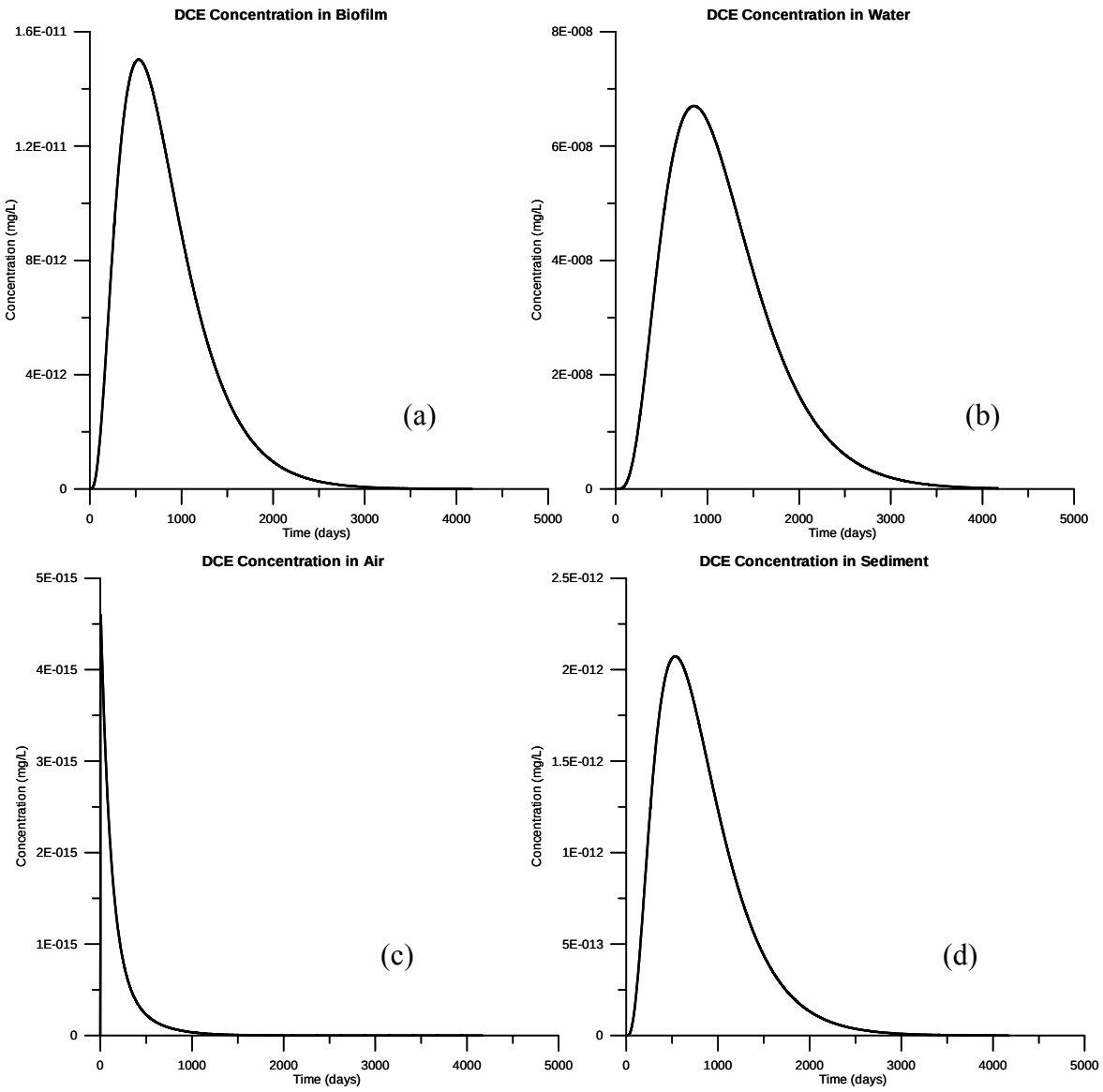

Figure 6.7 DCE concentration in (a) the biofilm compartment, (b) the water column (c) the air, and (d) sediment

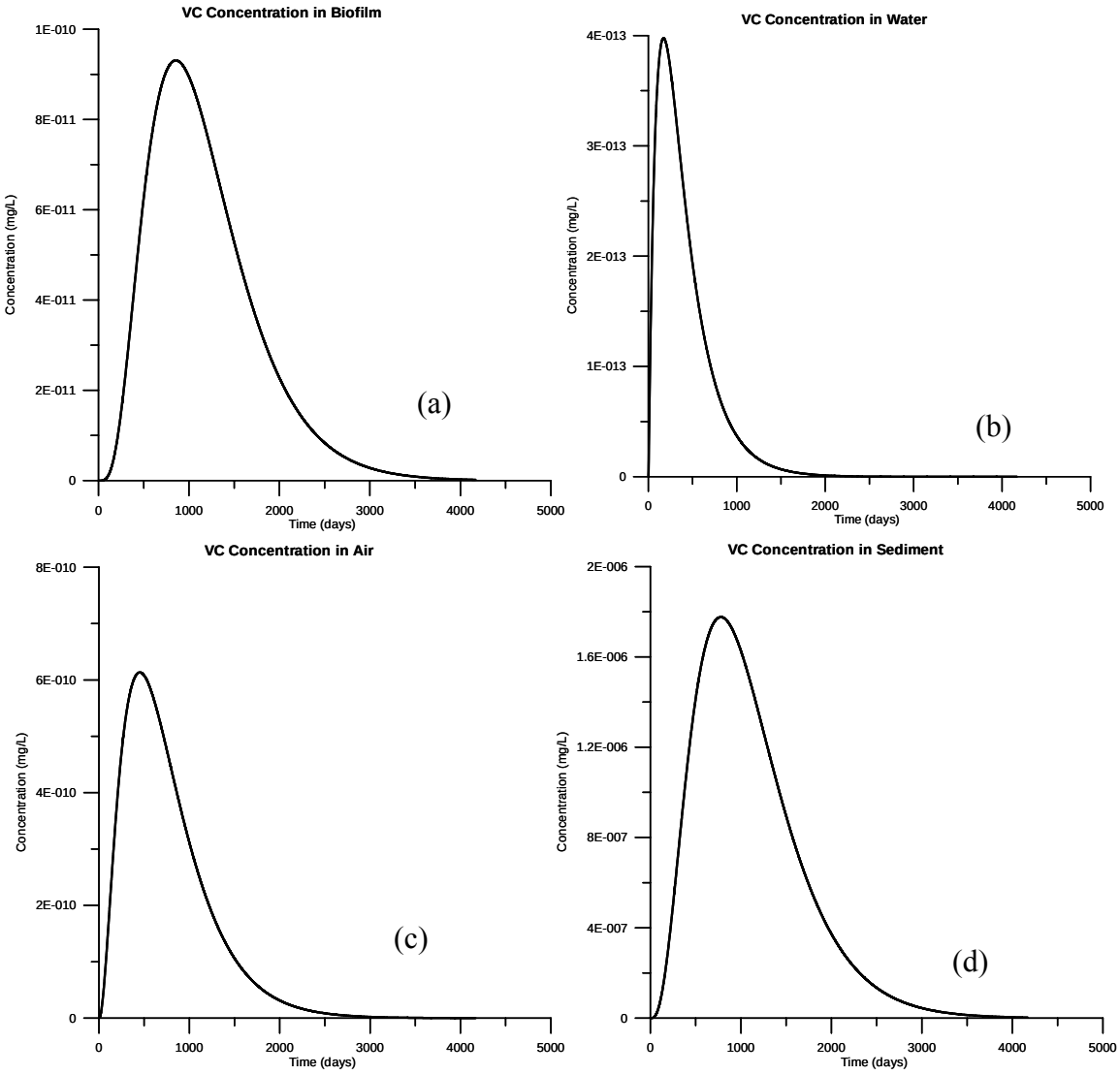

Figure 6.8 VC concentration in (a) the biofilm compartment, (b) the water column, (c) the air, and (d) sediment

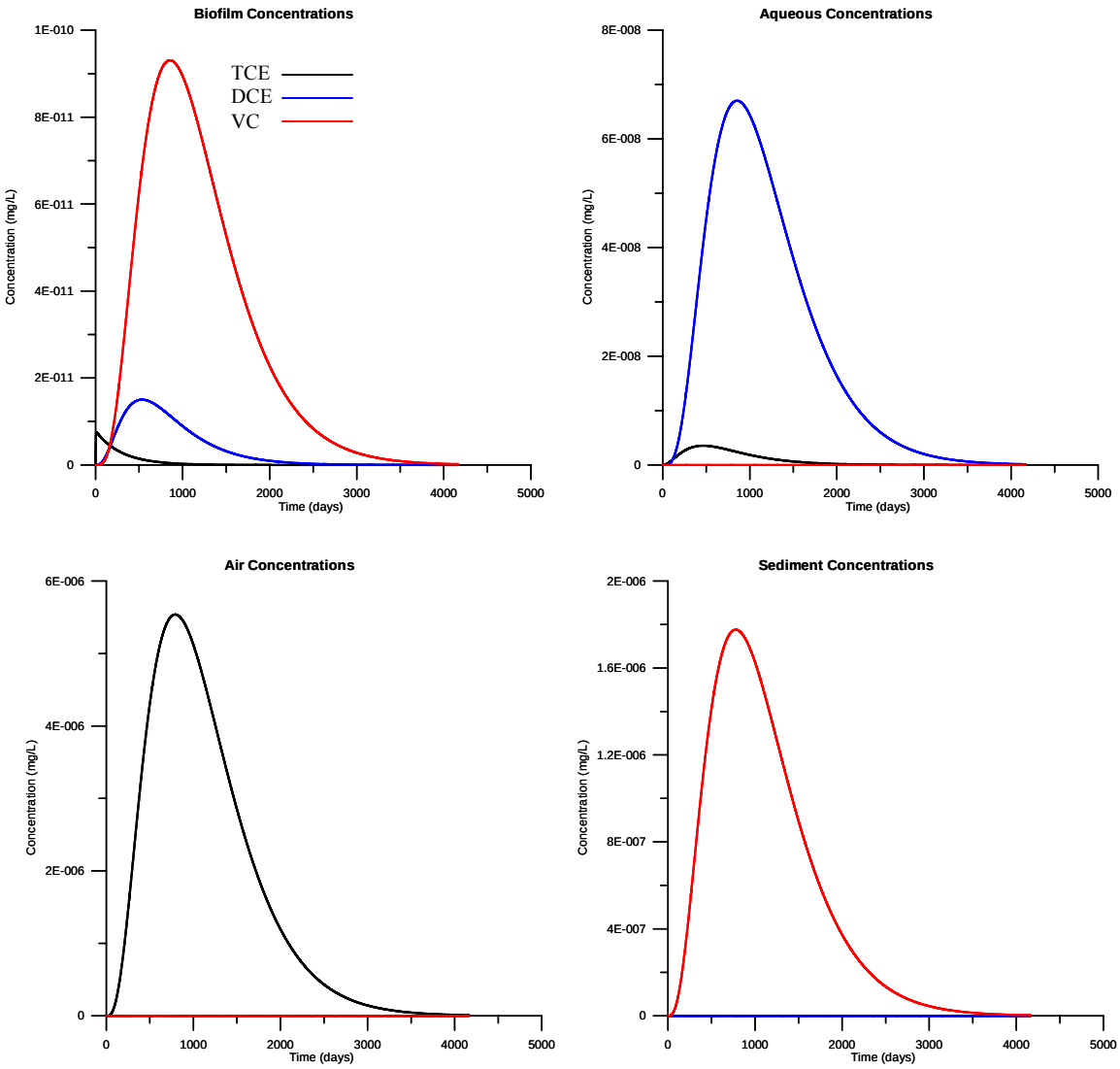

Figure 6.9 Concentration of all three chemicals in each compartment

TCE produces DCE and the amount decreases due to both biological transformation and partitioning into the water column and then volatilizing into the air. Once TCE produces DCE, DCE produces VC. DCE has higher concentrations in the water column, where it is most comfortable. VC, however, prefers the solid phases such as the biofilm and sediment compartments. In addition, from Figure 6.8, the highest concentration belongs to TCE, from which the other two chemicals are produced.

6.5 The Governing Equations for the Fate and Transport of TCE and its Daughter Products in a River

The same principles can be used to model the fate and transport of TCE and its daughter products as well as any other multispecies contaminant in rivers. As explained in Chapter 4, rivers have a more dynamic nature than lakes, so completely mixed reactor type models do not represent a river system accurately. Therefore, more rigorous hydrodynamics are required to thoroughly represent the characteristics of the water movement in rivers. The same hydrodynamics model developed in Chapter 4 can be used to supply the necessary velocity, depth, and width distribution of a river. Advection-dispersion equations can then be developed for the derivation of mass-balance for TCE, DCE, and VC in each compartment in the same manner such equations were developed in Chapter 5, but for a multispecies contaminant. The same formulae developed and solved in the previous section for lake application can be used with the addition of advection and dispersion terms in the mass-balance equations of a water column. Water is mobile, biofilm and sediment compartments are immobile, and the air compartment is semi-infinite. Although interactions between the air and water compartments take place, they do not alter the amount of chemical in the air. The concentrations of chemicals in the air remain constant. Then the set of nine equations for the nine unknown fugacity values are developed and given in Equations 6.16 through 6.24, starting with the biofilm compartment, where all biotransformations take place.

$$V_w Z_{bw} \frac{dF_W^{TCE}}{dt} = (K_{aw} A_w Z_w + Q_{dry} Z_{aerosol} + Q_{wet} Z_{aerosol}) F_A^{TCE} + (Q_{res} Z_p + K_{bw} A_s Z_w) F_B^{TCE} - (k_w V_w Z_w + Q_{dep} Z_p + Q_{out} Z_{bw} + K_{aw} A_w Z_w) F_W^{TCE} \quad (6.16)$$

$$V_b Z_{bb}^{DCE} \frac{dF_B^{DCE}}{dt} = (Q_{dep} Z_p^{DCE} + K_{bw} A_w Z_w^{DCE}) F_W^{DCE} + (K_{sb} A_s Z_b^{DCE}) F_S^{DCE} - (Q_{dep} Z_p^{DCE} + K_{bw} A_w Z_w^{DCE} + K_{bs} A_s Z_b^{DCE}) F_B^{DCE} - r_{DCE} \quad (6.17)$$

$$V_b Z_{bb}^{VC} \frac{dF_B^{VC}}{dt} = (Q_{dep} Z_p^{VC} + K_{bw} A_w Z_w^{VC}) F_W^{VC} + (K_{sb} A_s Z_b^{VC}) F_S^{VC} - (Q_{dep} Z_p^{VC} + K_{bw} A_w Z_w^{VC} + K_{bs} A_s Z_b^{VC}) F_B^{VC} - r_{VC} \quad (6.18)$$

$$V_w Z_{bw} \frac{\partial F_W^{TCE}}{\partial t} = -V_w Z_{bw} \frac{\partial (u F_W^{TCE})}{\partial x} + V_w Z_{bw} \frac{\partial}{\partial x} \left(D_H \frac{\partial (F_W^{TCE})}{\partial x} \right) + (K_{aw} A_w Z_w^{TCE} + Q_{dry} Z_{aerosol}^{TCE} + Q_{wet} Z_{aerosol}^{TCE}) F_A^{TCE} + (Q_{res} Z_s^{TCE} + K_{sw} A_s Z_w^{TCE}) F_B^{TCE} - (k_{TCEdecay} V_w Z_w^{TCE} + Q_{dep} Z_p^{TCE} + Q_{out} Z_{bw}^{TCE} + K_{aw} A_w Z_w^{TCE}) F_W^{TCE} \quad (6.19)$$

$$V_w Z_{bw} \frac{\partial F_W^{DCE}}{\partial t} = -V_w Z_{bw} \frac{\partial (u F_W^{DCE})}{\partial x} + V_w Z_{bw} \frac{\partial}{\partial x} \left(D_H \frac{\partial (F_W^{DCE})}{\partial x} \right) + (K_{aw} A_w Z_w^{DCE} + Q_{dry} Z_{aerosol}^{DCE} + Q_{wet} Z_{aerosol}^{DCE}) F_A^{DCE} + (Q_{res} Z_s^{DCE} + K_{sw} A_s Z_w^{DCE}) F_B^{DCE} - (k_{DCEdecay} V_w Z_w^{DCE} + Q_{dep} Z_p^{DCE} + Q_{out} Z_{bw}^{DCE} + K_{aw} A_w Z_w^{DCE}) F_W^{DCE} \quad (6.20)$$

$$V_w Z_{bw} \frac{\partial F_W^{VC}}{\partial t} = -V_w Z_{bw} \frac{\partial (u F_W^{VC})}{\partial x} + V_w Z_{bw} \frac{\partial}{\partial x}\left(D_H \frac{\partial (F_W^{VC})}{\partial x} \right)$$
$$+ (K_{aw} A_w Z_w^{VC} + Q_{dry} Z_{aerosol}^{VC} + Q_{wet} Z_{aerosol}^{VC}) F_A^{VC}$$
$$+ (Q_{res} Z_s^{VC} + K_{sw} A_s Z_w^{VC}) F_S^{VC}$$
$$- (k_{VCdecay} V_w Z_w^{VC} + Q_{dep} Z_p^{VC} + Q_{out} Z_{bw}^{VC} + K_{aw} A_w Z_w^{VC}) F_W^{VC} \quad (6.21)$$

As water is mobile, Equations (6.19) through (6.20) for the water column have advection and dispersion terms. The set of mass-balance equations for the TCE, DCE, and VC in the sediment compartment follows:

$$V_s Z_{bs}^{TCE} \frac{dF_S^{TCE}}{dt} = (Q_{dep} Z_p^{TCE} + K_{sb} A_s Z_b^{TCE}) F_B^{TCE}$$
$$- (K_{sb} A_s Z_s^{TCE} + Q_{bury} Z_s^{TCE} + k_{TCEdecay} V Z_s^{TCE}) F_S^{TCE} \quad (6.22)$$

$$V_s Z_{bs}^{DCE} \frac{dF_S^{DCE}}{dt} = (Q_{dep} Z_p^{DCE} + K_{sb} A_s Z_b^{DCE}) F_B^{DCE}$$
$$- (K_{sb} A_s Z_s^{DCE} + Q_{bury} Z_s^{DCE} + k_{DCEdecay} V Z_s^{DCE}) F_S^{DCE} \quad (6.23)$$

$$V_s Z_{bs}^{VC} \frac{dF_S^{VC}}{dt} = (Q_{dep} Z_p^{VC} + K_{sb} A_s Z_b^{VC}) F_B^{VC}$$
$$- (K_{sb} A_s Z_s^{VC} + Q_{bury} Z_s^{VC} + k_{VCdecay} V Z_s^{VC}) F_S^{VC} \quad . \quad (6.24)$$

In the solution of river water quality, the air compartment is considered semi-infinite and the water flow from one reach into the other in the river is fast. Although interactions between the water column and the air play an important role in the fate and transport of

chemicals, these interactions cannot sufficiently change concentrations in the air, the volume of which is large compared with that of the water column, the biofilm, and the sediment compartments. In this case, these compartments remain stagnant under the air, as they did in the lake application. Therefore, only nine equations define the system of a river with a constant air fugacity value, which affects the fate and transport of the three chemicals.

The same set of fugacity capacities and half-lives are used for the river application. The dissolved oxygen value in the Altamaha River system, where the application is performed, is also about 4.5 mg/L, so the same ratio of 0.32 can be used for the aerobic portion of bacteria.

Since the water column mass-balance equations use the same dynamic advection and dispersion terms in the application of river water quality, the equations are no longer linear. The finite difference solution of advection and dispersion requires a delicate treatment of these terms, as explained in Chapter 5. The QUICKEST algorithm, which was used in the solution of a single species with abiotic interactions in Chapter 5, is used for the solution of multispecies with biotic transformations. This case involves three sets of equations for three chemicals (TCE, DCE, VC) in each compartment instead of one. The QUICKEST algorithm allows the chemicals to advect first in the current time step from one element to the next, and then disperse, and then all the reactions are calculated for the next time step for all the elements.

6.6. Results of River Application

In this section, the model derived for fate and transport of TCE and its daughter products in a river is applied first to a straight trapezoidal channel and then to Ohoopee River in the Lower Altamaha River system. The hydrodynamic model derived in Chapter 4 is solved for the velocity, depth, and width distribution in the river. Using this information, the system of nine equations for TCE and its daughter products, described in the above section, are solved.

The results of the application are illustrated in graphical format. The results of the straight trapezoidal channel are demonstrated first. It is easier to comprehend the results in this system. The natural channel has many variations due to changes in geometry of the channel as well as the depth, surface width, and velocity in the channel. With so many changes occurring simultaneously, it is not easy to isolate the production of daughter products. Hence, a more in depth analysis has been performed in the application of a straight trapezoidal channel and then the results of the Ohoopee River application are demonstrated graphically in this section.

The concentration of TCE, DCE, and VC in water column, sediment, and biofilm compartments of the river system are plotted as concentration versus time and concentration versus location on the Ohoopee River. Figure 6.10 below shows the aqueous TCE concentration at three different locations of the river. The results show that TCE moves along the river in a plug flow fashion.

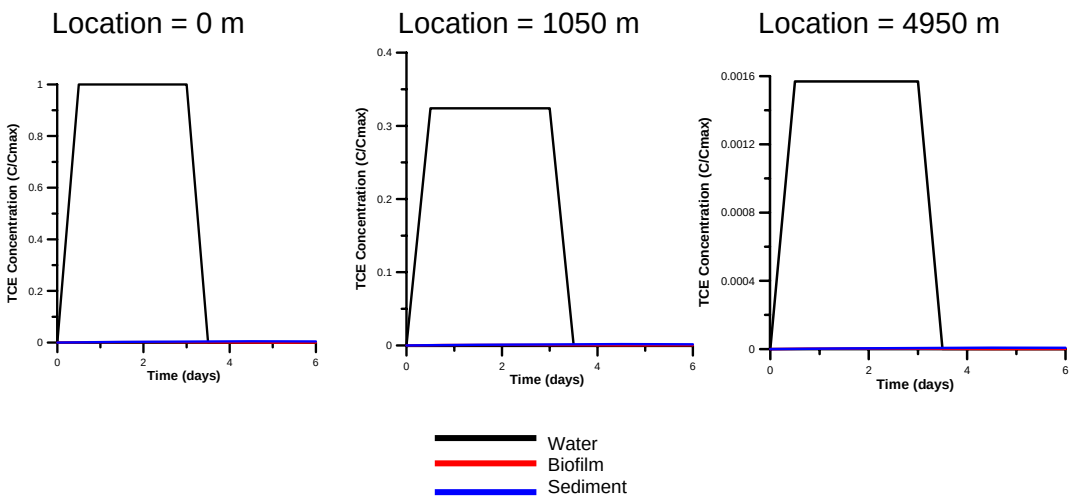

Figure 6.10 TCE concentrations at three different locations of the river

Figure 6.11 below illustrates the TCE, DCE, and VC concentrations at the most upstream location where TCE source is introduced into the water column of the river system. The results indicate that as TCE partitions into the biofilm, DCE and VC are produced and in turn they partition into other compartments. DCE mainly partitions into sediments rather than water column. VC partitions into water column and sediments as well but not as significantly.

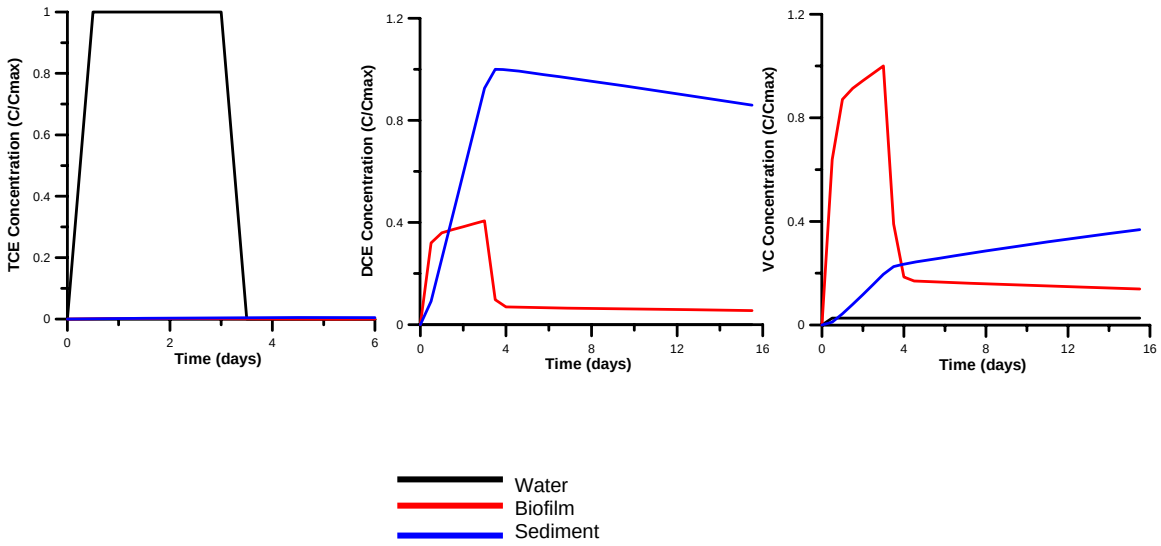

Figure 6.11 TCE, DCE, and VC concentrations at the most upstream location

The same type of results can be observed at 1 km downstream of the source location. These plots emphasize the previous discussions. TCE moves downstream in a plug flow fashion, and partitions into biofilm compartment as it moves along, so even further downstream the production of daughter products, DCE and VC are observed. DCE partitions into sediments as it forms and VC partitions into water column more than the sediments. These results can be observed in Figure 6.12 below.

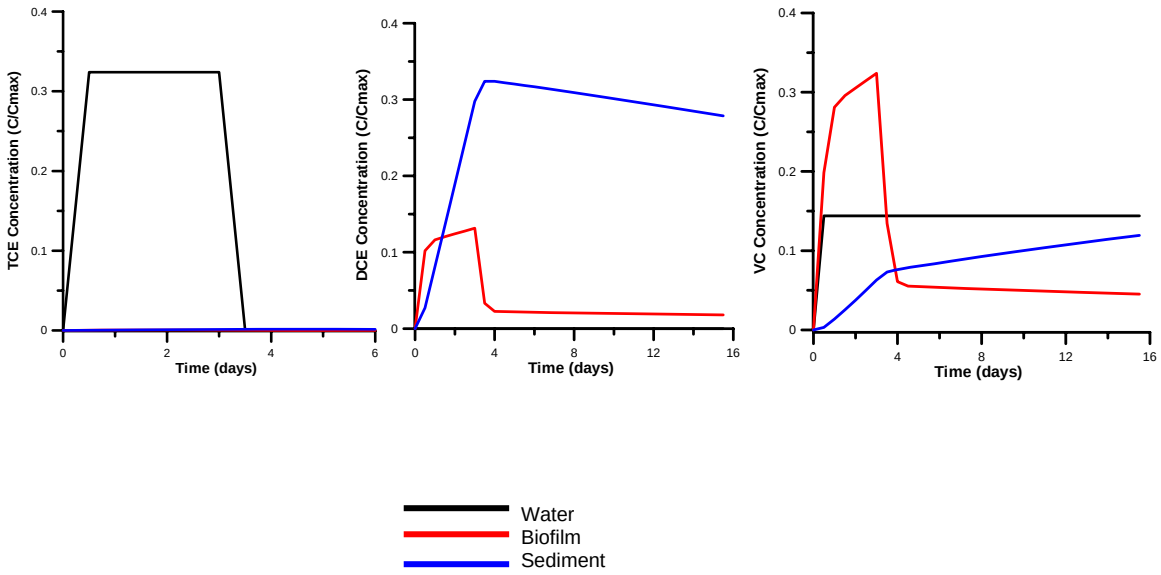

Figure 6.12 TCE, DCE, and VC concentrations 1 km downstream of the source location

In the application of straight trapezoidal channel, Figure 6.13 illustrates the same results looking from a concentration versus location perspective at a specific time. This is a snapshot of the response of the channel to TCE contamination 12 hours after the introduction of the TCE into the water column.

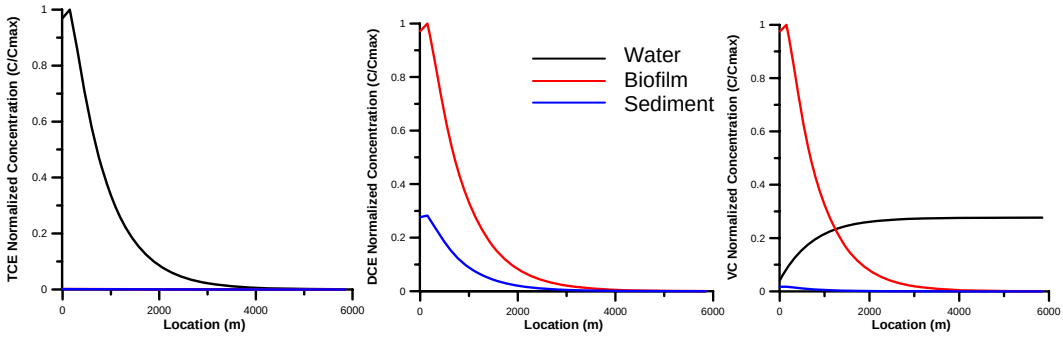

Figure 6.13 TCE, DCE and VC concentrations along the channel at time=0.5 days

The next set of figures are the results of the Ohoopee River application. In this case, the results of the Chapter 4 hydrodynamic analysis have been used to calculate the fate and transport of TCE pollution.

The concentration of TCE, DCE, and VC in water column, sediment, and biofilm compartments of the river system are plotted as concentration versus time and concentration versus location on the Ohoopee River. Figure 6.14 below shows the aqueous TCE concentratiol along the river immediately after the release of TCE into the water column and 4 days after the release. TCE concentration decreases as TCE travels downstream from the source point. 4 days later, the amount of TCE observed in the river is negligible compared to the initial concentrations.

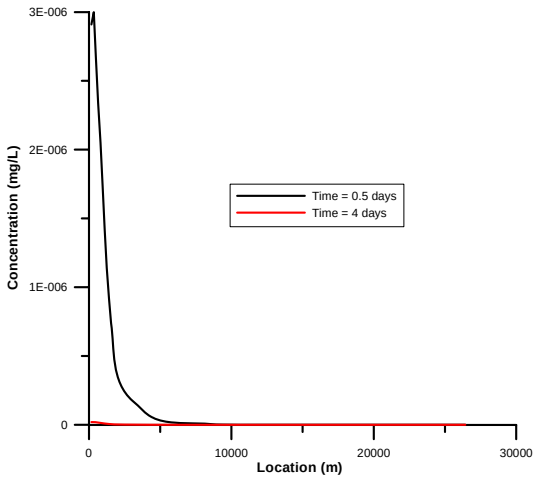

Figure 6.14 Aqueous TCE concentrations along the Ohoopee River

Figure 6.15 below illustrates the TCE concentration in the biofilm along the river. From this figure, it can be deduced that TCE in the water phase transfers into biofilm as TCE travels within the water phase downstream. The concentration in biofilms is higher after days compared to water phase.

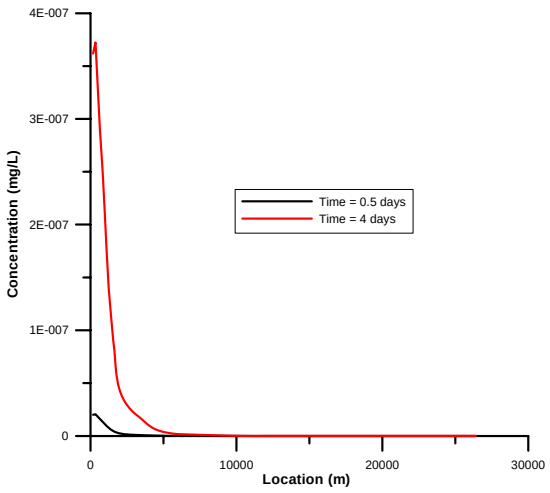

Figure 6.15 Biofilm TCE concentration along Ohoopee River

In Figure 6.16 below, TCE concentration in sediments along the river is shown. The concentration profile is very similar to the concentration profile in sediments. Actually, TCE in sediments reaches a little higher concentration compared to biofilm.

Figure 6.17 to 6.19 shows the concentration of DCE in water, biofilm and sediment compartments. DCE follows a similar pattern to TCE in Ohoopee River. The aqueous DCE concentration is not a smooth line. DCE is produced in the biofilm compartment and released into the water column by diffusive flux. Also the volume of water column changes throughout the river, hence the concentration also varies. The same type of concentration changes can be observed for aqueous VC concentration plot given in Figure 6.20 as well. The volume of sediment and biofilm compartments does not change as much as the volume of the water compartment. At the beginning, DCE and VC cannot be observed in the river, as time passes, some concentration of DCE and VC occurs in the

river. TCE transforms into DCE and then VC in the biofilm compartment and diffuses into water column. As DCE is more water soluble among the three compounds, the concentration of DCE in water is higher compared to TCE and VC.

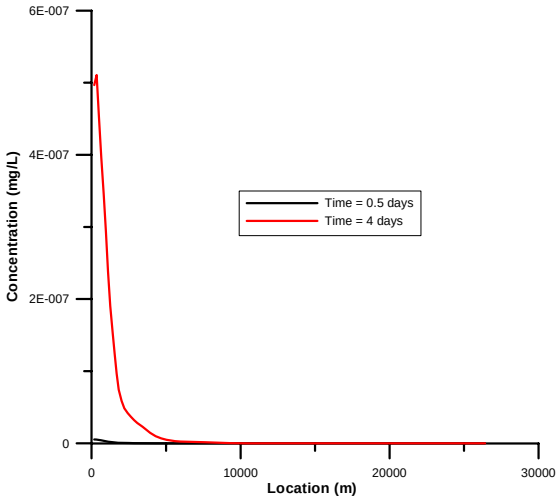

Figure 6.16 TCE sediment concentrations along Ohoopee River

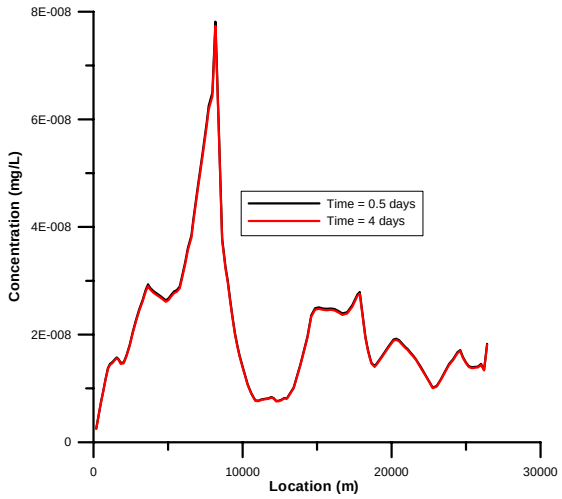

Figure 6.17 Aqueous DCE concentrations along Ohoopee River

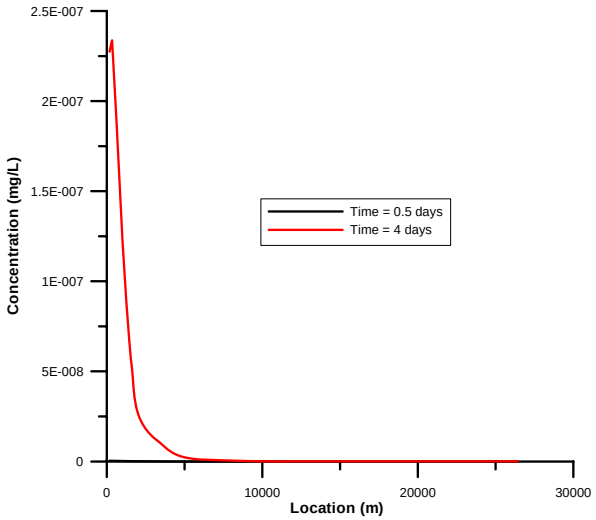

Figure 6.18 DCE sediment concentrations along Ohoopee River

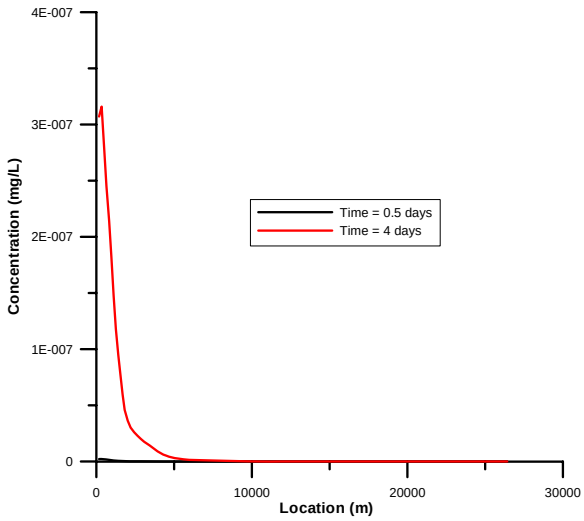

Figure 6.19 DCE biofilm concentrations along Ohoopee River

Figures 6.20 through 6.22 show the concentration of VC in water, biofilm, and sediment compartments along the river. VC and DCE show similar trends to each other.

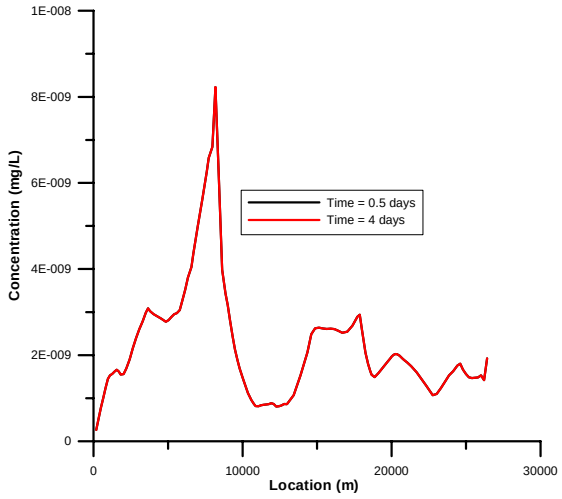

Figure 6.20 Aqueous VC concentrations along Ohoopee River

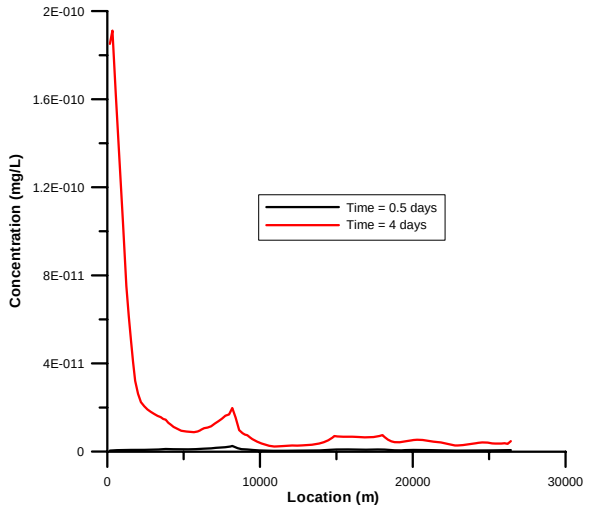

Figure 6.21 VC biofilm concentrations along Ohoopee River

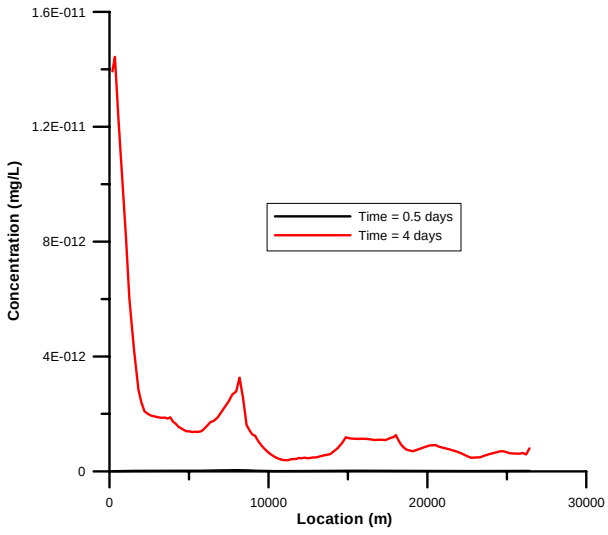

Figure 6.22 VC sediment concentrations along Ohoopee River

Figures 6.23 through 6.25 show the TCE concentration in water, biofilm, and sediment compartments at three different locations in Ohoopee River. Aqueous concentration of TCE increases with the loading of TCE, and then decrease after the TCE pollution load ceases. TCE partitions into other compartments in the river, and transforms into daughter products or decays. As a result, TCE concentration is significantly lower in downstream locations in the river. TCE also volatilizes into the air compartment. Figure 6.19 and 6.20 show that TCE partitions immediately into biofilm and sediment compartments close to the source of TCE load. Concentration of TCE in these compartments are negligible further downstream.

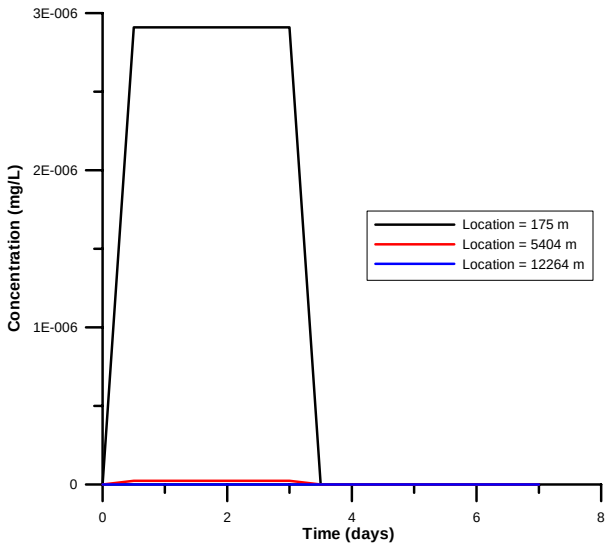

Figure 6.23 TCE water concentrations in Ohoopee River

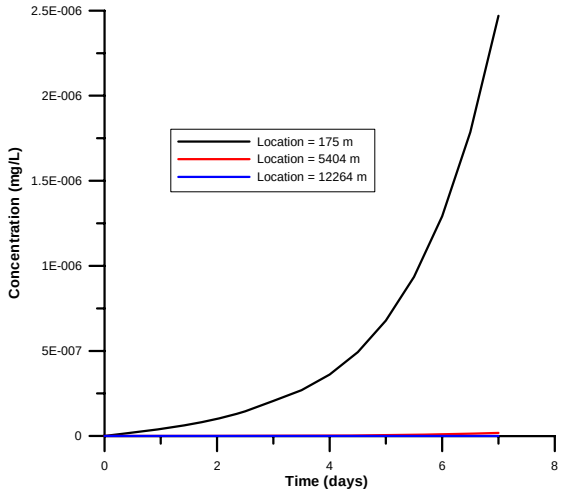

Figure 6.24TCE biofilm concentrations in Ohoopee River

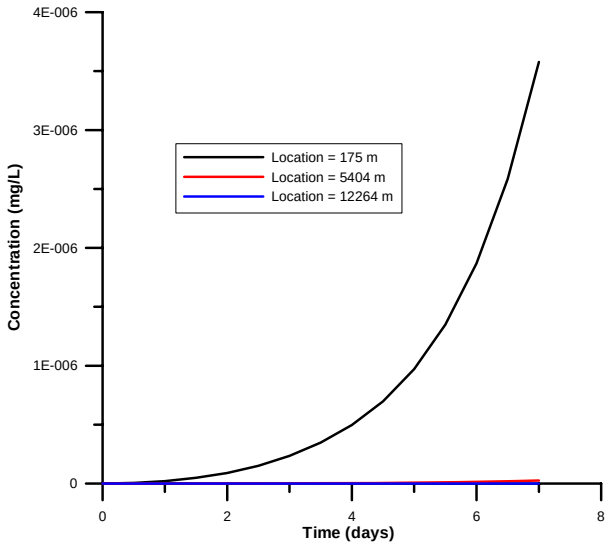

Figure 6.25 TCE sediment concentrations in Ohoopee River

Figures 6.26 through 6.28 show DCE concentration at three locations in Ohoopee River; and Figures 6.29 through 6.31 show VC concentrations at the same three locations in Ohoopee River. Aqueous concentrations of both DCE and VC follow a similar trend to aqueous TCE concentration.

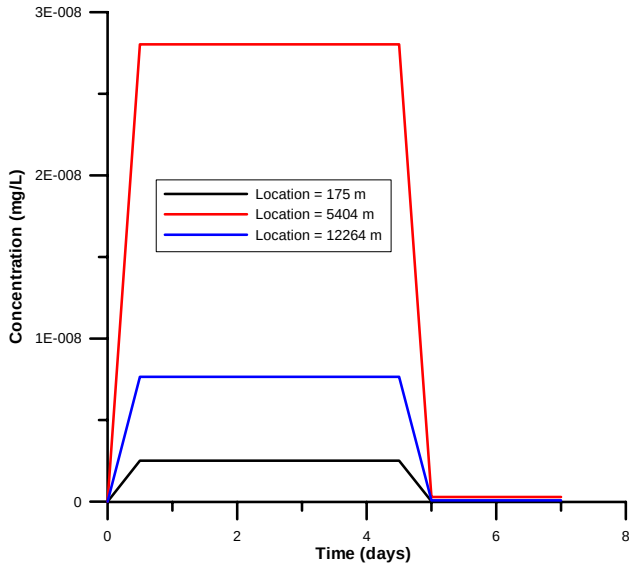

Figure 6.26 Aqueous DCE concentrations in Ohoopee River

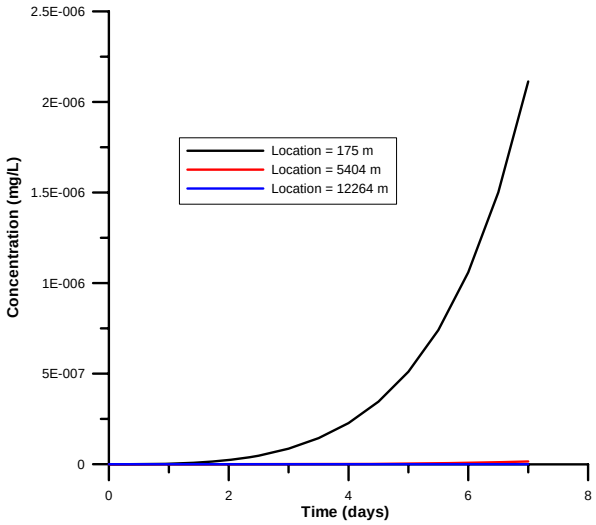

Figure 6.27 DCE sediment concentrations in Ohoopee River

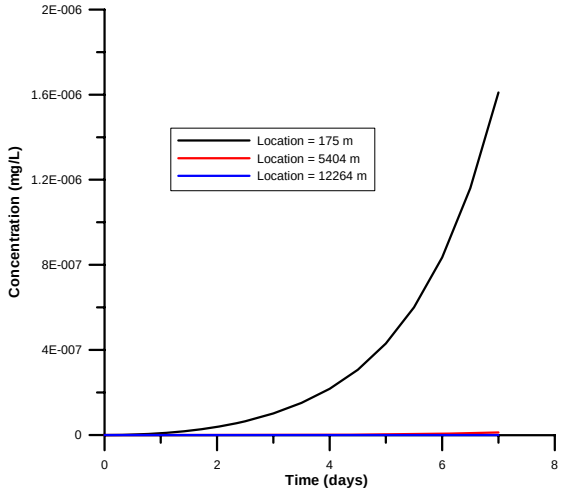

Figure 6.28 DCE biofilm concentrations in Ohoopee River

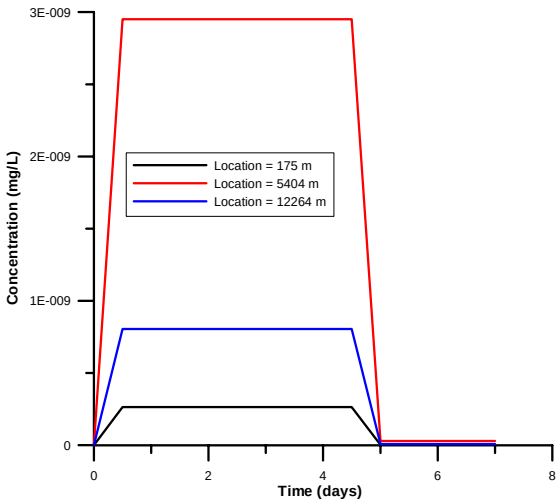

Figure 6.29 Aqueous VC concentrations in Ohoopee River

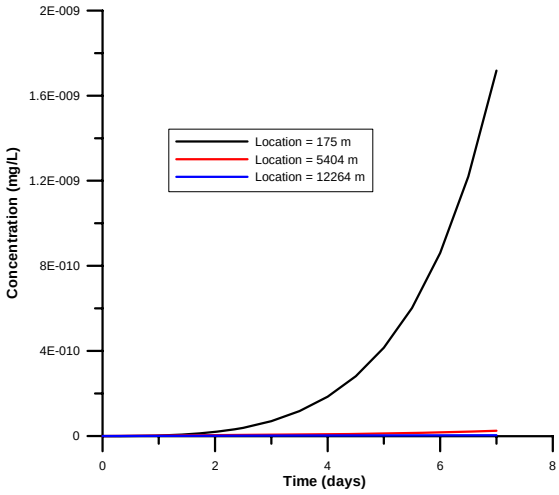

Figure 6.30 VC biofilm concentrations in Ohoopee River

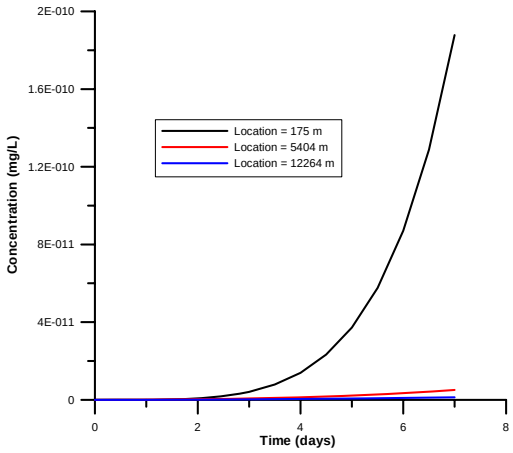

Figure 6.31 VC sediment concentrations in Ohoopee River

In this section of this thesis, a dynamic, continuous, fugacity based contaminant fate and transport model has been developed for a multispecies contaminant. Not only the fate and transport of contaminant itself is examined and analyzed, bit also its daughter products. More than one compartment is modeled as well as more than one contaminant. The environmental systems are very complex, different phases are interconnected, and existence of one compound usually has an effect on the fate of another. With the use of fugacity, this model reflects the processes occurring in a natural aquatic environment.

The fact that fugacity is continuous between phases has been put to good use in the development of a simple probabilistic model in the first part of this thesis. Decision makers are often forced to make snap judgments in the face of disasters without adequate time to examine the full extent of consequences of these decisions. A fugacity-based probabilistic model has been developed for shallow water systems with three compartments; water, sediment, and air. The fate of three representative contaminants, polychlorinated biphenyls (PCBs), atrazine, and benzene, are examined with this model, along with the concentration profile of each contaminant in all compartments. To resolve the uncertainty involved in the model parameters, Monte Carlo analysis is used. The resulting model is a simple, general, and effective tool that can be used as an emergency response model by decision makers. Various scenarios can be studied and an archive of responses can be recorded with this model. Each response is accompanied with its statistical analysis.

The second model developed in this thesis, is a continuous, dynamic river fugacity-based water quality model. It is our belief that this is the first time; a fugacity based model is developed to examine the fate and transport of a chemical in a river continuously. In the past, the fugacity concept has been applied to river water quality modeling with a simple approach in which many completely stirred tank reactors (CSTR) are connected in series and discrete analysis is performed. However, in this study, a fully dynamic and continuous contaminant fate and transport model for rivers is developed and solved. First, the velocity and the depth distribution in a river are established through the solution of river hydrodynamics. Saint-Venant Equations are derived and solved for a natural river

so that the hydrodynamics can be analyzed. As a result, the water depth and velocity at each node in the model are obtained. This information is then used for the fate and transport of a contaminant by application of advection-dispersion equation written in fugacity form, and all interactions between different phases available have been incorporated and solved numerically. This equation has been coupled with a mass balance equation derived for the same contaminant in the sediments, therefore incorporating more than just the aqueous transport.

The third model is a multispecies contaminant fate and transport model which can be used for the fate of a single contaminant and its daughter products. It is also our belief that this is the first application of a fugacity-based multispecies fate and transport model. TCE and its daughter products have been modeled both in a lake (well-mixed single cell) and a river (continuous multi-cell) application. The reactions which cause the daughter products of TCE to occur are biological and are called biotransformation. For biotransformation reactions to take place a new compartment has been added into the developed fugacity-based model. The new compartment, namely biofilm, is the top layer of sediments where most of the microbial population in aquatic environments is concentrated. Depending on the oxygen penetration depth of this biofilm, both aerobic and anaerobic transformations may take place in the biofilm compartment. With the addition of this compartment, a dynamic fugacity-based water quality model is developed for multispecies contaminants. With this approach, the fate of TCE and its daughter products, DCE and VC are followed in one single application.

The result of this research is the development of a fully dynamic fugacity-based model with a sophisticated representation of all the natural processes that may take place in a river or lake environment.

CHAPTER 7

CONCLUSIONS

Throughout history, all civilizations have been founded around rivers and lakes as human survival depend on fresh water sources. To protect these fresh water sources is crucial for the continuity of life and civilization. Unfortunately, they are under constant threat from contaminants. To prevent pollution or to examine its adverse effect if it happens, it is very important to understand the natural processes which occur in rivers and lakes. Many environmental scientists and engineers have studied the fate and transport of contaminants in surface waters.

There are many models in the literature that approach this topic and bring forth various solutions, ranging from very simple steady-state box models to complicated physical models. Box models are very simplistic and do not reflect the complexity and interconnectedness of natural processes in fresh water sources. If the model is very complex, then collection of data becomes tedious at best and very uncertain at worst. Also, many models use only aqueous phase transport, which can create false results. A hydrophobic contaminant would disappear rapidly from the water column of a river or a lake; however, it stays longest in the sediments of the river or the lake, eventually

releasing back into the water column for a long time. A model which only handles aquatic phase would miss the partitioning into solids phase and provide false results. Most of them have some limitations. Similarly, if a contaminant produces daughter products that are equally or even more toxic than itself, this has to be accounted for in the model.

This research tries to bring about a model which would overcome such limitations. It focuses on contaminants that are difficult to follow in the environment as they partition between different phases that exists in the water column. As these contaminants partition, they may follow various pathways, and pose myriad of risks, such as entering the food chain and pose health risk to humans.

To that end, fully-dynamic, continuous fugacity-based fate and transport models have been developed, in this thesis, to examine all natural processes and interactions in the aquatic water systems. Within a body of surface water such as a lake or a river, a dynamic interaction among different media takes place. Chemical compounds are continuously dissolving, adsorbing into solid particles, attaching to suspended particles, resuspending, reacting, diffusing, and advecting. As the inclusion of all these interactions into a model is complex, the use of fugacity concept instead of concentration, renders the modeling task relatively easy. Fugacity, which is described as the escaping tendency of a chemical from a medium, is continuous among different phases, thus easier to follow the movement of the chemical.

The fact that fugacity is continuous between phases has been put to good use in the development of a simple probabilistic model in the first part of this thesis. Decision makers are often forced to make snap judgments in the face of disasters without adequate time to examine the full extent of consequences of these decisions. A fugacity-based probabilistic model has been developed for shallow water systems with three compartments; water, sediment, and air. The fate of three representative contaminants, polychlorinated biphenyls (PCBs), atrazine, and benzene, are examined with this model, along with the concentration profile of each contaminant in all compartments. To resolve the uncertainty involved in the model parameters, Monte Carlo analysis is used. The resulting model is a simple, general, and effective tool that can be used as an emergency response model by decision makers. Various scenarios can be studied and an archive of responses can be recorded with this model. Each response is accompanied with its statistical analysis.

The second model developed in this thesis, is a continuous, dynamic river fugacity-based water quality model. It is our belief that this is the first time; a fugacity based model is developed to examine the fate and transport of a chemical in a river continuously. In the past, the fugacity concept has been applied to river water quality modeling with a simple approach in which many completely stirred tank reactors (CSTR) are connected in series and discrete analysis is performed. However, in this study, a fully dynamic and continuous contaminant fate and transport model for rivers is developed and solved. First, the velocity and the depth distribution in a river are established through the solution of river hydrodynamics. Saint-Venant Equations are derived and solved for a natural river

so that the hydrodynamics can be analyzed. As a result, the water depth and velocity at each node in the model are obtained. This information is then used for the fate and transport of a contaminant by application of advection-dispersion equation written in fugacity form, and all interactions between different phases available have been incorporated and solved numerically. This equation has been coupled with a mass balance equation derived for the same contaminant in the sediments, therefore incorporating more than just the aqueous transport.

The third model is a multispecies contaminant fate and transport model which can be used for the fate of a single contaminant and its daughter products. It is also our belief that this is the first application of a fugacity-based multispecies fate and transport model. TCE and its daughter products have been modeled both in a lake (well-mixed single cell) and a river (continuous multi-cell) application. The reactions which cause the daughter products of TCE to occur are biological and are called biotransformation. For biotransformation reactions to take place a new compartment has been added into the developed fugacity-based model. The new compartment, namely biofilm, is the top layer of sediments where most of the microbial population in aquatic environments is concentrated. Depending on the oxygen penetration depth of this biofilm, both aerobic and anaerobic transformations may take place in the biofilm compartment. With the addition of this compartment, a dynamic fugacity-based water quality model is developed for multispecies contaminants. With this approach, the fate of TCE and its daughter products, DCE and VC are followed in one single application.

The result of this research is the development of a fully dynamic fugacity-based model with a sophisticated representation of all the natural processes that may take place in a river or lake environment.

REFERENCES

Abramowicz, D. A. (1990). "Aerobic and Aerobic Biodegradation of PCBs: A Review." *Critical Reviews in Biotechnology*, 10(3), 241-251.

Alderink, R. H., Klaver, N. J., and Noorman, R. "DUFLOW V 2.0: Micro-computer Package for the Simulation of 1-Dimensional Flow and Water Quality in a Network of Open Water Courses. Modeling Water Quality and flow in River Vecht using DUFLOW. ." *International Conference on Water Quality Modeling*, Orlanda, FL.

Ambrose, R. B., and Martin, J. L. (1993). "The Water Quality Analysis Simulation Program, WASP5, Part a: Model Documentation." U.S. Environmental Protection Agency, Athens, GA.

ATSDR. (2003). "Toxicological Profile for Atrazine." U.S. Department of Health and Human Services. Public Health Service. Agency for Toxic Substances and Disease Registry, Atlanta, GA.

Baltas, E. A. (1988). "A State Space Model for River Routing," Georgia Institute of Technology, Atlanta, 120p.

Beck, M. B., and Reda, A. (1994). "Identification and Application of a Dynamic Model for Operational Management of Water Quality." *Water Science and Technology*, 30(2), 31-41.

Bedford, K., Findikasis, A., Larock, B. E., Rodi, W., and Street, R. L. (1988). "Turbulence Modeling of Surface Water Flow and Transport." *Journal of Hydraulic Engineering, ASCE*, 114(9), 970-1073.

Beurskens, J. E. M., and Stortelder, P. B. M. (1995). "Microbial Transformation of PCBs in sediments: What can we do to solve practical problems?" *Water Science and Technology*, 31(8), 99-107.

Brown, L. C., and Barnwell, T. O. (1987). "The Enhanced Stream Water Quality Models QUAL2E and QUAL2E-UNCAS: Documentation and User Manual." *EPA-600/3-87-007*, U.S. Environmental Protection Agency, Athens, GA.

Chapra, S. C. (1997). *Surface Water Quality Modeling*, McGraw-Hill, New York.

Chiarenzelli, J. R., Scrudato, R. J., and Wunderlich, M. L. (1997). "Volatile Loss of PCB Aroclors from Subaqueous Sand " *Environmental Science and Technology*, 31(2), 597-602.

Chin, D. A. (2000). *Water-Resources Engineering*, Prentice-Hall Inc., Upper Sadle River, New Jersey.

Chuco, T. D. (2004). "Dynamic Integrated Modeling of Basic Water Quality and FAte and Effect of Organic Contaminants in Rivers ", Ghent University, Ghent. 260p.

Citra, M. J. (2004). "Incorporating Monte Carlo Analysis into Multimedia Environmental Fate Models." *Environmental Toxicology and Chemistry*, 23(7), 1629 - 1633.

Costerton, J. W., Cheng, K. J., Geesey, G. G., Ladd, T. I., Nickel, J. C., Dasgupta, M., and Marrie, T. J. (1987). "Bacterial biofilms in nature and disease." *Annual Reviews of Microbiology*, 41, 435-464.

Cowan, C. E., Larson, R. J., Feijel, T. C. J., and R.A., R. (1993). "An Important Model for Predicting the Fate of Consumer Product Chemicals in Wastewater Treatment Plants." *Water Research*, 27, 561-573.

DHI. (1992). "MIKE11 User Manual." Danish Hydraulic Institute, Denmark.

DiGuardo, A., Calamari, D., Zanin, G., Consalter, A., and Mackay, D. (1994). "A Fugacity Model of Pesticide Runoff to Surface Water: Development and Validation." *Chemosphere*, 23, 511-531.

Eisenreich, S. J. (1987). "The Chemical Limnology of nonpolar organic contaminants: polychlorinated biphenyls in Lake Superior." Sources and Fates of Aquatic Pollutants, R. A. Hites and S. J. Eisenreich, eds., American Chemical Society, Wachington DC.

EPA. (2004). "Drinking Water Standards and Health Advisories." *EPA 822-R-04-005*, Environmental Protection Agency.

Fread, D. L. (1985). "Chapter 14: Channel Routing." Hydrological Forecasting, M. G. Anderson and T. P. Burt, eds., John Wiley and Sons Ltd., 437-503.

Gentle, J. E. (2003). *Random Number Generation and Monte Carlo Methods*, Springer, New York, 381p.

Gevao, B., Hamilton-Taylor, J., Murdoch, C., Jones, K. C., Kelly, M., and Tabner, B. J. (1997). "Depositional time trends and mobilization of PCBs in lake sediments." *Environmental Science and Technology*, 31, 3274-3280.

Ghosh, U., Zimmerman, J. R., and Luthy, R. G. (2003). "PCB and PAH Speciation in Contaminated Harbor Sediments and Effects on PAH Bioavailability." *Environmental Science and Technology*, 37, 2209-2217.

Gobas, F., and MacLean, L. (2003). "Sediment-Water distribution of organic contaminants in aquatic ecosystems: the role of organic carbon mineralization." *Environmental Science and Technology*, 37, 735-741.

Gunduz, O. (2004). "Coupled Flow and Contaminant Transport Modeling in Large Watersheds," Georgia Institute of Technology, Atlanta, 466p.

Gunduz, O., and Aral, M. M. (2004). "Surface and Subsurface Flow and Contaminant Transport Modeling in Lower Altamaha Watershed." *MESL-01-04*, Multimedia Environmental Simulations Laboratory, School of Civil and Environmental Engineering, Georgia Institute of Technology, Atlanta, 245p.

Haque, R., Schmedding, D. W., and Freed, V. H. (1974). "Aqueous Solubility Adsorption and Vapor Behavior of Polychlorinated Biphenyl Aroclor 1254." *Environmental Science and Technology*, 8(2), 139-142.

Hibiya, K., Nagai, J., Tsuneda, S., and Hirata, A. (2004). "Simple prediction of oxygen penetration depth in biofilms for wastewater treatment." *Biochemical Engineering Journal*, 19, 61-68.

Higashino, M., and Stefan, H. G. (2005). "Sedimentary microbial oxygen demand for laminar flow over a sediment bed of finite length." *Water Research*, 39, 3153-3166.

Holmer, M., and Storkholm, P. (2001). "Sulphur reduction and sulphur cycling in lake sediments: a review." *Freshwater Biology*, 46, 431-451.

Howard, P. H. (1989). *Handbook of Environmental Fate and Exposure Data for Organic Chemicals*, Lewis Publishers, Boca Raton.

Imamoglu, I. (2001). "PCB Sources and Degradation in River Sediments by Receptor Modeling," University of Wisconsin-Milwaukee, Milwaukee, Wisconsin.

Imamoglu, I., and Christensen, E. R. (2002). "PCB Sources, Transformations, and Contributions in Recent Fox River, Wisconsin Sediments Determined from Receptor Modeling." *Water Research*, 36, 3449-3462.

Iwasa, Y., and Aya, S. "Predicting longitudinal dispersion coefficient in open channel flows." *International Symposium on Environmental Hydrology*, HongKong, 505-510.

Khlebnikov, A., Samb, F., and Peringer, P. (1998). "Use of a dynamic gassing-out method for activity and oxygen diffusion coefficient estimation in biofilms." *Water Science and Technology*, 37(4-5), 171-175.

Kilpatrick, F. A., and Wilson, J. F., Jr. (1989). "Measurement of Time of Travel in Streams by Dye Tracing Book 3 Chapter A9." USGS, Denver.

Lewis, D. R., Williams, R. J., and Whitehead, P. G. (1997). "Quality simulation along Rivers (QUASAR): An Application to the Yorkshire Quese." *Science Total Environment*, 194, 399-418.

Mackay, D. (2001). *Multimedia Environmental Models: The Fugacity Approach*, Lewis Publishers, Boca Raton, 261p.

Mackay, D., and Hickie, B. (2000b). "Mass Balance Model of Source Apportionment, Transport and Fate of PAHs in Lac Saint Louis, Quebec." *Chemosphere*, 41, 681-692.

Mackay, D., Paterson, S., DiGuardo, A., and Cowan, C. E. (1996b). "Evaluating the Fate of a Variety of Types of Chemicals using EQC Model." *Environmental Toxicology and Chemistry*, 15, 1627-1637.

Mackay, D., Paterson, S., Kisci, G., Cowan, C. E., DiGuardo, A., and Kane, D. M. (1996a). "Assessment of Chemical Fate in the Environment Using Evaluative, Regional and Local-scale Models: Illustrative Application to Chlorobenzene and Linear Alkylbenzene Sulfonates." *Environmental Toxicology and Chemistry*, 15, 1638-1648.

Mackay, D., and Diamond, M. (1989). "Application of the QWASI (Quantitative Water Air Sediment Interaction) Fugacity Model to the Dynamics of Organic and Inorganic Chemicals in Lakes." *Chemosphere*, 18(7-8), 1343-1365.

Mackay, D., Shiu, W. Y., and Ma, K. C. (1992). *Illustrated Handbook of Physical-Chemical Properties and Environmental Fate of Organic Chemicals: MonoaromaticHydrocarbons, Chlorobenzenes and PCBs*, Lewis, Boca Raton.

MacLeod, M., Fraser, A. J., and Mackay, D. (2002). "Evaluating and Expressing the Propagation of Uncertainty in Chemical Fate and Bioaccumulation Models." *Environmental Toxicology and Chemistry*, 21(4), 700 - 709.

Maddalena, R. L., McKone, T. E., LaytonDennis, D. W., and Hseih, P. H. (1995). "Comparison of Multi-media Transport and Transportation Models: Regional Fugacity Model vs. CALTOX." *Chemosphere*, 30, 869-889.

Mahmood, K., and Yevjevich, V. (1975). *Unsteady Flow in Open Channels*, Water Resources Publications, Fort Collins, CO.

Marshall, K. C. (1992). "The Effects of Surfaces on Microbial Activity." Water pollution microbiology, R. Mitchell, ed., Wiley-Interscience, New York, 51-70.

Masch, F. D., and Associates. (1970). "QUAL-1 Simulation of Water Quality In-Stream and Canals. Program Documentation and User's Manual." Texas Water Development Board, Texas.

McFarland, V. A., and Clarke, J. U. (1989). "Environmental occurence, abundance, and potential toxicity of polychlorinated biphenyl congeners: consideration for a congener-specific analysis." *Environmental Health Perspectives*, 81, 225-239.

McKone, T. E. (1993). "CalTOX, a multimedia total exposure model for hazardous-waste sites." *UCRL-CR-111456PtI-IV,* Lawrence Livermore National Laboratory, Livermore, CA.

Neitsch, S. L., Aanold, J. G., and Williams, R. J. (2000). "Soil and Water Assessment Tool User's Manual Version 200." Grassland, Soil and Water Research Laboratory, Agricultural Research Service, Temple, TX.

Park, S. S., and Lee, Y. S. (1996). "A Multiconstituent Moving Segment Model for the Water Quality Predictions in Steep and Shallow Streams." *Ecological Modeling*, 152, 65-75.

Park, S. S., and Lee, Y. S. (2002). "A Water Quality Modeling Study of the Nakdong River, Korea." *Ecological Modeling*, 89, 121-131.

Rauch, W., Vanhooren, H., and Vanrolleghem, P. A. (1999). "A Simplified Mixed-Culture Biofilm Model." *Water Research*, 33, 2148-2162.

Reichert, P., Borchardt, D., Henze, M., Rauch, W., Shanahan, P., Somlyody, L., and Vanrolleghem, P. A. (2001). "River Water Quality Model No.1 (RWQM1):II. Biochemical Processes Equations." *Water Science and Technology*, 45(3), 11-30.

Reible, D. D. (1998). *Fundamentals of Environmental Engineering*, Lewis Publishers, Boca Raton, 544p.

Ronen, Y. (1988). *Uncertainty Analysis*, CRC Press, Inc., Boca Raton, 282p.

Sanders, G., Jones, K. C., Hamilton-Taylor, J., and Dorr, H. (1992). "Historical inputs of polychlorinated bipheyls and other organochlorides to a dated lacustrine sediment core in rural England." *Environmental Science and Technology*, 26, 1815-1821.

Schowanek, D., Fox, K., Holt, M., Schroeder, F. R., Koch, G., Cassani, G., Metthies, M., Boeije, G., Vanrolleghem, P. A., Young, A., Morris, G., Gandolfi, C., and Feijel, T. C. J. (2001). "GREAT-ER: a new too for management and risk assessment of chemicals in river basins. Contribution to GREAT-ER#10." *Water Science and Technology*, 43(2), 179-185.

Shanahan, P., Henze, M., Koncsos, L., Rauch, W., Reichert, P., Somlyody, L., and Vanrolleghem, P. A. (2001b). "River Water Quality Model No.a (RWQM1): II. Problems of the Art." *Water Science and Technology*, 38(11), 245-252.

Sincock, A. M., and Lees, M. J. (2002). "Extension of the QUASAR River Water Quality Model to Unsteady Flow Conditions." *Journal of Chart. Ins.Water Environ. Manage. (CIWEM)*, 16, 12-17.

Stumm, W., and Morgan, J. J. (1996). *Aquatic Chemistry: Chemical Equilibria and Rates in Natural Waters*, John Wiley and sons, New York, 1022p.

Sturm, T. W. (2001). *Open Channel Hydraulics*, McGraw Hill Inc., Boston, 493p.

Tank, J. L., and Dodds, W. K. (2003). "Nutrient limitation of epilithic and epixylic biofilms in ten North America streams." *Freshwater Biology*, 48, 1031-1049.

Tartakovsky, B., Manuel, M. F., and Guiot, S. R. (2005). "Degradation of trichloroethylene in a coupled anaerobic-aerobic bioreactor: Modeling and experiment." *Biochemical Engineering Journal*, 26, 72-81.

USGS. (2002). "Environmental Atlas of Lake Pontchartrain Basin." *Open Report 02-206*, United States Geological Survey.

Valsaraj, K. T. (2000). *Elements of Environmental Engineering Thermodynamics and Kinetics*, Lewis Publishers, Boca Raton, 717p.

WallingfordSoftware. (1994). "ISIS." Wallingford, Oxfordshire, UK, River Water Quality Software.

WaterResourcesEngineers. (1973). "Computer Program Documentation for the Stream Quality Model QUAL-II." U.S. Environmental Protection Agency, System Analysis Branch, Washington D.C.

Wiegel, J., and Wu, Q. (2000). "Mini Review: Microbial Reductive dehalogenation of polychlorinated biphenyls." *FEMS Microbiology Ecology*, 32, 1-15.